IMMOBILIZED HEPARIN VIA A LONG CHAIN POLY(ETHYLENE OXIDE) SPACER FOR PROTEIN AND PLATELET COMPATIBILITY

by
Suzanne Winters

A dissertation submitted to the faculty of
The University of Utah
in partial fulfillment of the requirements for the degree of

Doctor of Philosophy

Department of Pharmaceutics

The University of Utah

June 1987

THE UNIVERSITY OF UTAH GRADUATE SCHOOL

SUPERVISORY COMMITTEE APPROVAL

of a dissertation submitted by

Suzanne Winters

This dissertation has been read by each member of the following supervisory committee and by majority vote has been found to be satisfactory.

Chairman:

SungWan Kim

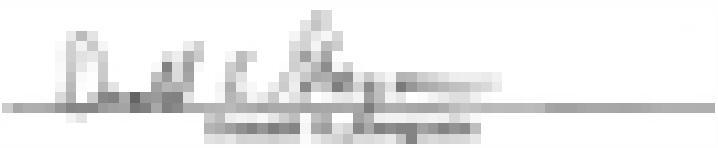

3/13/87

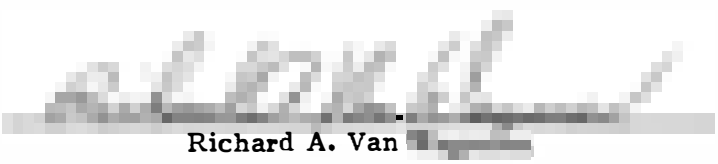

Richard A. Van

THE UNIVERSITY OF UTAH GRADUATE SCHOOL

FINAL READING APPROVAL

To the Graduate Council of The University of Utah:

I have read the dissertation of Suzanne Winters its final form and have found that (1) its format, citations, and bibliographic style are consistent and acceptable; (2) its illustrative materials including figures, tables, and charts are in place; and (3) the final manuscript is satisfactory to the Supervisory Committee and is ready for submission to the Graduate School.

Date

D. Andrade
Chairperson, Supervisory Committee

Approved for the Graduate Council

ABSTRACT

Poly(ethylene oxide) has some unique solubility and hydrogen-bonding characteristics which have been used to explain its apparent inertness with regard to blood protein adsorption and platelet interactions. A method has been developed to immobilize long chains of this hydrophilic and amorphous polymer by derivatization of the end hydroxyl groups allowing attachment to and extension out from the surface. This creates an "excluded volume" which is inaccessible to large protein molecules and cells.

Four derivatives of poly(ethylene oxide) (PEO) have been synthesized: PEO-bis isocyanate, PEO-bis isothiocyanate, PEO-bis chloroformate, and PEO-bis thiochloroformate. The cyanate derivatives were synthesized using the lithium salt of cysteamine to form diamine-terminated PEO chains which were subsequently reacted with phosgene or thiophosgene. The chloroformate derivatives were produced by directly reacting the hydroxyl groups of the PEO with phosgene and thiophosgene. Molecular weights of PEO ranging from 1,000 to 18,000 daltons were used.

Heparin was immobilized onto the reactive free ends of these PEO derivatives via the free amine and hydroxyl groups of the heparin molecule, permitting extension of the anticoagulant from the surface, allowing it to assume its native and active conformation for interaction with specific blood proteins.

Surfaces prepared by this method were characterized by X-ray photoelectron spectroscopy and found to be stable in aqueous environments. Minimal nonspecific protein adsorption and adhesion of platelets to the PEO

surfaces without heparin was demonstrated by Total Internal Reflection Fluorescenne Spectroscopy (TIRF) and ^{125}-iodine labeled proteins. It was found that there is a small inverse relationship between chain length of the PEO and the quantity of protein adsorbed onto the surface, confirming earlier reports. Platelet retention has been studied by exposing platelet rich plasma to derivatized glass beads and has demonstrated significantly less retention than the control surfaces.

Quantitation was accomplished using tritiated heparin. The activity of the heparin was shown by the ability of these surfaces to bind antithrombin-III and by significantly increased whole blood clotting times and activated partial thromboplastin times.

The results reported here suggest that long chain poly(ethylene oxide) offers a relatively inert surface for the immobilization of biologically active molecules, minimizing nonspecific interactions and providing a mechanism for these active molecules to react freely, mimicking their solution activities.

TABLE OF CONTENTS

ABSTRACT iv

ACKNOWLEDGMENTS vi

LIST OF FIGURES ix

LIST OF TABLES xiv

1. INTRODUCTION 1

1.1 Perspectives on Biocompatibility and Rationale 1
1.2 Poly(ethylene oxide) Background 7
1.2.1 Physiochemical Properties 7
1.2.2 Theory of the Passivating Nature of PEO 12
1.2.3 Biomedical and Biochemical Applications 18
1.3 Heparin Background 23
1.3.1 Structure and Pharmacology 23
1.3.2 Immobilized Heparin Materials 29

2. METHODS 34

2.1 Derivatization of Poly(ethylene oxide) 34
2.1.1 Isocyanates 34
2.1.2 Chloroformates 37
2.2 Quartz Substrate Preparation 42
2.2.1 Cleaning 42
2.2.2 Vapor Phase Silanization 42
2.2.3 Silanization of Quartz Beads 43
2.3 Poly(ethylene oxide) Immobilization 43
2.3.1 Poly(ethylene oxide) Coupling to Quartz Plates 43
2.3.2 Poly(ethylene oxide) Coupling to Quartz Beads 47
2.4 Heparin Immobilization 47
2.4.1 Coupling to Quartz Plates 47
2.4.2 Coupling to Quartz Beads 48
2.5 Quantitation of Immobilized Heparin 48
2.5.1 Tritium Labeling of Heparin 48
2.5.2 Quantitation Procedure 49
2.5.3 Heparin Depletion from Surface 49
2.6 Radiolabeling of Bovine Serum Albumin and Antithrombin III . 50
2.7 Characterization 51
2.7.1 X-Ray Photoelectron Spectroscopy 51
2.7.2 Variable Angle XPS 52
2.7.3 Wilhelmy Plate Contact Angle 53
2.8 Protein Adsorption Studies 54
2.8.1 Total Internal Reflection Fluorescence Spectroscopy . 54

2.8.2 ^{125}Iodine Protein Adsorption 59
2.9 Stability Studies in Aqueous Buffer 61
2.10 Heparin Activity Testing 62
2.10.1 Whole Blood Clotting Times 62
2.10.2 Activated Partial Thromboplastin Time Test 63
2.11 Platelet Interactions 64
2.11.1 Platelet Retention 65
2.11.2 Platelet Factor 4 Release 66

3. RESULTS 67

3.1 APS Coupling to Quartz Plates and Beads 67
3.1.1 XPS Characterization of Surface 67
3.1.2 Variable Angle Thickness 71
3.1.3 Wilhelmy Plate Characterization 74
3.2 Poly(ethylene oxide) Coupling to Quartz Plates and Beads 79
3.2.1 XPS Characterization of Surface 79
3.2.2 Variable Angle XPS Thickness 97
3.3 Heparin Coupling to Quartz Plates and Beads 102
3.3.1 XPS Stability Characterization of Surface 102
3.3.2 Variable Angle XPS Thickness 108
3.3.3 Quantitation 110
3.4 Protein Adsorption Studies 112
3.4.1 Total Internal Relfection Fluorescence (TIRF) 112
3.4.2 ^{125}I-Labeled Proteins 116
3.5 Whole Blood Clotting Times 119
3.6 Activated Partial Thromboplastin Times 121
3.7 Platelet Retention 125
3.8 Platelet Factor 4 Release 129

4. DISCUSSION

4.1 Poly(ethylene Oxide) Derivatization 133
4.2 Protein Resistance of PEO Surfaces 135
4.3 Heparin Immobilization 138
4.4 Blood and Protein Interactions 141
4.5 Summary and Conclusions 142
4.6 Future Studies 147
4.6.1 Derivatization of Graft Materials 147
4.6.2 *In-Vivo* Characterization 148
4.6.3 Feasibility for Long Term Applications 148

REFERENCES 149

LIST OF FIGURES

1. Factors affecting interfacial phenomena of blood contacting foreign surfaces and some of the possible reactions that may occur. 4

2. The possible orientations of poly(ethylene oxide) chains physically adsorbed onto a surface. The long chains may run along the surface, form loops and form tails which extend out from the surface. 11

3. Model of the interaction of a linear polymer (cylinder) with a large protein molecule (sphere) developed originally by Ogston and Laurent.[44] 14

4. The main sugars found in the heparin molecule which are linked by 1-4 glycosidic bonds. 1) 2-deoxy-2sulfoamino-α-D-glucose; 2) a-L-iduronic acid 2-sulfate (2-sulfoiduronic acid); 3) 2-acetoamido-2-deoxy-α-D-glucose (acetylglucosamine); 4) β-D-glucuronic acid; and 5) α-L-iduronic acid. 25

5. Schematic representation of the mechanism of heparin, antithrombin III (AT-III) and thrombin interaction. Heparin binds to the positively charged lysine residues on the AT-III molecule resulting in a subsequent conformational change in the AT-III molecule. This renders the active arginine center more accessible to the thrombin serine residue facilitating binding. 28

6. The four derivatives of poly(ethylene oxide) synthesized for immobilization onto quartz substrates. The bifunctional molecules permit attachment to the substrate with the extension of the other free reactive end group out from the surface for subsequent reaction with heparin. 35

7. The chemistry involved in the synthesis of the four derivatives of poly(ethylene oxide). 36

8. Infrared spectrum of poly(ethylene oxide) derivatives. a. bis-isocyanate MW 6,000; b. bis-isothiocyanate MW 6,000; c. bis-chloroformate MW 6,000; d. bis-thiochloroformate MW 6,000 . 38

9. The elemental percent of carbon of the PEO immobilized surfaces resulting from reaction in 1 percent and 5 percent solutions for various lengths of time..... 45

10. The reaction involved in the coupling of the four derivatives of PEO to the silanized quartz substrate. The amine of the silane couples to the functionalized PEO. Using a large excess of PEO minimizes the possibility of the formation of loops resulting from both ends of the PEO coupling to the surface. 46

11. Schematic of the TIRF apparatus. The components are (UV) UV excitation light source; (ExM) excitation monochromator; (S) shutter; (L) collamating lense; (P) polarizer; (F) flow cell; (EmM) emission monochromator; (PM) photomultiplier tube; (PhC) photon counter; and (R) recorder. 56

12. Components of the TIRF flow cell. The derivatized quartz slide was optically coupled to the quartz prism with glycerol. Flow volume created by the silastic gasket was 0.8 ml..... 57

13. The adsorption scheme used for TIRF protein adsorption studies. Tryptophan standards were followed by successively increasing concentrations of AT-III and the plasma. 60

14. The XPS elemental analysis of quartz surfaces derivatized with -aminopropyltriethoxy silane following exposure to PBS for various times. 68

15. The XPS spectrum of the nitrogen 1S signal of APS-coupled quartz slides following exposure to PBS. The doublet presumably is due to the presence of NH_2 and NH_3. 69

16. The XPS elemental analysis of clean quartz slides following exposure to PBS for various times. 70

17. The ratio of the nitrogen to silicon XPS signals of APS and clean quartz control surfaces following exposure to PBS for various times. 72

18. Plot of the equation for a theoretical uniform overlayer of APS on quartz of various thicknesses. The astericks (*) indicate actual data obtained in variable angle XPS experiments..... 73

19. Plot of the equation for a theoretical 10 Å patchy overlayer of APS on quartz for varying surface coverages (γ). The astericks (*) indicate actual data obtained in variable angle XPS experiments. 75

20. Plot of the equation for a theoretical 30 Å patchy overlayer of APS on quartz for varying surface coverages (γ). The astericks (*) indicate actual data obtained in variable angle XPS experiments. 76

21. Plot of the equation for a theoretical 50 Å patchy overlayer of APS on quartz for varying surface coverages (γ). The astericks (*) indicate actual data obtained in variable angle XPS experiments. 77

22. The contact angles of clean and APS derivatized quartz measured by the Wilhelmy Plate method as a function of hydration time in PBS. 78

23. The carbon 1S XPS spectra of surfaces analyzed. a) pure PEO; b) aliphatic carbon of an APS silanized quartz slide; c) PEO immobilized onto quartz via APS. 80

24. The curve-resolved carbon 1S spectrum of PEO immobilized on quartz via APS coupling agent. It is the ether carbon component of the carbon 1S signal that was used to monitor the stability of the PEO grafted surface. 82

25. The total XPS elemental signals of PEO-bis chloroformate MW 6,000 immobilized onto a quartz slide as a function of hydration time in PBS. 83

26. The total XPS elemental signals of PEO-bis thiochloroformate MW 6,000 immobilized onto a quartz slide as a function of hydration time in PBS. 84

27. The total XPS elemental signals of PEO-bis isocyanate MW 6,000 immobilized onto a quartz slide as a function of hydration time in PBS. 85

28. The total XPS elemental signals of PEO-bis isothiocyanate MW 6,000 immobilized onto a quartz slide as a function of hydration time in PBS. 86

29. The total XPS elemental signals of PEO-bis chloroformate MW 18,000 immobilized onto a quartz slide as a function of hydration time in PBS. 87

30. The total XPS elemental signals of PEO-bis thiochloroformate MW 18,000 immobilized onto a quartz slide as a function of hydration time in PBS. 88

31. The total XPS elemental signals of PEO-bis isocyanate MW 18,000 immobilized onto a quartz slide as a function of hydration time in PBS. 89

32. The total XPS elemental signals of PEO-bis isothiocyanate MW 18,000 immobilized onto a quartz slide as a function of hydration time in PBS. 90

33. The percent of the total carbon XPS signal due to the ether carbon component of the control surfaces. The underivatized PEO was physically adsorbed to the APS/quartz surfaces and slowly leached from the surface. 91

34. The carbon to silicon ratio of the XPS elemental analysis of control surfaces as a function of hydration time in PBS. 92

35. The percent of the total carbon XPS signal due to the ether carbon component of the four PEO derivatized surfaces MW 6,000 as a function of PBS exposure time. 94

36. The carbon to silicon ratio of the XPS elemental analysis of the four PEO derivatized surfaces MW 6,000 as a function of PBS exposure time. 95

37. The percent of the total carbon XPS signal due to the ether carbon component of the four PEO derivatized surfaces MW 18,000 as a function of PBS exposure time. 96

38. The carbon to silicon ratio of the XPS elemental analysis of the four PEO derivatized surfaces MW 18,000 as a function of PBS exposure time. 99

39. The carbon 1S spectrum of PEO derivatized glass beads. The small peak at 284 ev is the hydrocarbon contamination of the indium foil on which the sample beads were run. 100

40. Plot of the equation for a theoretical 70 Å patchy overlayer of PEO on APS derivatized quartz for varying surface coverages (γ). The astericks (*) indicate actual data obtained in variable angle XPS experiments. 101

41. The sulfur 2P XPS signal from heparin. a) pure heparin powder; and b) heparin immobilized via PEO-bis isothiocyanate. he sulfur of the isothiocyanate is charge shifted enabling differentiation of the sulfur of heparin. 104

42. The sulfur 2P XPS signal of the four PEO/heparin surfaces MW 6,000 as a function of PBS exposure time. 106

43. The sulfur 2P XPS signal of the four PEO/heparin surfaces MW 18,000 as a function of PBS exposure time. 107

44. Plot of the equation for a theoretical 90 Å patchy overlayer of heparin on PEO coupled quartz surfaces for varying surface coverages (γ). The astericks (*) indicate actual data obtained in variable angle XPS experiments. 109

45. Quenching of the TIRF signal due to the presence of increasing concentrations of PEO. 113

46. The Activated Partial Thromboplastin Times of various quantities of immobilized heparin/PEO glass beads. 123

47. A typical curve generated in the platelet retention studies using immobilized heparin beads plotted as a function of whole blood incubation time. 126

48. A typical standard curve generated during each series of the sample Platelet Factor 4 release studies. 130

49. Platelet Factor 4 levels in plasma exposed to derivatized beads for various times with and without heparin. 131

LIST OF TABLES

I. Covalently Immobilized Heparin Surfaces 30

II. Elemental Analysis of PEO Stability on Glass Beads 98

III. Elemental Content of Heparin and Heparin Derivatized PEO Surfaces (MW 3,000) 103

IV. Quantitation of Surface Immobilized Tritiated Heparin 111

V. Protein Adsorption From Solution Measured by Total Internal Reflection Fluorescence 114

VI. Adsorbed ^{125}I-Proteins Onto PEO and PEO/Heparin Surfaces 117

VII. Whole Blood Clotting Times 120

VIII. Activity of Immobilized Heparin Surfaces Determined by APTT 124

IX. Mean Platelet Retention Index for Whole Blood and Platelet Rich Plasma 128

ACKNOWLEDGMENTS

I wish to thank the members of my Supervisory Committee for their encouragement, direction and inspiring comments. My sincere thanks to all the people at the University of Utah for their friendship and technical assistance which helped to make graduate school an enjoyable experience. This work was partially supported by NIH Training Grant HL-07520.

I would also like to express my deepest appreciation to the mentors of my life, without whose encouragement I would not have succeeded in this endeavor; first to my parents who have given me guidance and support, and particularly to my father, William E. Winters, who has provided me a role model; to Robert I. Leininger, who introduced me to the field of biomaterials and motivated me in this direction; and finally to Joseph D. Andrade, for his constant encouragement, motivation and contagious enthusiasm. I would also like to thank my husband, Robert H. Ramsey, who gave me the motivation and courage to finish this dissertation.

CHAPTER 1

INTRODUCTION

1.1 Perspectives on Biocompatibility and Rationale

Among the various kinds of interfacial phenomena in the field of biomaterials chemistry, the adsorption of biomolecules at the interface between a liquid and solid phase is one of the most significant areas to be first studied. This adsorption influences subsequent biochemical or biological phenomena such as platelet or leukocyte adhesion, thrombus formation, and local tissue or systemic reactions.

Compatibility of a material with blood requires no adverse effect on blood or any of its components. The complex nature of blood, with its formed elements, coagulation system, and multitude of proteins, puts not only a variety of restrictions on the blood contacting surface, but also makes the determination of blood compatibility a significant problem. The reverse requirement is also true: that the blood have no adverse or incapacitating effect on the material.

A systematic approach to the development of safe and suitable implant materials for human use requires: 1) matching of the engineering properties of the material and the finished devices with those of the corresponding human tissues; 2) knowledge of the properties of the implant materials which might exert an effect on the biological system; and 3) an understanding of the properties of the biological environment which might have an effect on the material. Following the development of materials intended for biological purposes, extensive testing for the complex interactions must be completed. It

is surprising that there is incomplete agreement on how these materials are to be standardized in terms of chemical, physical, mechanical or biological properties in order to determine their relative biocompatability with human tissues, the lack of hazardous side effects on the human patient, or their effectiveness as reconstruction materials.

Various recommendations have recently been published in an attempt to standardize blood testing protocols and to provide appropriate statistical verification for claims of improved "blood compatibility." Unfortunately, it has been demonstrated that *in-vivo* results of implanted polymers do not necessarily correlate with the results of *in-vitro* and *ex-vivo* testing of biomedical implants. P. Didisheim has recommended nine tests for describing compatibility including protein adsorption in terms of type and amount, complement activation, cellular adhesion, and calcification. (1) J. Anderson has developed several tables listing level I and level II type tests describing minimum requirements for characterization of new compatible materials. (2) Perhaps the most comprehensive testing procedures have been outlined in the recently published "Guidelines for Blood Material Interactions" by the National Heart, Lung, and Blood Institute. (3) These guidelines offer recommendations for material characterization, *in-vitro* interactions, and testing in appropriate animal models.

Due to legal, ethical, and religious reasons, our society is not conducive to the use of human volunteers for the testing of new biomedical materials. Therefore, current techniques for the evaluation of these materials are by nature indirect, limited both in accuracy and scope of prediction for human applications. Any scientist working in the field of bioengineering must be aware of the limitations of both the existing and potential future indirect methods used for assessing the biohazards and biocompatibility of new candidate materials.

It is known that adsorption of proteins is one of the first events when blood contacts a foreign surface. (4) Moreover, the nature of the protein layer influences subsequent reactions that involve platelets and leukocytes, complement activation, and finally, the formation of crosslinked fibrin and thrombus. Thrombus formation is by far the most debilitating and obvious response to foreign material in contact with the blood. Fig. 1 shows some of the major factors which influence the ultimate biocompability and the possible course of reactions that may occur.

Due to the importance of protein adsorption on the fate of a material, this area has received the most attention in investigations of the biocompatibility of materials. The emphasis in these studies has been on the composition of the adsorbed layer, rate of adsorption, and possible changes, such as conformation or denaturation over time. This has proven difficult, and most studies have been done on solutions of single proteins or simple mixtures. Rates have been measured using labels, analysis of the eluted protein, and spectroscopic analysis. However, problems have been encountered when applying such measurements to the behavior of blood itself.

In the past, the thrombogenicity of implants has been sufficiently overcome by the administration of systemic anticoagulants such as heparin or coumadin. However, long term anticoagulation therapy is not advisable due to deleterious side effects. For this reason, there have been extensive efforts to develop materials which can be used with minimal or no anticoagulation. A number of surface parameters have been evaluated in an attempt to correlate these properties with the coagulation of blood. Efforts have been made to develop new materials, predominately polymeric, which are, by themselves, thromboresistant. Comprehensive reviews of individual polymers tested have been published (5) and will not be repeated here. Developments include anionic

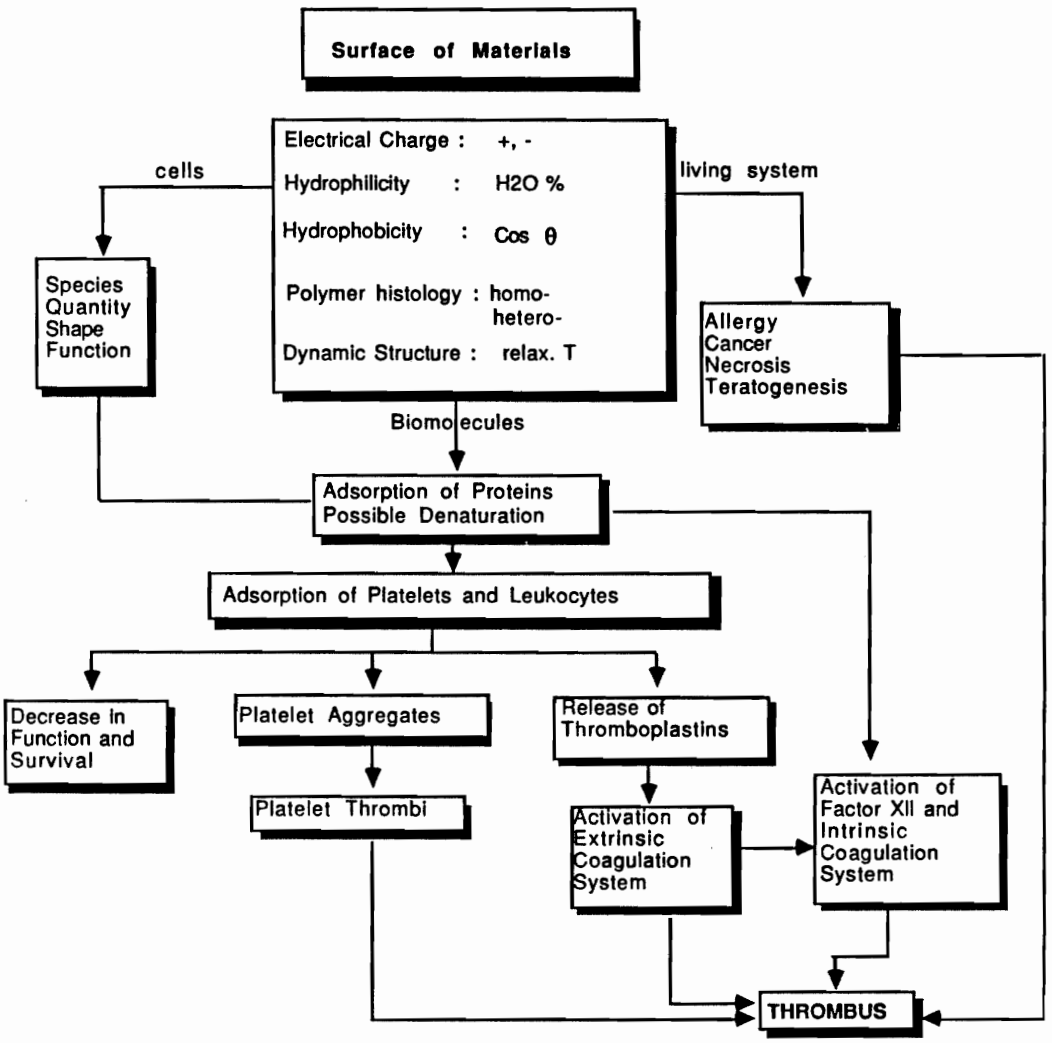

Figure 1. Factors affecting interfacial phenomena of blood contacting foreign surfaces and some of the possible reactions that may occur.

polymers, low surface energy materials, hydrogels, urethanes, and biologically modified surfaces such as preadsorption of polymers with albumin. The factors increasing thromboresistance include increased surface smoothness, increased negative surface charge, and increased hydrophilicity. To date no single definitive parameter appears to govern the thrombogenic response of the blood to the material.

Surface modification of polymeric materials offers the advantage of optimizing the chemical nature of the blood/polymer interface while allowing the choice of the substrate to be on the basis of the necessary mechanical properties. With this technique, variables such as hydrophilicity and ionic charge may be varied without consideration of other stringent requirements on the material. An excellent review of the surface modification of polymers to improve blood compatibility has been published by Kim and Feijen. (6)

Early in the development of a thromboresistant material was the finding that heparin ionically bound to a surface provides a very significant degree of thromboresistance. (7) Since that time, investigators have attempted numerous methods to ionically and covalently bind anticoagulants onto polymers. Some of these attempts have had limited success in clinical use. The problems encountered in the ionically bound systems have been depletion of the heparin by ion exchange with the blood constituents. In the covalently bound systems, the problems have been a decrease or lack of activity of the pharmacon.

The study presented herein was undertaken to develop a new thromboresistant material. In an attempt to identify and develop an optimally blood compatible system, a number of desirable qualifications can be listed. The "ideal" polymer would be one which would not initiate the sequence of events in any of the coagulation mechanisms, would interact favorably with the cellular components, and would not cause tissue reaction or inflammation. If

anticoagulation therapy is necessary, emphasis should be placed on developing ways to minimize harmful side effects. The material developed during the course of this study uses a polymer coating, poly(ethylene oxide), with heparin immobilized covalently.

Poly(ethylene oxide) (PEO) has recently received much attention as a potential biomaterial. PEO has some unique properties which have led to its consideration for application in implants, oxygenators, dialysis membranes, contact lenses, and in immunoassays. Current evidence shows that PEO, either by itself or as a component in copolymers, is relatively inert in terms of protein adsorption and platelet adhesion. (8,9,10,11,12) The unusual solubility characteristics and solution properties of PEO have been used to explain its apparent inertness towards blood proteins and platelets. (13) For these reasons, PEO was chosen as a good candidate for the development of a biocompatible material.

Heparin is the most frequently prescribed anticoagulant in use today. It is a mucopolysaccharide, highly sulfonated, and contains a number of other charged functional groups. There are large variations in the individual sugar units and in the molecular weight of commercial preparations. Heparin enhances the inactivation of thrombin by antithrombin III, thereby inhibiting the fibrinogen to fibrin conversion process. Heparin has been used in a variety of ways to increase the thromboresistance of polymeric materials. It has been dispersed within a matrix and ionically or covalently bound to materials for the purpose of improving compatibility. All of these methods have had limited success. However, if heparin can be covalently bound to a surface and still maintain its anticoagulant activity, the possibility of depletion of the pharmacon will be avoided. This is the approach used in this study.

To create a biocompatible surface, long PEO chains were immobilized to a surface via a silane coupling agent and heparin molecules were covalently attached to the PEO. This provides for a protein resistant surface (the PEO chains) and for the local action of heparin. By virtue of the flexibility and extension into solution of the PEO chains, the heparin has the freedom to assume its native and active conformation. This approach has been tested for its stability, protein resistance, and anticoagulant activity.

1.2 Poly(ethylene Oxide) Background

1.2.1 Physiochemical Properties

Poly(ethylene oxide) was first reported by Lourenco in 1860 by the condensation of ethylene glycol and ethylene dibromide. (14) With the development of the macromolecule concept in the mid-1900s, PEO of high molecular weight was one of the first polymers prepared and studied by Herman Staudinger. The first synthesis of truly high polymers was announced in 1957. PEO was one of the first polymers to be crosslinked by radiation and to have inter- versus intramolecular crosslinking delineated in terms of molecular weight. (15) The low molecular weight members of the PEO series with n (number of repeat units) up to about 150 are generally known as polyethylene glycols while the higher members are known as poly(ethylene oxide).

The two extremes of molecular weight have sufficiently different properties as to form two classes. The low molecular weight species range from relatively viscous fluids to waxy solids while the higher polymers are true thermoplastics. An excellent review of PEO has been published by Bailey and Koleske. (16)

In recent years, PEO and its derivatives have proven valuable in a variety of diverse chemical and biological applications. These include peptide synthesis,

phase transfer catalysis, pharmaceutical modification, protein and cell purification, polymer-bound reagents and binding assays. The wide range of possible applications is due to some very unique properties of PEO.

PEO is soluble in water and a number of organic solvents including acetonitrile, chloroform, benzene, and dimethyl formamide. At room temperature, it is completely miscible with water in all proportions. The extreme water solubility is of particular importance in light of the insolubility in water of such closly related polymers as poly(methylene oxide) and poly(propylene oxide). Aqueous solutions of PEO are elastic in their behavior and the viscosity decreases with increasing shear stress. There is an inverse solubility-temperature relationship exhibited by aqueous solutions: as these solutions are increased in temperature to near the boiling point of water, the polymer precipitates. (17) For very dilute solutions (0.2 percent or less), the precipitation is observed as a cloud point. For slightly more concentrated solutions (0.5 percent), the polymer precipitates as a gel that slowly shrinks and retains the shape of the container on standing at the precipitation temperature. This has been explained by the dual nature of the polymer structure (Doolittle). (18) There is a hydrophobic character to the polymer due to the ethylene units. As a result of bound water molecules, which are presumably associated with the ether oxygen, (19) it also exhibits a hydrophilic character. Another way to explain the inverse solubility-temperature relationship of PEO has been suggested by Nemethy as a result of a disordering of bound water or "icebergs" that exist about the polymer molecule. (20) These "icebergs" correspond to a layer of highly oriented water which would surround the polymer in aqueous solution. Increasing the temperature causes a disruption of this water and allows relatively strong polymer-polymer interactions, which are mainly entropic in nature.

The conformations and crystallinity of PEO in the solid, melt and in organic and aqueous solutions have been studied. In the absence of crystallinity, the amorphous material is a rubber of low glass transition temperature (Tg typically -60°C) and exhibits a maximum Tg at molecular weights in the range of 4000 daltons. Having no chiral centers and no sidegroups, the polymer is normally highly crystalline with the melting points up to a theoretical value of 70°C for infinite molecular weight. (21) The crystalline structure of linear PEO has been determined by X-ray diffraction as a 7_2 helix: seven mer units and two turns in a fiber identify period of 19.3 A. (22) Further studies by Miyazawa confirmed that the PEO repeating unit is in the trans-gauche-trans (TGT) conformation of the COCCOC sequence. (23) Previous work by infrared and NMR techniques suggests that the TGT sequence is retained to a large degree in aqueous solution. (24) However, Maxfield and Shepard, using Raman scattering, found that the ordered nature of the polymer is lost at a critical concentration, approximately 50 percent by weight, in both aqueous and chloroform solutions. (25)

While it is more common to study the properties of polymers either in solution or as solid materials, many of the practical applications for PEO involve its use at or on surfaces. Glass measured the adsorption characteristics of PEO at aqueous-air interfaces as a function of polymer molecular weight, concentration and temperature. (26) His data indicate that the polymer is adsorbed at the interface, for all molecular weights, with portions of the polymer chains oriented out of the interfacial region. However, in low molecular weight glycols, the terminal hydroxyl groups may have a predominating influence and one half of the potentially adsorbed segments are actually oriented in the interfacial region.

Cosgrove *et al.* studied the conformation of PEO at the solid/solution interface. (27) The conformational behavior of linear, homopolymer PEO physisorbed and terminally bonded to polystyrene latex particles was studied by these investigators. By using a multipulse NMR relaxation time method which reflects both molecular structure and motion, they were able to differentiate segments on the chains having different mobility as a function of the method of attachment to the surface. In this manner, the ratio of segments in each state and the fraction of bound segments may be calculated. It was found that the conformation of the polymer chains adsorbed to a surface contains loops and trains close to the surface with the long tails extending into solution as schematically depicted in Fig. 2. This is for a surface completely covered with polymer (i.e., $\Theta = 1.0$). The effect of degree of coverage was studied and segment density distributions could be determined.

Studies of the characteristics of PEO at aqueous-organic liquid interfaces are of considerable interest. PEO in water retains the TGT sequence and helical conformation of the crystalline state to a large degree. (28,29) However, in organic solvents such as chloroform or benzene, PEO assumes a more random conformation. (30) Interfacial pressures of PEO with various molecular weights at benzene-water interfaces with PEO initially dissolved in either phase demonstrated that equilibrium is attained surprisingly quickly. (17) The interfacial tension of dextran - PEO water systems has demonstrated that two immiscible water phases are obtained. (31) This has been used as selective and mild partitioning systems for separation of various biological materials such as proteins, nucleic acids and cell particles. (32)

PEO is known to form associated complexes with other molecules in aqueous solutions. Formation of the association complexes occurs at the expense of ordered water associated with the polymer. (33) This disruption of the water

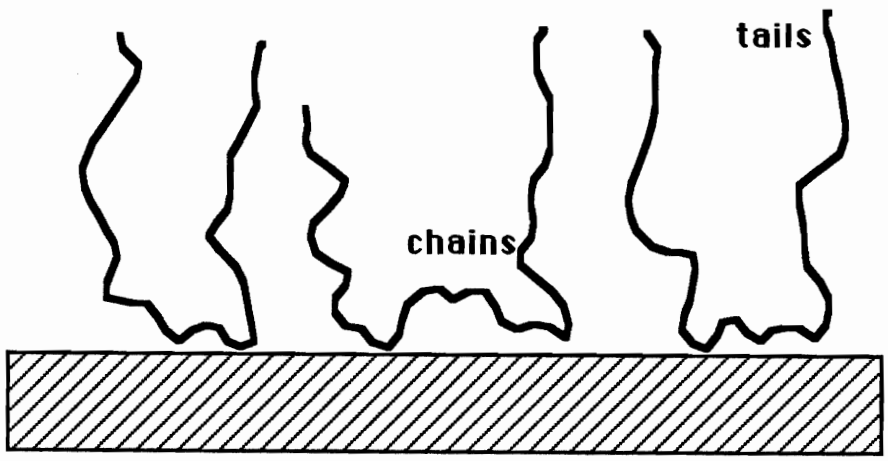

Figure 2. The possible orientations of poly(ehtylene oxide) chains physically adsorbed onto a surface. The long chains may run along the surface, form loops and form tails which extend out from the surface.

structure provides an added entropic driving force favoring complex formation. When aqueous solutions of PEO and poly(acrylic acid) are mixed in approximately equal proportions, a precipitate is immediately formed. (34) The formation of these insoluble hydrogels is due to the formation of hydrogen bonds between the poly-acid and the ether oxygens of the PEO which are weakly basic.

Evidence exists for the interaction of PEO with metal salts such as potassium iodide. This interaction is sufficiently marked such that the incorporation of 10-30 percent of the salt in the bulk polymer substantially reduces crystallinity while retaining compatibility. (35) No interaction other than a very small salting-out effect is observed with potassium iodide and PEO in water solution. It has been suggested that the association is due to an ion-dipole interaction. The anion is tentatively postulated as the species directly associating with the polymer resulting in the concurrent disruption of the crystalline structure. (36) Other materials, such as urea and thiourea, have also been shown to form associated complexes with PEO, although these are highly crystalline complexes. (37) Linear PEO is also able to complex with neutral molecular iodine in the solution and solid state to produce I_3^- ions, demonstrating the ability of PEO to mimic the complexation features of the macrocyclic crown ethers. (38)

1.2.2 Theory of the Passivating Nature of PEO

The behavior of solutions containing globular proteins and PEO has been of great interest to protein chemists. The use of PEO to crystalize proteins for crystallographic studies is well established (39) and PEO provides an attractive alternative to other agents used for protein precipitation. PEO has been used for the prevention of macromolecular adsorption (40,41) and for the stabilization of colloidal dispersions. (42)

The theory developed by Ogston and Laurent and readdressed by Topchieva (43) described the exclusion properties of polymers and greatly simplified the problem by considering the model of the interaction of a linear polymer, represented by a long thin rod, with globular particles which are assumed to be spherical (Fig. 3). The greatest exclusion effect is expressed as the excluded volume for S, with respect to unit mass of R. The center of the spherical particle S cannot approach R to a distance less than r_s. The excluded volume for the center of S is equal to the volume of the cylinder bounded by dashed lines whose radius is equal to the sum of the radii $r_s + r_r$ (r_r = the radius of the rod). If the end group effect can be neglected, then the volume excluded for the sphere is $\pi\, l_r\, (r_s + r_r)^2$, where l_r is the length of the rod. If d is the density of the rod, then its mass is $\pi l_r\, r^2_r d$, and the excluded volume v_{excl} with respect to unit mass of R is:

$$v_{excl} = \frac{\pi l_r (r_s + r_r)^2}{\pi l_r\, r^2 r d} = \frac{1}{d}\left(\frac{r_s}{r_r} + 1\right)^2. \qquad (1)$$

The degree of exclusion increases with increasing radius of S and with decreasing radius of R or with increasing asymmetry of the polymer. The overall volume (K_{av}) accessible to spheres with radius r_s in the space containing randomly distributed long rods with radius r_r is:

$$K_{av} = \exp\left(-\pi\, L\, (r_s + r_r)^2\right) \qquad (2)$$

where L is the sum of the lengths of all the rods per unit volume. It can be seen that the concentration of the rods and the square of the radius of the spheres are the only parameters which determine the accessible volume for the case where $r_r << r_s$. The fraction of the volume accessible for a given substance (K_{av},) is related to the excluded volume by the expression:

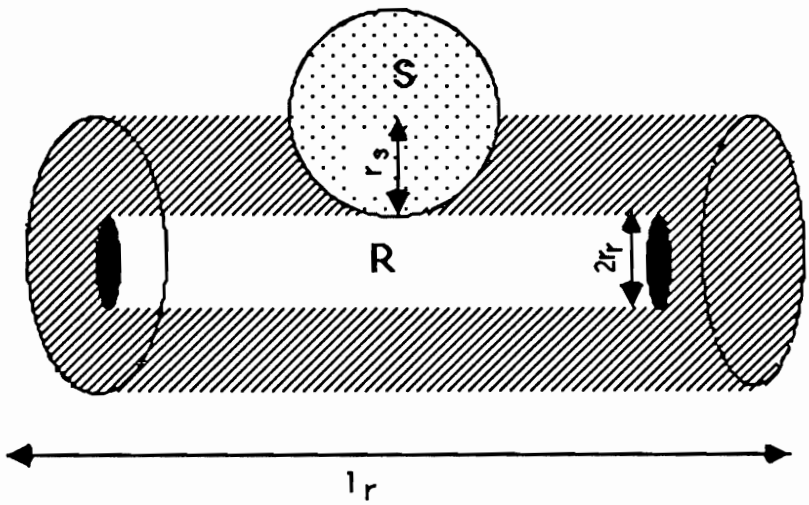

Figure 3. Model of the interaction of a linear polymer (cylinder) with a large protein molecule (sphere) developed originally by Ogston and Laurent.[44]

$$v_{excl} = (1 = K_{av}) / C_R \quad (3)$$

where C_R is the concentration of the rods R expressed in terms of mass with respect to volume.

This excluded volume theory was further refined by Knoll and Hermans (44) to take into consideration protein size, conformations, and polymer chain statistics. The excluded volume (V_{12}) in this theory is defined similarly as the effective volume of a solution that is not available to particles of species 1 as a result of the introduction of species 2 strictly for steric reasons. Beginning with the expression for this:

$$v_x = N_1 V_{12} \quad (4)$$

where v_x is the average number of particles of species 1 which are excluded from the total volume (V_{tot}) by the volume occupied by species 2. The geometry of the excluding and excluded species has been taken into consideration for cases where the excluding species is either a sphere or a long rod described by a cylinder. Conformational freedom of the polymer requires that the excluded volume be calculated as an average overall possible conformations of the polymer chain.

The result of the theory is an expression for the excluded volume in terms of the root mean square end to end distance of the polymer chain (h_o) and the radius of the protein, assuming a globular protein and infinitely long randomly coiled polymer molecules. Using a probability function for the location of the beginning and end of the polymer chains and a Gaussian distribution for the number of chain segments, an expression has been derived for the excluded volume: (45)

$$V_{12} = v_x/N_1 = V_2 + \quad (2/3 \quad)S_2h_o \tag{5}$$

where S_2 is the surface area of the sphere, V_2 is the volume occupied by species 2 and N is defined as above. Values of h_o were estimated from intrinsic viscosities; values of protein radii were based upon molecular weight, intrinsic viscosity, frictional coefficient and knowledge of molecular conformation.

Measurement of thermodynamic interaction parameters of bovine serum albumin and PEO of varying molecular weights using light scattering techniques were correlated with theoretical calculations of interactions based on size, radius of gyration and solubilities in two solvents. Using this method, these investigators were able to predict with relative accuracy the composition and distribution of the two phases at equlibrium in terms of thermodynamics and statistical mechanics even for dilute solutions in which PEO is a poor protein precipitating agent.

Maroudas presented similar evidence for the exclusion of molecules by adsorbed polymer as it relates to cell adhesion and membrane fusion. (45) This model comprises not only geometric exclusion by rigid molecules, such as rods and spheres, but also unfavorable thermodynamic parameters such as free energy, summed up over many segments, and for random coil polymers, entropy resulting from the ability of each molecule to claim extra extension space for its own. This steric exclusion model provides a general physiochemical basis for the observation of fusion and for the low adhesivity of neutral hydrophilic gels.

Another approach explaining the repulsion of two long chain molecules (i.e., PEO and proteins) has been described by Klein *et al.* (46) This investigation determined the forces as a function of distance, F(D), and the mean refractive index n(D), of the medium separating two smooth curved mica surfaces in the presence or absence of adsorbed layers of monodispersed PEO of two molecular

weights. Interactions between bare mica surfaces were characteristic of electrostatic double-layer overlap and strongly repulsive as described by DLVO theory. Following incubation in PEO polymer solution, no attraction between the two layers was detectable as might be expected if bridging or depletion layer forces were present. It was determined that the adsorbed PEO was irreversibly adsorbed. The distance of onset of repulsive interactions is typically twice the extension of the adsorbed polymer layers from the surfaces. In terms of unperturbed radii of gyration R_g, the extension from the surfaces is approximately 3 R_g for polymers of the two molecular weights. The repulsive forces between the mica plates as the adsorbed PEO layers come into overlap were attributed to local rise of osmotic interactions between the opposing segments. This is to say at the simplest level, that as the surfaces approach, the mean concentration of polymer in the overlap region increases with consequent increasing repulsion.

Merrill and Salzman have used the unique solubility and solution properties of PEO to explain its favorable interaction with blood proteins when used as a biomaterial. (47) These investigators claim that a two-phase equilibrium between aqueous solution of high molecular weight PEO and crystalline PEO is never realized when the PEO is bound to a surface or exists in a network because the effective chain molecular weights are too low and the hydroxyl containing unit, by which the PEO sequence of PEO is tied, acts as a diluent comonomer. This depresses the crystalline melting point of PEO in the anhydrous state which is further depressed by the imbibition of water from plasma. Therefore, the surface presented to the blood is "liquid-like," capable of segmental motion and fluctuation constrained only at the chain ends.

The passive behavior of PEO towards cellular components can be considered an extension of this theory because cell membranes are coated by a

hydrated layer of long-chain glycocalyx molecules. George Bell has addressed the thermodynamics of cell adhesion in which the steric compression resulting in repulsion of the polymer chains plays a major role. (48) He describes the repulsive force at distance S given by F(S) as a function of the free energy of nonspecific repulsion per unit area of contact r(S):

$$\Gamma(S) = \int_S^\infty F(s)\, dS. \qquad (6)$$

Qualitatively, the repulsive energy falls roughly as the reciprocal of the separation distance out to a distance, after which it drops more rapidly. A parameter g is developed as a measure of the combined thickness of the polymer layers and the ease with which the polymer layers between cells can be compressed. Theoretical estimates of g can be derived by considering the statistical mechanics of chain molecules anchored to rigid surfaces.

In summary, the apparent inertness of PEO towards the adsorption of proteins and cells is due to the unfavorable entropy of mixing of two long chain molecules, an active repulsion force generated by steric exclusion and interaction parameters and the imbibition of water molecules by an amorphous already hydrophilic material leading to a flexible, liquid like surface.

1.2.3 Biomedical and Biochemical Applications

Low molecular weight poly(ethylene oxide)s are widely formulated in ointments because of their broad compatibility and water solubility. This characteristic permits the ointments to be readily washed off with water. These rather inert polymers do not interfere with release of medications and can be applied to both moist and dry skin areas with equal ease. PEO with molecular weights ranging from 1,000 to 4,000 are used as suppository bases. The softening point of the suppository can be controlled by the relative amounts of the higher

or lower molecular weight PEO in the formulation. PEO is also used as a dry binder, in tablet coating, and for lubrication in the formulating and manufacture of compressed tablets. In cosmetics, PEOs are formulated in creams, lotions, cakes, sticks, and powders.

PEO polymers have found a number of clinical applications and are the basis of many commercial products. Vigilon™ is a radiation crosslinked high molecular weight PEO which swells to a high degree with water and is sold as a sheet wound covering material. A contraceptive sponge which has been well received in the USA is a crosslinked PEO foam containing the spermicide nonoxynolphenol. Smith and Nephew have patented a wound healing laminate described by Lang (49) in which a hydrophilic open-celled PEO foam is sandwiched between an inner poly(urethane) open-pore net and an outer continuous layer which prevents the ingress of bacteria and controls the egress of water.

Poly(ethylene oxide) has found numerous applications in both gas and liquid chromatography. Castello *et al.* have evaluated the retention characteristics of PEO used as liquid phases in gas chromatography. (50) Effects of molecular weight, temperature and of the effect of the hydroxyl group were examined in eight different grades of PEO, and their activity coefficients were calculated. The presence of impurities was found to significantly affect these experiments.

The adsorptivity of glass capillary columns has been suppressed by application of a thin nonextractable layer of Carbowax™, high molecular weight PEO which is highly polydisperse, to the glass surface. (51) The properties of PEO surfaces were found to differ greatly with the etching technique used on the glass, the type of glass and the procedure of Carbowax™ application. Columns prepared from etched Pyrex glass showed the highest stability, and have been used regularly for the separation of polycyclic aromatic

hydrocarbons at temperatures up to 300°C. By using a column packing consisting of chemically bonded PEO 20M on Sepharose 6B and an isotonic buffered solution containing dextran T40 and T500 as mobile phase, Matsumoto *et al.* were able to separate human blood cells and studied the influence of mobile phase composition on the retention behavior. (52) When neutral salts, such as sodium chloride, were added to the mobile phase while maintaining the isotonicity, an increase in the retention volumes of erythrocytes, granulocytes, and lymphocytes was observed. In a similar exclusion chromatography procedure, PEO was used at low concentrations to passivate controlled pore glass and prevent the adsorption of rabies virus. (53)

Ling and Matthiasson explored the possibility of using PEO with intermediate hydrophobicity as ligands in hydrophobic interaction chromatography. (54) In this procedure, glucose oxidase was modified by covalent attachment of monomethoxypoly(ethylene glycol) and conjugation with gentamicin. Two fractions were obtained when the product was run on monomethoxypoly(ethylene glycol)-Sephadex at high ionic strengths.

The behavior of solutions containing globular proteins and PEO has been of great interest to protein chemists. The only noticeable effect of PEO on protein structure is the shift of the pK of the ionizable groups at high PEO concentration. (55) In some situations, the use of PEO has definite advantages over the use of high salt concentrations, where salting-in and salting-out phenomena and specific interaction with both cations and anions complicate the interpretation of results and the extrapolation to well defined, biologically relevant states. (56) To validate the theory of volumetric displacement put forth by Laurent, (57) Hasko *et al.* (58) studied the solubility of plasma proteins at various pH values as a function of PEO concentration and were able to develop

equations which describe the relationship between protein solubility and PEO concentration.

When PEO is used for the fractionation and purification of proteins from human plasma as an alternative to cold ethanol precipitation techniques, it can be removed from these preparations by adsorption chromatography on polystyrene beads. (59) PEO concentrations were reduced by 80 percent in IgG preparations by this procedure. It was determined that the oxyethylene groups of the PEO are involved in the adsorption to the polystyrene Biobeads^{TM} and that this adsorption increases with decreasing mean molecular weight.

Poly(ethylene oxide) has recently been reported to stabilize solutions of dissolved proteins and to prevent their denaturation and aggregation. Thurow and Geisen have demonstrated that insulin solutions can be stabilized and protected from surface-induced adsorption and aggregation by the preadsorption of PEO-PPO-PEO triblock and related copolymers onto hydrophobic surfaces. (60) Suzuki *et al.* similarly used PEO to stabilize IgG solutions and found that the formation of dimers and trimers of IgG was prohibited by the addition of PEO. (61)

Immunologists have recently used PEO to modify proteins and drugs by the covalent attachment of PEO chains to produce a molecule with minimal antigenicity. (62) Attachment of PEO in sufficient quantities to a protein often produces a conjugate which circulates for extended periods in the blood and does not elicit an immune reaction. (63) Abuchowski *et al.* have altered the immunological properties of a number of enzymes and drugs by the covalent attachment of PEO. (64,65,66)

The attachment of PEO to oligopeptides has produced soluble conjugates which enable ^{1}H-NMR conformational studies to be performed. (67) A thorough

knowledge of the conformation of proteins and biologically active peptides is necessary for the understanding of their structure-activity relationships.

Poly(ethylene oxide) surfaces are becoming recognized as exhibiting properties offering an excellent candidate material for biomaterial applications. To date, PEO surfaces which have been used for biomaterials and medical devices applications generally consist of PEO block copolymers. Nagaoka *et al.* prepared hydrogels containing methoxy poly(ethylene glycol) monomethacrylates with PEO side chains of various lengths and investigated their interactions with blood components. (68,69,70) These investigators have shown that the surface mobility of PEO chains is maximal when n, the number of repeat units, approaches 100. They further showed that a PEO graft copolymer (many free ends) is more effective than a network or block system for minimizing the adsorption of blood components including proteins and platelets.

The adsorption of proteins onto a series of oligomers, all containing ethers in the molecules copolymerized with β-hydroxyethyl methacrylate (HEMA), was studied by Lin *et al.* (71) The water content of these copolymers was tested and the adsorption of albumin was studied using radiotracer techniques. It was found that there is an enhancement of albumin adsorption by ether groups which is also found in the copolymers having higher water contents than that of poly(HEMA). However, these investigators did no surface characterization of the copolymer systems and their apparently contradictory results may stem from microdomains of the hydrophobic portions of the system present on the surface.

Matsuda *et al.* have done extensive testing of hydrophilic segmented polyurethanes containing PEO as the soft segment in which the hard segments cluster to form the domain dispersed into the matrix phase of the soft segments. (72) The *in-vitro* blood/material interactions show that both contact phase activation of plasma intrinsic coagulation pathway and platelet adhesion

are much greater for the hard segment analogous polymer than for soft segment versions. The least adsorptional and adhesional behaviors of platelets and plasma proteins were observed in the hydrophilic segmented urethane systems.

Similarly, Merrill and Salzman have observed the platelet compatibility of hydrophilic segmented polyurethanes containing PEO soft segments. (73, 74) According to their studies, amorphous PEO swollen in water appears to interact little, if at all, with proteins including at least some of those relevant to blood. When incorporated into networks having defined surfaces, PEO seems to favor little adsorption of platelets and this adsorption is independent of the material used as a junction of the networks provided this material is not accessible to the proteins or platelets of blood.

1.3 Heparin Background

1.3.1 Structure and Pharmacology

Herapin is a sulfated polysaccharide well known for its anticoagulant and antithrombotic properties. It was discovered by McLean in 1916 (75) but was not introduced into routine clinical use until the 1930's. Heparin is present in numerous animal and human tissues but is found in the highest concentration in the lung and intestinal mucosa, which are used for commercial sources of both animal and human heparins. It is synthesized in the mast cells. The enzymatic steps involved in the biosynthesis of heparin were elucidated by Riesenfeld. (76)

Commercial heparin preparations exist as a population of sulfoglucosamine and hexuronic acid units linked by 1–4 glycosidic bonds to form linear anionic carbohydrate molecules ranging in molecular weight from 3,000 to 40,000 daltons. The main sugars occurring in heparin are: 1) 2-deoxy-2-sulfoamino-α-D-glucose; 2) α-L-iduronic acid 2-sulfate (2-sulfo-iduronic acid); 3) 2-acetamido-2-deoxy-α-D-glucose (acetylglucosamine); 4) β-D-glucuronic

acid; and 5) ∝-L-iduronic acid, in order of their decreasing concentrations. (77) Structures of these sugar units are shown in Fig. 4. The variations in molecular weight coupled with single sugar unit variations lead to the very polydisperse nature of commercial preparations.

It was found that approximately one third of commercial heparin preparations are active in their ability to bind to antithrombin III (AT-III). (78) Even this small fraction is highly polydisperse, ranging in molecular weight from 7,000 to 20,000. A unique tetrasaccharide sequence was found to be present in the active heparin fraction. (79,80) The tetrasaccharide sequence (L-iduronic acid, N-acetylate-D-glucosamine 6-sulfate, D-glucuronic acid, N-sulfated-D-glucosamine 6-sulfate) was found in only 2.6 percent of the molecules present in the inactive fraction, while every molecule in the active population possessed at least one tetrasaccharide sequence. (79) Studies conducted to define the location of the unique tetrasaccharide sequence in heparin have demonstrated that these are located at or near the non-reducing terminus of the heparin chain. (81) Dusulfination of bulk heparin leads to a rapid loss in anticoagulant activity and yet the L-iduronic acid is not sulfated in the tetrasaccharide sequence. (82) There is a strong correlation between the anticoagulant activity and the relative abundance of the unique tetrasaccharide sequence, suggesting that this represents the AT-III binding site. However, because additional properties such as molecular weight, thrombin affinity and charge density can markedly affect the activity of heparin, the molecule must have multiple functional domains. (83, 84)

Other chemical groups are present in the molecular structure of heparin. Amino acids, in particular glycine, cysteic acid, alanine, aspartic acid and serine, have been found (between 0.3 and 2.3 weight percent depending upon the source). (79) These amino acids can be covalently linked to heparin or may

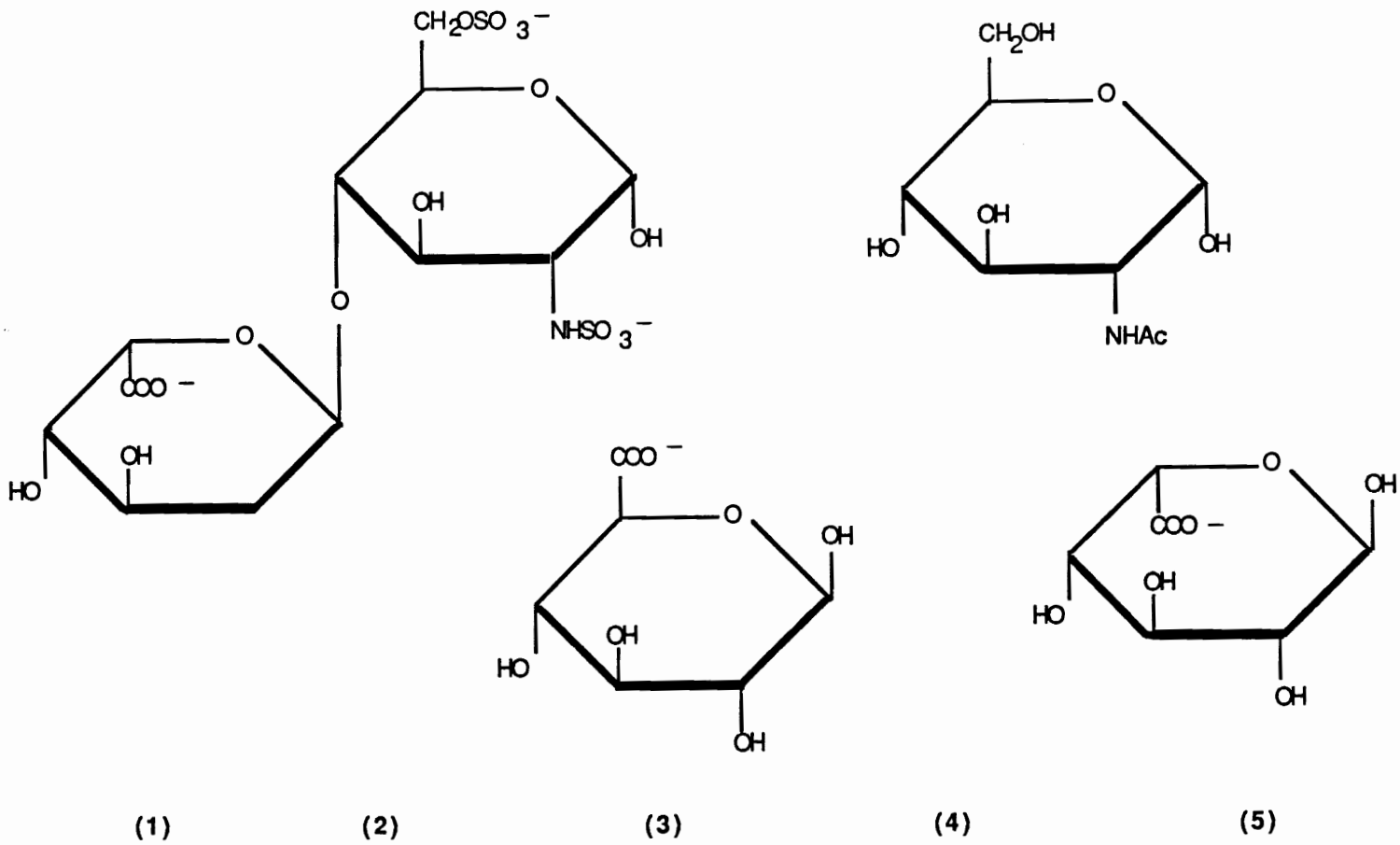

Figure 4. The main sugars found in the heparin molecule which are linked by 1-4 glycosidic bonds. 1) 2-deoxy-2sulfoamino - α-D-glucose; 2) a-L-iduronic acid 2-sulfate (2-sulfoiduronic acid); 3) 2-acetoamido-2-deoxy-α-D-glucose (acetylglucosamine); 4) β-D-glucuronic acid; and 5) α-L-iduronic acid.

simply be ionically bound and represent impurities from the native heparin protein complex.

The anticoagulant effect of heparin is due to its interaction with the proteolytic enzyme, thrombin. The generation of thrombin represents the central event in the coagulation of blood. Its formation proceeds via two pathways, the intrinsic and extrinsic, in which plasma proteins initiate a cascade of sequential reactions. These pathways have been summarized previously and will not be recounted here. (85,86) However, heparin has a variety of interactions with coagulation factors and cofactors including Factor Xa, XIIa, IXa, antithrombins and thrombin. Heparin has been shown to independently induce platelet aggregation and to potentiate platelet release reactions caused by exogenous agents. High molecular weight fractions are apparently more reactive toward platelets and platelet function than low molecular weight fractions. (87) Numerous other pharmacological functions have been reported for heparin which affect the activity of more than 50 enzymes. (88) For example, heparin can trigger the release of lipoprotein lipases from endothelium, adipose tissues and liver, (89) initiate secretion of histaminase from intestinal mast cells, (90) and inhibit secretion of aldosterone resulting in lower adrenal function. (91)

By far the most significant and extensive interaction of heparin is its ability to bind AT-III and thrombin, increasing the inactivation rate of thrombin up to 500-fold. The presence of a reactive serine center on thrombin is crucial to its binding to heparin as demonstrated by studies which artifically block this amino acid. (92) While the exact mechanism of the heparin/AT-III/thrombin reaction is currently unknown, three predominate theories have emerged.

The most popular of these is that heparin binds to the positively charged lysine residues on the AT-III molecule thus forming a heparin/AT-III complex.

This induces a conformational change in the AT-III molecule, rendering the active arginine center more accessible to the thrombin, thus neutralizing it from further interaction with fibrinogen (93,94) (Fig. 5). This would infer that active serine sites on other coagulation proteases would also bind AT-III and that this reaction would be enhanced by the presence of heparin. This was found to be the case for Factor XIIa, (95) Factor IXa, (96) and Factor XIa. (97) However, the reaction with Factor Xa apparently occurs by a different mechanism. (98) This lends more evidence for multiple functional domains on the heparin molecule.

In a second theory of the mechanism of heparin's action, the high binding constant of thrombin with heparin supports the idea that heparin first binds to thrombin, and then as a complex binds to AT-III. However, this mechanism is thought to be of minor importance in the physiological state. (99) The third model, based on the binding constants of AT-III and thrombin, suggests that both these molecules bind to different sites on the heparin molecule and, due to their proximity, an enhancement of the rate of reaction is observed. (100)

Regardless of the exact mechanism, it is evident that heparin works in a catalytic fashion. (101) The initial reaction velocity can be described by the general rate equation for a random-order two reactant, enzyme catalyzed reaction which is mathematically identical to the "template" model. (102) In principle, the template model for the heparin mechanism implies that the binding of thrombin and AT-III to heparin is required for the catalytic activity of heparin. (103,104) This also supports the position that heparin can be released for further AT-III binding after the thrombin-AT-III complex has been formed. (105) It has been found that the binding of thrombin to the heparin/AT-III complex results in the discharge of heparin, leaving the thrombin/AT-III complexes with little ability to bind heparin. The binding affinity of the heparin

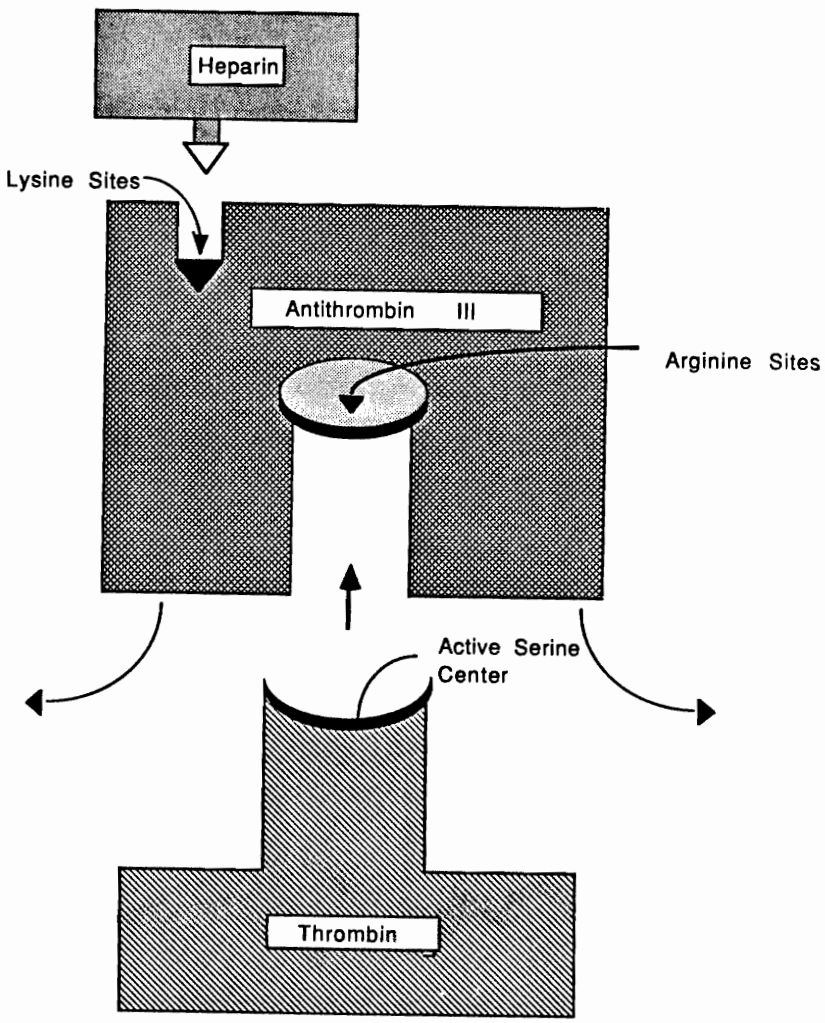

Figure 5. Schematic representation of the mechanism of heparin, antithrombin III (AT-III) and thrombin interaction. Heparin binds to the positively charged lysine residues on the AT-III molecule resulting in a subsequent conformational change in the AT-III molecule. This renders the active arginine center more accessible to the thrombin serine residue facilitating binding.

molecule for AT-III remains unchanged following the release of the thrombin/AT-III complex.

1.3.2 Immobilized Heparin Materials

Due to the numerous pharmacological effects associated with heparin and the high risks involved in long term systemic heparin dosing, efforts have been made to decrease the risk of anticoagulation therapy for patients using biomedical devices in contact with blood. Many investigators have attempted to incorporate heparin and other anticoagulants into or onto the polymeric devices themselves. These have taken a variety of forms, but may be considered in two categories: 1) materials providing a controlled release of heparin at the interface, either by exchange with blood components or by diffusion through the polymer, and 2) materials which have the pharmacon immobilized on the surface. In light of the recent, comprehensive review of the approaches taken by numerous investigators to modify polymers with heparin, (106) a summary of the immobilized herapin surfaces is given in Table I. Some of these approaches have demonstrated promising results.

Part of the difficulty encountered in the testing of these surfaces is due to the complex interactions and protein adsorption reactions which occur. For example, the increased clotting times observed may be a result of heparin leaching from the surface. They may also be attributable to the protein interactions with the highly negative surface. The surface may actually be coated with a layer of adsorbed proteins which act to passivate the material and with time the blood proteins and platelets may never really be in contact with the heparin surface. Many studies have not determined whether the immobilization of heparin through a specific functional group affects the anticoagulant activity of the heparin. It may be that blocking these groups by a

Table I

Covalently Immobilized Heparin Surfaces

Investigators and References	Material Treatment	Comments
Grode (108)	Covalent coupling of a heparin / cyanuric chloride adduct to amino-propyl-triethoxysilane treated silicone rubber.	Produces a permanent heparin surface; effects of forming the heparin / cyanuric complex on the anticoagulant activity were not investigated. Prevented thrombus formation for 6 months.
	Radiation grafting of polystyrene, chloromethylated, then treated with heparin /cyanuric chloride adduct.	Also permanent surface and increased whole blood clotting times
Merrill (109)	Glutaraldehyde crosslinking of heparin to poly(vinyl alcohol).	Permanent crosslinked heparin surface that adsorbs coagulation factors; Decreased platelet function; No investigation of heparin crosslinking effects; No release of heparin from surface detected.
Lagergren (110)	Cationic surfactant adsorption ontopolypropylene followed by ionic binding of heparin and subsequent crosslinking with glutaraldehyde.	No clotting observed after 3 hours of blood contact; Shunts were viable for 12 hours; Leaching of ~3% of heparin from surface during initial 10 hours; Clotting times were a function of degree of crosslinking; Improved platelet compatibility.
Schmer (111)	Direct coupling of heparin to cyanogen bromide activated agarose.	Less heparin immobilized onto the spacer arm than with other methods used.

Table I (continued)

Investigators and References	Material Treatment	Comments
Schmer (111)	Coupling of heparin to putrescine on putrescine derivatized agarose.	Coupling was via primary amine groups on heparin Greater amounts of heparin than on the direct coupling method; Increased ability to bind antithrombin III.
	Coupling of heparin to amino caproyl to amino caproyl derivatized agarose via carbodiimide.	Indistinguishable from above method.
Labarre (112,113)	Heparin- methyl methacrylate copolymer	Dose related anticoagulant activity observed due to copoymer consisting of heparin core with p-MMA chains extending out. Increased clotting times result of ionically bound heparin leaching from surface.
Danishefsky (114)	Heparin coupled to agarose via an amino-ethyl spacer arm.	No leaching of heparin upon storage; Saturation of heparin binding sites and significant binding of Factors IX, XI, and antithrombin III.
Sefton (115)	Heparin coupled to poly(vinyl alcohol) via acetal bridge of various aldyhydes,then applied to hydroxylated styrene-butadiene -styrene block copolymer.	Insignificant leaching of heparin; Increased partial thromboplastin and recalcification times observed; High shear rates however, produced no differences between heparin surfaces and controls; Evidence for binding of thrombin to heparin contrary to popular belief of heparin mechanism.

Table I (continued)

Investigators and References	Material Treatment	Comments
Muria (116)	Coupling of heparin to cyanogen bromide activated sepharose.	Greatly prolonged plasma recalcification times; Indication that using amine groups of heparin renders it incapable of interacting with antithrombin III.
	Coupling of heparin to cyanogen bromide activated poly(hydroxy-ethyl methacrylate).	Greatly prolonged recalcification times; Indication that using amine groups of heparin renders it incapable of interacting with antithrombin III.
	Coupling of heparin to cyanogen bromide activated poly(vinyl alcohol).	No indication of prolongation of recalcification times. Indication that using amine groups of heparin renders it incapable of interacting with antithrombin III.
Larsson (117)	Partially degraded fragments of heparin coupled to polyethylene-amine activated poly(ethylene).	Surface is stable; Heparin fragments capable of reacting with thrombin; Increased whole blood clotting times observed.
Ebert (118)	Heparin coupled via various length alkyl spacer groups to diaminoal-kane derivatized sepharose, and cellulose, agarose.	Increasing activated partial thromboplastin times with increasing spacer arm length; no adverse inter-action with platelets.
Heyman (119)	Heparin coupled via various length alkyl spacer groups to polyurethane.	Heparin retained its activity towards thrombin and Factor Xa but caused only slight increase of partial thrombo-plastin times; No significant release of heparin from surface; Decreased thrombus formation in implanted shunts.
Lindberg (120)	Crosslinked heparin with glutar-aldehyde stabilized by hexadecylamine.	Inhibition of thrombin activity observed; Minimal platelet adhesion.

reaction similar to those used for the immobilization process also results in loss of anticoagulant activity. Several of the heparinized polymers involve crosslinked herapin, and the effect of this on heparin activity has not been clearly established.

CHAPTER 2

METHODS

2.1 Derivatization of Poly(ethylene oxide)

Four different derivatives of PEO of two molecular weights were synthesized using modifications of the procedure developed by D. Gregonis (personal communication) (Fig. 6): PEO-bis isocyanate, PEO-bis isothiocyanate, PEO-bis chloroformate, and PEO-bis thiochloroformate. Each of these derivatives was synthesized starting with PEO molecular weights of 6,000 and 18,000 (Polysciences). The PEOs were dried under vacuum overnight prior to use.

2.1.1 Isocyanates

The PEO was dissolved in tetrahydrofuran (THF) under nitrogen. A 20 percent excess of 2.2 M n-butyl lithium (Aldrich Chemical) in hexane was added and stirred for 1 hour. A 20 percent excess of tosyl chloride (Aldrich Chemical) was added to the solution and the reaction mixture stirred for 3 days (Step I in Fig. 7).

The lithium salt of cysteamine was prepared (Step II in Fig. 7) by adding equivalent amounts of n-butyl lithium to cysteamine (Aldrich Chemical) in THF dropwise to the solution and stirring overnight. The PEO-tosylate solution was added to the cysteamine salt and the mixture stirred for 3 days (Step III in Fig. 7). THF was removed under reduced pressure and toluene was added to dissolve the residue. The toluene was then washed with 40 percent KOH four times. The toluene was removed under reduced pressure and the amine capped PEO was

Four Derivatives of Poly(ethylene Oxide)

1. PEO - BIS ISOCYANATE

2. PEO - BIS ISOTHIOCYANATE

3. PEO - BIS CHLOROFORMATE

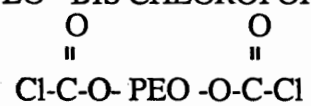

4. PEO - BIS THIOCHLOROFORMATE

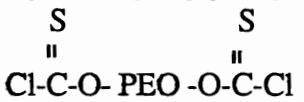

Figure 6. The four derivatives of poly(ethylene oxide) synthesized for immobilization onto quartz substrates. The bifunctional molecules permit attachment to the substrate with the extension of the other free reactive end group out from the surface for subsequent reaction with heparin.

I.

$$H\text{-}(OCH_2CH_2)_n\text{-}OH + 2\ n\text{-butyl lithium} \longrightarrow Li^+\ ^-(OCH_2CH_2)_n\text{-}O^-\ Li^+ + CH_3CH_2CH_2CH_3\ \uparrow$$

$$Li^+\ ^-(OCH_2CH_2)_n\text{-}O^-\ Li^+ + CH_3C_6H_4SO_2Cl \longrightarrow$$

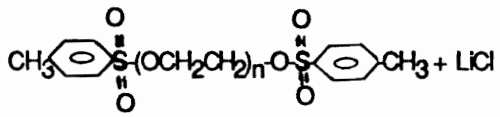

PEO di-tosylate

II.

$$HSCH_2CH_2NH_2 + n\text{-butyl lithium} \longrightarrow Li^+\ ^-SCH_2CH_2NH_2 + CH_3CH_2CH_2CH_3\ \uparrow$$

III.

$$PEO\ \text{di-tosylate} + 2\ Li^+S^-CH_2CH_2NH_2 \longrightarrow H_2NCH_2CH_2S\text{-}(OCH_2CH_2)_n\text{-}SCH_2CH_2NH_2 + 2\ TsOH$$

PEOdi-amine

IV.

$$PEOdi\text{-}amine + COCl_2 \longrightarrow O{=}C{=}N\text{-}CH_2CH_2\text{-}S\text{-}(OCH_2CH_2)_n\text{-}S\ CH_2CH_2N{=}C{=}O + HCl$$

PEO-bis isocyanate

$$H_2NCH_2CH_2S\text{-}(OCH_2CH_2)_n\text{-}SCH_2CH_2NH_2 + CSCl_2 \longrightarrow$$

$$S{=}C{=}N\text{-}CH_2CH_2\text{-}S\text{-}(OCH_2CH_2)_n\text{-}S\ CH_2CH_2N{=}C{=}S + HCl$$

PEO-bis isothiocyanate

V.

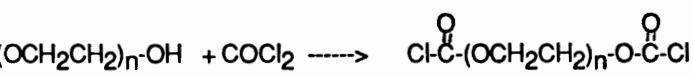

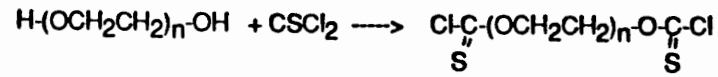

Figure 7. The chemistry involved in the synthesis of the four derivatives of poly(ethylene oxide).

reprecipitated three times in diethyl ether (cold) from a minimum amount of methylene chloride.

To determine the degree of conversion of PEO to diamino-PEO, the amine capped PEOs were titrated using 0.01 M perchloric acid (Fisher Scientific) and acetic acid anhydride (Fisher Scientific). Potassium acid phthalate (Mallinckrodt) was used as a standard in the titration. The conversion was determined to be 85 percent.

The amine capped PEO's were then reacted with a 100 percent excess of phosgene in toluene (12 percent) (MCB) and stirred for 2 hours (Step IV in Fig. 7). The excess phosgene was removed by distillation and the toluene removed by rotoevaporation. In the case of the thiocyanate, a 100 percent excess of thiophosgene in toluene (Aldrich Chemical) was used instead of phosgene. Infrared spectra of each of the derivatives were run (Figs. 8a and 8b). All derivatives were stored under nitrogen until used to prevent hydrolysis of the end groups.

2.1.2 Chloroformates

The chloroformate derivatives were prepared by dissolving PEO (hydroxyl terminated) in toluene (Step V in Fig. 7) to which was added a four times excess of phosgene or thiophosgene. The reaction was accomplished by stirring overnight and heating to reflux, then removing the solvent until the solution was no longer acidic. The toluene was removed by rotoevaporation. Infrared spectra were run to determine any remaining hydroxyl from the OH stretching region at 3333 cm^{-1} (Figs. 8c and 8d). These derivatives were stored under nitrogen until used.

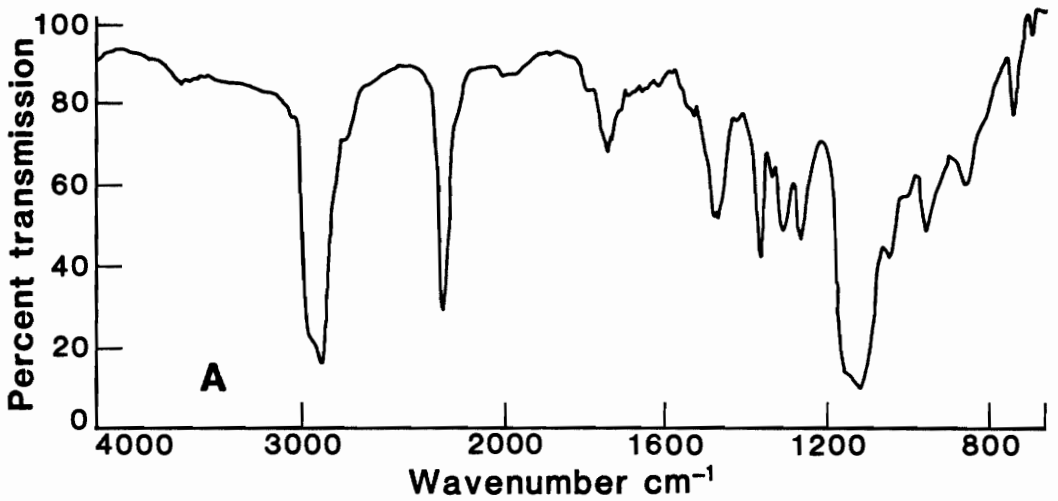

Figure 8. Infrared spectrum of poly(ethylene oxide) derivatives. a. bis-isocyanate MW 6,000; b. bis-isothiocyanate MW 6,000; c. bis-chloroformate MW 6,000; d. bis-thiochloroformate MW 6,000.

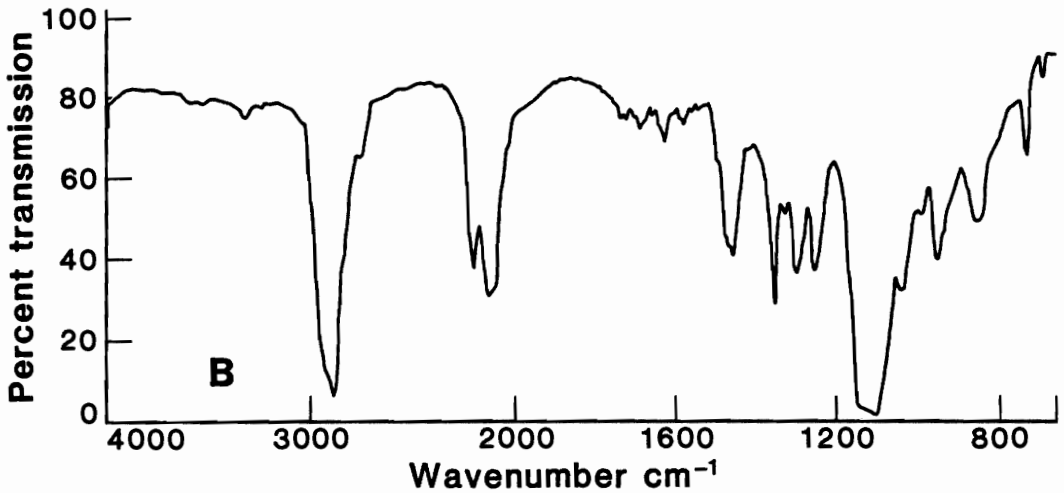

Figure 8. (continued)

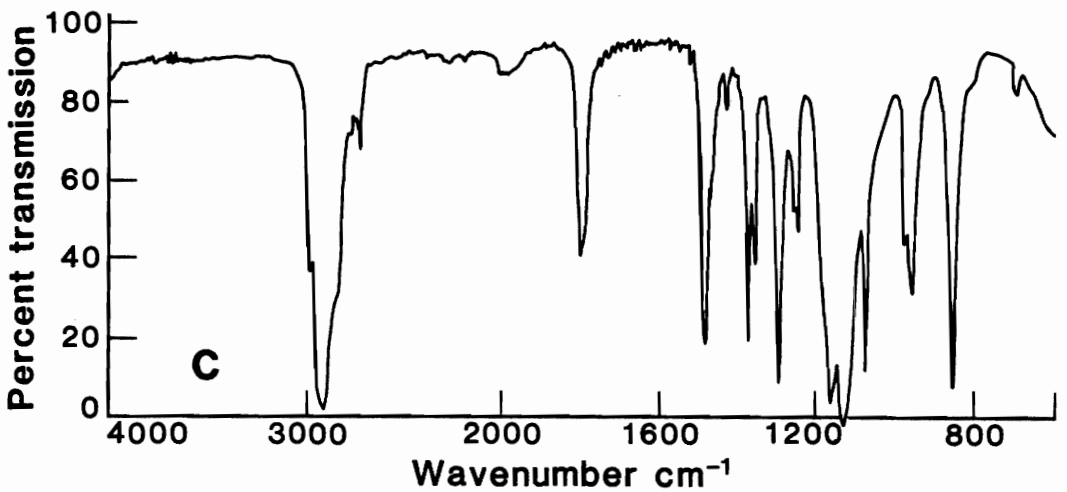

Figure 8. (continued)

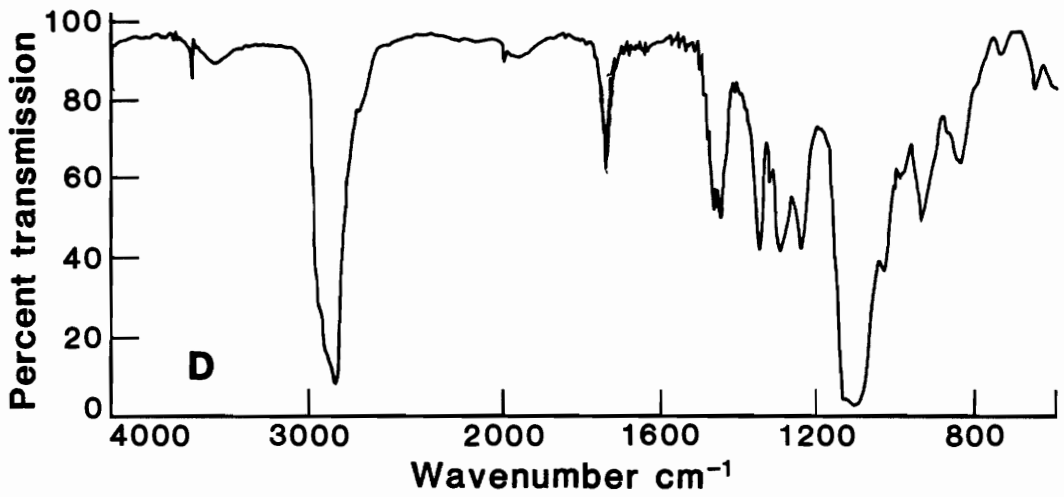

Figure 8. (continued)

2.2 Quartz Substrate Preparation

2.2.1 Cleaning

The quartz slides (7 x 10 mm, ESCO Products) were prepared for PEO immobilization by soaking in a dichromate-sulfuric acid solution (25 ml Monostat Chromerge chromic acid in 4.1 kg of concentrated sulfuric acid) at 80° for 20 minutes. The slides were then rinsed with distilled water four times for 3 minutes each, rinsed four times in ethanol and radio frequency glow discharged at 35 watts (Plasmod, Tegal) under 200u pressure oxygen for 3 minutes. The slides were then heated to 100°C overnight to remove any residual water. Wilhelmy plate contact angle and X-ray photoelectron spectroscopy spectra (XPS) were obtained to determine any residual contamination. If the carbon content of the XPS spectra of clean surfaces exceeded 12 percent, or if the contact angle was greater than 0° and/or demonstrated hysteresis, the slides were not used.

The quartz beads were 50u Unispheres™ (Ferro Corp). These were placed in the same dichromate-sulfuric acid solution and stirred for 20 minutes. They were then rinsed extensively with distilled water by filtering through a buchner funnel until no remaining acid color could be detected visually. They were then rinsed with an additional 16 liters of distilled water through the funnel. The beads were dried overnight at 100°C. To determine cleanliness, XPS spectra were run by pressing the beads into indium foil and scanning for carbon and sulfur remaining from the sulfuric acid.

2.2.2 Vapor Phase Silanization

All glassware used for the silanization was oven dried (100°C) following the cleaning procedure. The clean quartz slides were vapor phase silanized immediately after removing from the 100° oven by placing them in a vapor

chamber through which 10 ml γ-aminopropyl-triethoxysilane (APS) (Aldrich Chemical) in 250 ml dry p-xylene (Fisher Scientific) was refulxed for 12 hours. The APS had been recently distilled to remove any dimer or trimers and stored under nitrogen at 4oC. They were then refluxed for an additional 12 hours in toluene dried over molecular sieve, rinsed to remove any unbound APS. XPS analysis was done to determine the extent of silane coverage (see Section 3.1).

2.2.3 Silanization of Quartz Beads

The silanization of the quartz beads was done in a round bottom flask fitted with a nitrogen bubbler, a condenser and thermometer. The beads were suspended in dried p-xylene by use of a stir bar and the nitrogen bubbler. After perfusion with nitrogen for 2 hours, the nitrogen was turned off. Ten ml distilled APS were then added to the flask and the mixture was refluxed for 12 hours. After removing the APS/xylene mixture and rinsing the beads with toluene three times, the beads were then refluxed with toluene for an additional 12 hours. XPS analysis was done to determine the extent of silane coverage.

2.3 Poly(ethylene oxide) Immobilization

2.3.1 Poly(ethylene oxide) Coupling to Quartz Plates

The conditions for the immobilization of the PEO derivatives were established from experiments to determine the optimum time and concentration. Initially, PEO derivatives of various molecular weights and concentrations were dissolved in methylene chloride, and then added to the silanized slides in staining jars. In order to minimize the formation of loops by the PEO coupling via both ends, the highest concentration of PEO solution was used. The results indicated that raising the PEO solution concentration greater than 3 percent did not increase the PEO coupling to the surface. These early coupling experiments demonstrated that some of the reactive end groups, particularly the

chloroformates, had been hydrolyzed before coupling to the silane coated slides. It was determined that the hydrolysis was due to the condensation of moisture from the air during the evaporation of the methylene chloride.

Therefore, the PEO derivatives were dissolved in chloroform, which is less volatile and the coupling efficiency was again determined. In the presence of atmospheric moisture, however, the end groups were still being hydrolyzed prior to coupling.

In order to prevent this problem, the coupling reactions were performed in a nitrogen glove bag. All glassware and solvents were purged for 2 hours with nitrogen prior to beginning the reaction. The final reaction conditions were a 1.5 percent (w/v) solution for the 6,000 molecular weight derivatives and 3 percent (w/v) for the 18,000 derivatives. This was done to normalize the molar ratio of end groups available for the reaction in both molecular weights. From the results of the coupling efficiencies as a function of time, it was determined that a minimum of 12 hours coupling time be used (Fig. 9). The reaction was left overnight, after which the slides were rinsed with methylene chloride three times to remove the unbound PEO. The reaction involved in the coupling of the four derivatives is given in Fig. 10. Because of early experiments indicating instability of PEO, a large brown cardboard box was placed over the entire nitrogen glove bag assembly in an attempt to exclude room light which has been indicated as a potential cause of chain scission. (121) The reactive end groups on the PEO chains not involved in the coupling reaction were hydrolyzed with water before analysis. However, no water was used if the slides were to be used for subsequent heparin immobilization.

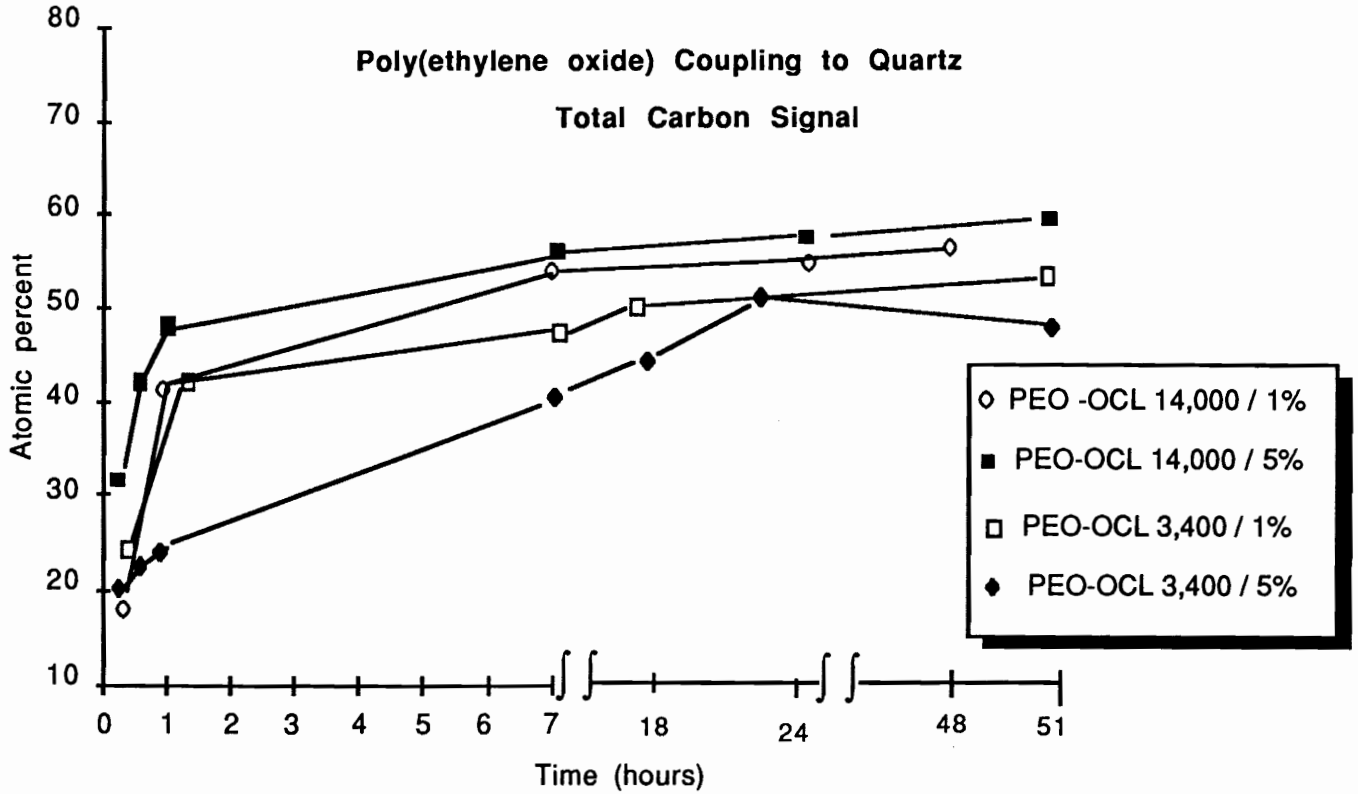

Figure 9. The elemental percent of carbon of the PEO immobilized surfaces resulting from reaction in 1 percent and 5 percent solutions for various lengths of time.

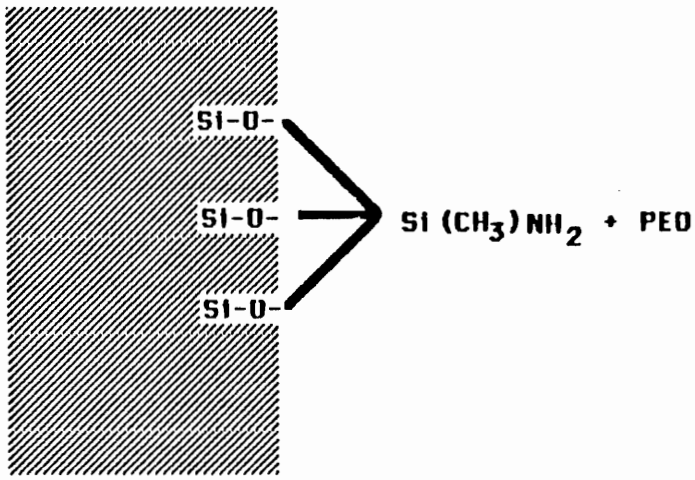

1.  $-NH-\overset{O}{\overset{\|}{C}}-NH-(CH_2CH_2O)_n-CH_2-CH_2-N=C=O$

2. 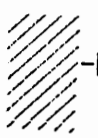 $-NH-\overset{S}{\overset{\|}{C}}-NH-(CH_2CH_2O)_n-CH_2-CH_2-N=C=S$

3. 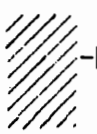 $-NH-\overset{O}{\overset{\|}{C}}-O-(CH_2CH_2O)_n-\overset{O}{\overset{\|}{C}}-Cl$

4. 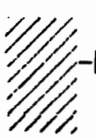 $-NH-\overset{S}{\overset{\|}{C}}-O-(CH_2CH_2O)_n-\overset{S}{\overset{\|}{C}}-Cl$

Figure 10. The reaction involved in the coupling of the four derivatives of PEO to the silanized quartz substrate. The amine of the silane couples to the functionalized PEO. Using a large excess of PEO minimizes the possibility of the formation of loops resulting from both ends of the PEO coupling to the surface.

2.3.2 Poly(ethylene oxide) Coupling to Quartz Beads

Coupling of the PEO derivatives to the quartz beads was achieved using an apparatus similar to the APS silanization described above. The silane treated beads were suspended in methylene chloride by using a magnetic stir bar and nitrogen bubbler. The PEO derivatives were added to this mixture so as to make 1.5 percent and 3.0 percent solutions of the 6,000 and 18,000 derivatives, respectively. The flasks were covered with aluminum foil to exclude room light and left overnight. They were then rinsed three times with methylene chloride to remove the unbound PEOs. Those beads not used for further reaction with heparin were then removed from the flask and rinsed with ethanol and distilled water.

2.4 Heparin Immobilization

2.4.1 Coupling to Quartz Plates

The PEO reacted slides were taken directly from the PEO immobilization reaction vessels and rinsed once with methylene chloride. This procedure was conducted in the nitrogen glove bag in order to prevent end group hydrolysis. The quartz slides were then immersed in a saturated solution of bovine intestinal mucosa sodium heparin (Diosynth) in formamide (MCB) with 1 percent pyridine added as a catalyst. The heparin was used as received. The heparin solution was prepared one day prior to use and stored under nitrogen to eliminate any possible moisture contamination. The reaction was left for 3 hours. The slides were withdrawn from solution and rinsed in ethanol, water, ethanol and methylene chloride for drying. They were stored under vacuum for further drying until analysis.

The coupling of the heparin is presumed to occur through the hydroxyl and the relatively few amine groups of the heparin molecule and should be

instantaneous. Of course, any carboxyl groups on the heparin would be expected to react with the PEO derivatives, and this would presumably be accomplished faster than reaction with the hydroxyl groups due to their higher reactivity. However, the resultant anhydride type linkage would be unstable and rearrangement to the urethane or urea coupling would be expected to occur. For this reason, the reaction was allowed to run for 3 hours.

2.4.2 Coupling to Quartz Beads

The immobilization of heparin to the quartz beads was achieved by transferring the PEO coupled beads to another round bottom flask in the nitrogen glove bag. The saturated formamide/heparin solution with 1 percent pyridine, which had been stored under nitrogen overnight, was then added to the flask and immediately fitted with the nitrogen bubbler and stir bar. This flask was left for 3 hours, after which the beads were rinsed three times with ethanol, twice with distilled water, and once with methylene chloride for drying. The beads were then stored under vacuum for further analysis.

2.5 Quantitation of Immobilized Heparin

2.5.1 Tritium Labeling of Heparin

The procedure used for the tritium labeling of heparin was a modification of that used by Dottavia-Martin *et al.* (122) This procedure uses sodium cyanoborohydride as the reducing agent because it is stable in aqueous solutions and may be used at pH 7.0. Briefly, the procedure entailed mixing 300 uCi ^{3}H-formaldehyde (New England Nuclear) diluted with 2.0 ml double distilled water and 1 gm heparin (Diosynth) dissolved in 2.0 ml double distilled water. This mixture was diluted with an additional 10 ml water and then 0.7 gm sodium cyanoborohydride was added and left stirring for 24 hours. The heparin was then precipitated out of solution using 200 ml ethanol and freeze dried. The labeling

procedure used results in a labeled methyl group coupled to the free amines. The specific activity of heparin was determined by preparing five solutions of known amounts of heparin, adding scintillation cocktail to make 10 ml and counting on a Beckman LS 7500 scintillation counter. The background of 47.3 dpm was subtracted from all samples. The specific activity of the labeled heparin was determined to be 63,530 $\pm$ 1,042 dpm/mg. The ^{3}H-heparin was stored at 4°C until used.

2.5.2 Quantitation Procedure

Quantitation of the immobilized heparin was performed by reacting PEO-bis isocyanate derivatized (MW 6,000 and MW 18,000) beads with a saturated solution of ^{3}H-heparin in a formamide/pyridine solution similar to that described in Section 2.4.2 for 3 hours. Various quantities of these labeled beads were weighed out, total surface area calculated and mixed for 4 hours with minimum amounts of concentrated NaOH in order to hydrolyze the heparin from the surface. Aliquots of the NaOH were withdrawn and counted after addition of enough scintillation cocktail to make 10 mls. Triplicate samples of each bead solution were used. Controls consisted of clean quartz beads and PEO-bis isocyanate without heparin. For each molecular weight of the PEO used, the quantity of heparin was determined per unit surface area.

2.5.3 Heparin Depletion From Surface

In order to determine if heparin was leaching from the surfaces used for the activity tests, two different sets of heparin reacted beads were tested. The first group was the beads which were rinsed in the same manner as those used in the initial whole blood clotting tests which failed to produce clots even after 2 hours. These beads were washed repeatedly with PBS, each rinse being

subsequently counted. Typically, after the eighth washing with 10 ml PBS no more heparin was detected.

The method used for the second group of beads was ultimately determined to be the method of choice in the whole blood clotting tests. This procedure involved soaking the beads in PBS for at least 2 hours, then rinsing three times with distilled water and drying. These beads were then rinsed repeatedly in the same manner as those above. All rinses were counted. Even after the first rinse, no heparin was detected in solution, indicating no leaching from the surface.

2.6 Radiolabeling of Bovine Serum Albumin and Antithrombin III

The method used for the iodination of protein for quantitative analysis of protein adsorption was a modification of the Chloramine T method, originally developed by Greenwood *et al.* (123) and modified by Chuang. (124) Briefly, this involves the iodination of the tyrosine residues present in the protein molecules using ^{125}I-sodium iodide. A commercial Chloramine T kit was purchased from Amersham Corp. and 500 uCi of ^{125}I-sodium iodide per 100 ug of protein were used. The proteins used were bovine serum albumin Fraction V (Sigma Chemical) and Antithrombin III. The AT-III was the generous gift provided by Dr. Wickerhauser of the American Red Cross. Both proteins were used as received and rehydrated in PBS. Fifty ul of a chloramine T solution (40 mg/10 ml water) were added to the protein solution and mixed gently for one minute. Fifty ul of a sodium metabisulfite (SMB) solution (48 gm/10 ml water) were added to stop the reaction. Removal of the free ^{125}-I from the labeled protein was done according to procedures described in (124) using plastic mini-columns which had the reservoir cut off, allowing solution to flow out the bottom. The tube was packed with approximately 1.3 ml of a thick slurry of Sephadex G-25 (Sigma)

which had been equilibrated for 24 hours, and centrifuged piggy-back in a 12 x 75 cm plastic tube at 400 rpm for 1 minute.

The effluent was tested for the presence of free ^{125}-I after separation with the following procedure: 45 ul PBS, 5 ul ^{125}-I protein, and 50 ul TCA solution were added to column 1; column 2 contained 95 ul PBS and 5 ul ^{125}-I protein. These were centrifuged for 10 minutes at 10,000 rpm. Five ul of both control sample and supernatant of the precipitated sample were removed and counted. The ratio typically showed that after separation, greater than 95 percent of the ^{125}-I was bound to the protein. The approximately 5 percent free ^{125}-I was presumed to not irreversibly adsorb to the surfaces and was accounted for in the quantitation by reducing the total adsorbed count by 5 percent. This may be an invalid assumption, particularly for the PEO surfaces which may be capable of complexing free iodide. This will be discussed later in the results of the protein adsorption experiments.

Efficiency of labelling and specific activities were determined. The specific activity of the BSA was found to be about 1.17 uCi/ug and that of the AT-III, 0.92 uCi/ug. The labeled protein was stored at 4°C until used. Each sample was counted twice in a ^{125} I-gamma well counter (Beckman) using 1 minute counting times. Small aliquots of labeled protein were added to unlabeled protein of known concentrations immediately prior to the adsorption experiments.

2.7 Characterization

2.7.1 X-Ray Photoelectron Spectroscopy

Photoelectron spectroscopy is very surface sensitive, analyzing the first 50 -100 A of a polymer surface. It was chosen as the primary means of characterization of the PEO and PEO/heparin surfaces because of its

quantitative abilities, the ease of differentiation of functional groups, and elemental analysis. To analyze the polymer surfaces, the samples are placed under high vacuum (10-9 torr), and bombarded with photons from a monochromatic X-ray source. The instrument used in this study was a Hewlett Packard 5950B spectrometer equipped with a monochromatic Al k α 1,2 source at 1487 ev, with anode power of 800 watts. An electron flood gun operating at 0.6 mA supplied a source of low energy electrons to compensate for charging of the sample. Samples of the quartz plates and beads from every reaction were analyzed. Carbon 1S, oxygen 1S, nitrogen 1S, silicon 2S and sulfur 2P spectra were taken and normalized by their Scofield cross sections. (128) Data were stored on a Hewlett Packard 9845 computer which allowed for data analysis. Percent elemental composition of the surfaces was determined. A curve fitting routine using a least squares fit was applied to the carbon 1S spectra of the PEO surfaces in order to differentiate the aliphatic, ether, and carboxylic carbon species on the surface. It was assumed that all ether carbon detected from the surface was due to the PEO.

XPS spectra were also obtained on heparin powder and underivatized PEO as received from Polysciences, Inc.

2.7.2 Variable Angle XPS

Variable angle XPS was run on the APS and PEO coupled slides to determine thickness and homogeneity of the surface. Photoelectron take off angles were varied from 10 - 85°. Using models for both a uniform overlayer and patchy overlayers of varying thicknesses, these data were fit to the appropriate equations. (125)

2.7.3 Wilhelmy Plate Contact Angle

Contact angle measurement by the Wilhelmy Plate method (126) provides both advancing and receding angles on either dry or hydrated samples. The apparatus used consisted of a Cahn electrobalance supported above a beaker of 2X distilled water. A thin thread was connected to the electrobalance which was used to support the test material as it is submerged and withdrawn from the beaker of water. The beaker was raised and lowered at 40 mm/minute. The sample chamber was maintained at 30 percent relative humidity and 21°C. The angles were determined from the following equation:

$$\text{measured force } F_m = mg + \rho\gamma + Pg\cos\theta - V\rho g$$

or

$$\cos\theta = \frac{F_m - mg + V\rho g}{\rho\gamma}$$

where

F_m is the mass of slide as measured with electrobalance;

g is the local gravitational force (979.3 dynes/g in Salt Lake City);

P is the perimeter of the slide;

γ is the surface tension of wetting liquid (water = 72.6 dynes/cm at 20°C);

V is the volume of immersed sample at a particular depth, and

ρ is the density of wetting liquid (water = 0.998 g/cc at 20°C).

All treated slides were characerized using this method before and after various periods of hydration in PBS. Slides soaked in PBS were rinsed with distilled water and air dried prior to determining contact angle. However, it was found that the PEO reacted slides were not giving reproducible results presumbly because of some noncovalently bound polymer coming off. This will be discussed in Section 3.2.

2.8 Protein Adsorption Studies

The adsorption of proteins from solution was determined by two methods. Initially, experiments using Total Internal Reflection Fluorescence Spectroscopy (TIRF) were done in hopes that conformational information of the proteins interacting with the immobilized heparin could be obtained. However, problems inherent to the TIRF technique, which at that time had not yet been solved, precluded extensive experimentation with this technique. The experiments which were done using TIRF were not quantifiable* and for this reason, protein adsorption properties of the PEO and PEO/heparin surfaces were measured using ^{125}I-labeled proteins.

2.8.1 Total Internal Reflection Fluorescence Spectroscopy

Total internal reflection is a technique which takes advantage of the standing evanescent wave resulting from the superposition of incident and reflected radiation at a solid/liquid interface. Complete reviews of this phenomenon have been published and will not be discussed herein. (127) Let it suffice that internal reflection is dependent upon the refractive indices of the two media, the incident angle of radiation, and the amplitude of the electric field. The evanescent wave propagates perpendicular to the interface and decays exponentially into the less dense medium. In this way, information about the molecules at or near the interface can be obtained. Hirschfeld was the first to introduce the use of this technique using solid/liquid interfaces in the fluorescent mode which requires the presence of fluorescent species at the interface. (129)

---

*The TIRF method can now be used for quantitative studies; the quantitation method was developed too late to be used in this thesis. (128)

In the experiments done here, the intrinsic fluorescence of the tryptophan and tyrosine residues of antithrombin III (of which there are six) and other blood proteins were excited at 280 nm and the emission collected at right angles to the interface at 330 nm. A schematic diagram of the apparatus used is given in Fig. 11. The excitation beam of the broad band 150 watt xenon high pressure lamp (ILC Technology) was focused onto the entrance slit of an excitation monochromator (H10-UV, Instruments SA). The narrow band light was collimated with a 10 cm focal length UV lens (Oriel) and directed through a beam area limiting aperature (Model 1D 1.5, Newport Research Corp.). The beam struck at right angles to one face of a fused quartz dove-tailed prism (Harrick Scientific) such that it struck the optical interface at a 70° angle. This is greater than the critical angle required for total internal reflection. Coupling between the prism and quartz slides prepared as described above was facilitated by use of glycerol. The reflected beam was discarded.

The fluorescence emission was collected through the quartz prism and directly entered the emission monochomator (HR 640, instruments SA) and detected by a photomultiplier tube (Hamamatsu, Ortec model 9210 holder). A preamplifier/discriminator unit (model 9302, Ortec) was used to amplify the signal and to reject low noise signals. A photon counter (model 9315, Ortec) displayed the signal digitally, then converted it to a continuous analog signal (D/A model 9325, Ortec) and displayed the data on a strip chart recorder (model 48, Pharmacia).

The flow cell design is shown schematically in Fig. 12. It is a modification of an earlier design described by Van Wagenen *et al.* (130) The modifications involved changing the entrance and exit ports to point sources and an elliptical rather than rectangular flow volume was demonstrated to exhibit improved laminar flow by dye flow studies. The gasket material creating the 0.8 ml

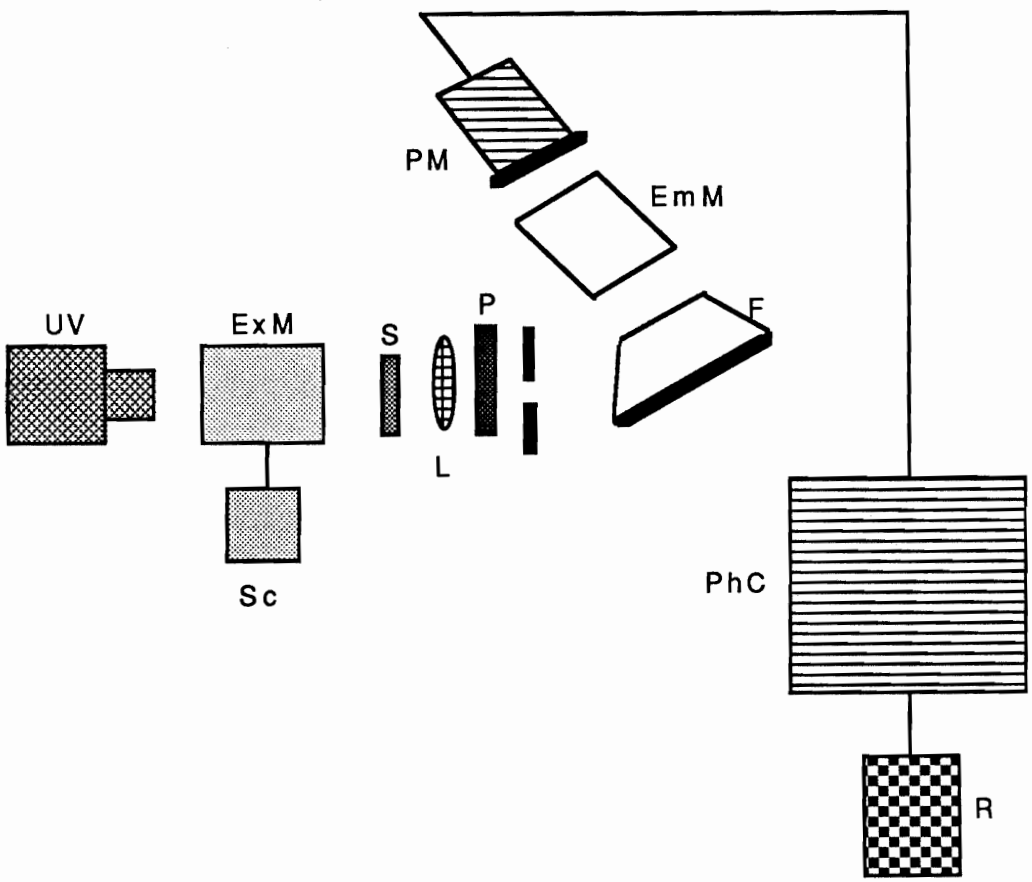

Figure 11. Schematic of the TIRF apparatus. The components are (UV) UV excitation light source; (ExM) excitation monochromator; (S) shutter; (L) collamating lense; (P) polarizer; (F) flow cell; (EmM) emission monochromator; (PM) photomultiplier tube; (PhC) photon counter; and (R) recorder.

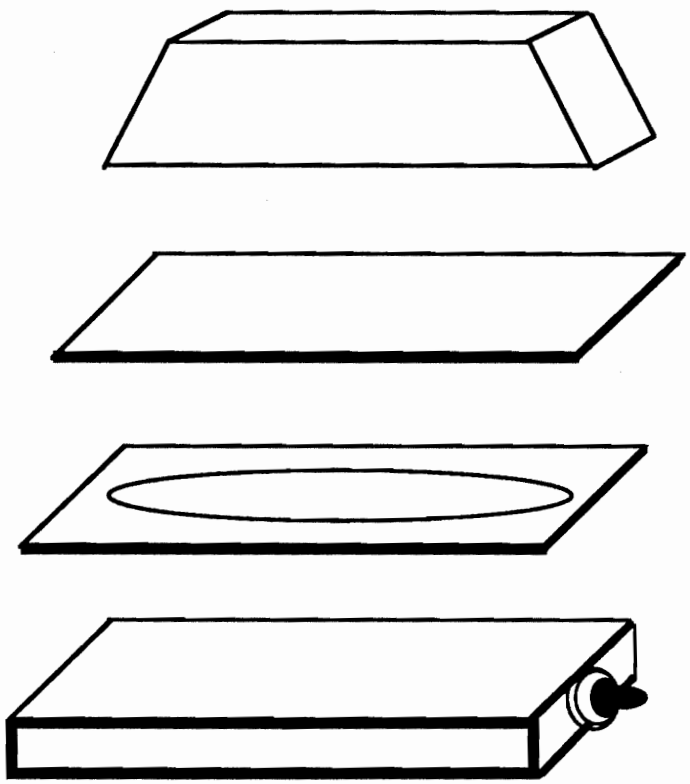

Figure 12. Components of the TIRF flow cell. The derivatized quartz slide was optically coupled to the quartz prism with glycerol. Flow volume created by the silastic gasket was 0.8 ml.

sample volume was 0.05 cm Silastic^{TM} which sealed the prepared quartz plate to the anodized aluminum flow cell. Threaded tubing connectors inserted to the base at the ports provided a means for connection of 1.57 mm 1D polyethylene tubing (Intramedic, Clay Adams). The exit port lead to a waste container. The inlet port tubing was connected to a three-way stopcock which was connected to syringe held in a syringe pump (341, Sage Instruments). The priming volume of the system was approximately 2.5 ml. The flow cell/quartz prism assembly was mounted flat against the aperture of the emission monochromator.

Transmission spectra were also taken of the proteins in the presence and absence of concentrations ranging from 5×10^{-2} to 5×10^{-6} M PEO in order to determine the occurance of fluorescence quenching by the PEO. This was done by focusing the incident beam perpendicular to a 1 cm path length cell and collecting at right angles as previously described.

The flowing experiments consisted of manually injecting a series of tryptophan solutions, of varying concentrations, into the flow cell and measuring the fluorescence emission. This was followed by a phosphate buffered saline (PBS) flush, after which the fluorescence was again measured. Tryptophan has been shown not to adsorb to clean quartz surfaces and was used as an external standard to quantitate the experiments. Following the wash out of the tryptophan solution, which was monitored by a return of the signal to background levels, a 0.25 mg/ml solution of AT-III in PBS was injected. The concentration of the protein solutions was determined by UV absorbance using 6.5 ml mg^{-1} cm^{-1} for the extinction coefficient. The initial flow rate was 15 ml/minute for 1 minute in order to fully fill the flow cell and to minimize diffusion problems. After the first minute, a reduced flow of 1 ml/minute was continued for 1 hour. During the first 10 minutes of adsorption, the signal was counted for 1 second intervals. After the first 10 minutes an excitation shutter was closed to

reduce any UV degradation of the protein and opened only to obtain several 1 second counts at 5 minute intervals. At the end of the 1 hour adsorption period, the signal was measured and a 20 ml bolus injection of PBS was used to flush out the bulk volume. PBS was then allowed to flow at 1 ml/min for 30 minutes after which the signal was recorded. It was found that after 30 minutes the decrease of the adsorbed protein signal was minimal. Following this, a 0.50 mg/ml solution of AT-III in PBS was similarly injected and allowed to adsorb for 1 hour. A buffer flush followed and signals recorded. The next step was the adsorption of a 1:10 dilution of a pooled human plasma (12 donors) in an identical flow scheme. Similarly a buffer flush terminated the adsorption after 1 hour. This adsorption scheme, shown schematically in Fig. 13, was used for clean, APS, PEO, and PEO/heparin surfaces. Spectral scans were taken from 270 to 400 nm in an attempt to see any conformational changes which may have occurred.

2.8.2 ^{125}Iodine Protein Adsorption

All protein solution concentration values were verified by UV absorbance (model 35, Beckman) using values for the extinction coefficient of 1.35 and 6.5 ml mg^{-1} cm^{-1} for BSA and AT-III, respectively. The labeled protein was added to a known solution concentration of unlabeled protein immediately prior to the adsorption. For the BSA adsorption, the total concentration was 1.0 mg/ml with the ratio of unlabelled to labelled protein of 84:1. A 0.36 mg/ml solution of AT-III was used due to the small amount of AT-III available. The labelling ratio was 58:1.

Quartz chips (1 x 2.5 x 0.1 cm, area of 5.7 cm^2), prepared as described in Section 2.2.1, were used for direct counting by a gamma well counter. The chips were immersed into 2 ml of the protein solution in a 12 x 25 mm test tube and allowed to adsorb at room temperature for 1 hour. After an hour, they were

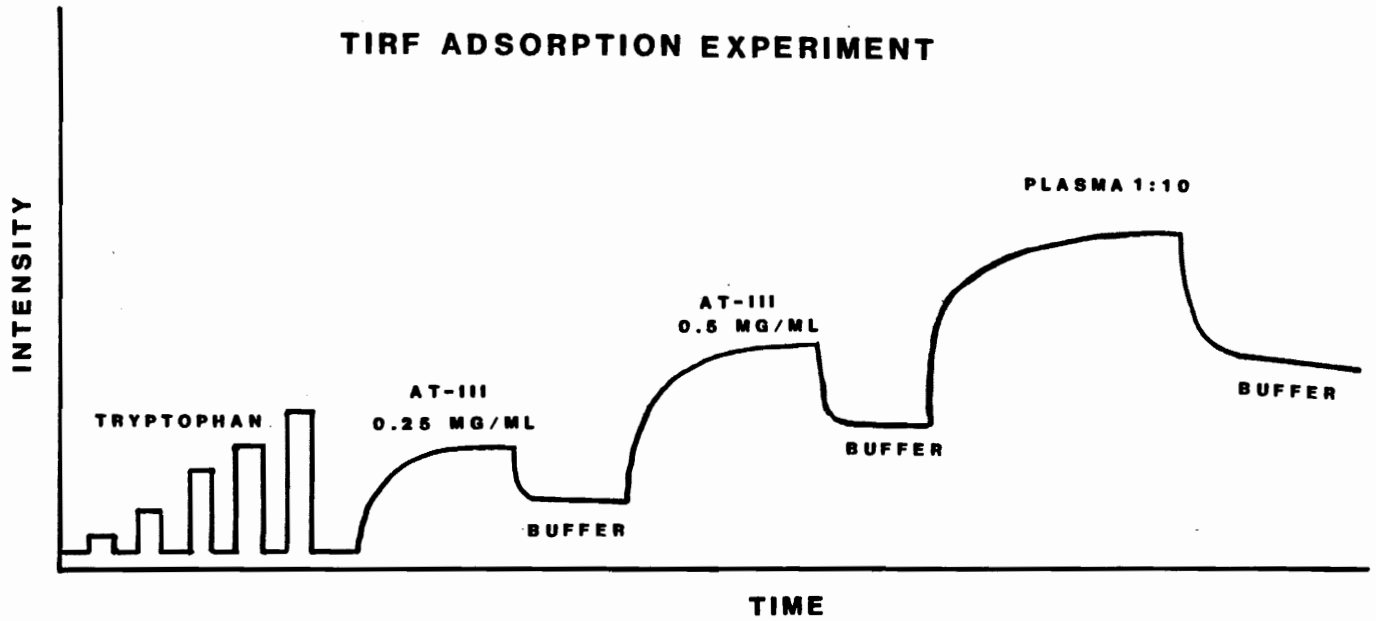

Figure 13. The adsorption scheme used for TIRF protein adsorption studies. Tryptophan standards were followed by successively increasing concentrations of AT-III and the plasma.

withdrawn, rinsed by placing them into a clean test tube and adding 5 x 2 ml PBS, again transferred to another clean test tube, and again rinsed five times with 2 ml PBS each. The chips were then placed into capped scintillation vials and counted on a well gamma counter for 1 minute. Each tube was counted twice and the average of the two counts recorded. In addition, 100 ul aliquots of the protein solutions were reserved after the adsorption and counted to determine if any significant solution depletion had occurred. All surfaces were tested in triplicate.

2.9 Stability Studies in Aqueous Buffer

The stability of the APS and PEO surfaces was determined by soaking them in a phosphate buffered saline solution for various periods of time and analyzing for the elemental content by XPS. This was done by placing them into staining jars with PBS (pH 7.4 with 0.01 percent sodium azide as a bacteriocide) and allowing them to soak without stirring. The PBS was changed daily. At times ranging from 1 to 72 hours, slides were removed, washed three times with distilled water, ethanol and methylene chloride for drying, and stored under vacuum until analysis was performed. Surfaces tested were from at least three different reaction sets, with n being the number of different reactions tested. Controls for these studies consisted of clean quartz slides and APS coupled slides. APS slides were underivatized PEO physically adsorbed under identical conditions as were used for the covalent coupling were also analyzed to determine the stability of nonspecifically bound PEO.

The surface elemental composition was analyzed by XPS using the cabon 1S, oxygen 1S, nitrogen 1S, silicon 2S, and sulfur 2P were taken and normalized by their Scofield cross sections. Plots of the percent of ether carbon, carbon to

silicon ratio and sulfur content (in the case of the slides reacted with heparin) versus time were recorded.

2.10 Heparin Activity Testing

2.10.1 Whole Blood Clotting Times

The anticoagulant activities of the derivatized glass beads prepared as described in Sections 2.3 and 2.4 were determined using a modification of the Lee White Whole Blood Clotting Test. (131) This test is by nature only a crude measure of coagulation activation and was used for screening which surfaces would be tested further for materials interactions.

Glass tubes (12 x 50 mm Fisher Scientific) were prepared for this test by silanizing them using the method described in Section 2.2.2 and reacting them overnight, under nitrogen, with a 1 percent solution of PEO-bis chloroformate MW 18,000 in methylene chloride. They were washed extensively with distilled water prior to use. Eighty mg of derivatized beads (calculated surface area of 66 cm^2) were added to each tube and equilibrated with 2 ml of PBS solution for 2 hours prior to the test. Immediately prior to the addition of blood, the PBS was withdrawn from the tubes using a glass pipet.

Blood was collected from the author using the double syringe technique and used within 10 seconds of drawing. Using a stop watch to record time, 1 ml of whole blood was added to each tube and stirred with a glass pipet to mix the beads thoroughly with the blood. Three tubes were used for each sample. At 15 second intervals the tubes were inverted in the same order each time, until a clot could be detected and the blood would no longer flow by inverting the tube. Time to clot was recorded for each sample and the time of clotting of the third tube of each sample was used according to protocol of the Lee-White method.

This test was performed on blood drawn at six different times and the results of these six tests averaged.

During the first test, the blood in contact with beads containing the heparin failed to clot even after 2 hours. The blood of these tubes was placed into tubes containing 80 mg of clean beads to determine if heparin had leached from the beads. After 3 hours, the blood still had not clotted and it was determined that more extensive washing of the heparin coupled beads was necessary. As a result, during succeeding tests, all heparin surfaces were soaked in buffer for at least 2 hours and rinsed with distilled water three times before equilibration with PBS for the test. This seems to have been sufficient to remove all leachable heparin as subsequent testing of these surfaces caused clotting of the whole blood within 2 hours of contact.

2.10.2 Activated Partial Thromboplastin Time Test

The surfaces tested using the Activated Partial Thromboplastin Time Test (APTT) (132) were chosen from the results of the Whole Blood Clotting Test. These were the PEO-bis chloroformate 18,000 and the PEO-bis isothiocyanate 18,000 with and without heparin and the appropriate controls of clean glass and APS reacted glass. Blood from the author was collected using the double syringe method into 3.8 percent sodium citrate (nine parts blood to one part citrate) and centrifuged to prepare a platelet rich plasma (PRP). The supernatant plasma was collected and stored at 4°C until testing, but no longer than 2 hours after drawing.

APTT tests were conducted by first incubating various quantities of the derivatized beads with 2 ml of the prepared plasma at room temperature for 30 minutes, stirring every 5 minutes with a glass pipet. Plasma, with known unit activities of heparin, was prepared for generation of calibration curves. One

hundred ul of the plasma exposed to the beads, or plasma containing known unit activities of heparin were withdrawn and incubated with 100 ul of activated thromboplastin reagent (Ortho Pharmaceutics) at 37oC for 5 minutes. One hundred ul of 0.3 M $CaCl_2$ in distilled water was then rapidly added to the incubated plasma and clotting times were determined with a fibrometer (Beckman). A plot of APTT (seconds) versus heparin activity in the plasma (units/ml) was first prepared with plasma heparinized in 0.1 unit/ml increments. A linear relationship is typically observed between 0.0 and 0.5 units/ml of heparin. Unheparinized plasma was evaluated before and after all samples were run to ensure that coagulation factors had not degraded during the course of testing. Each plasma sample was tested for APTT in triplicate for each of two batches of plasma drawn at different times. The APTTs of plasmas exposed to the beads were compared to the calibration plot of known heparin unit activities and the activities of the plasma exposed to the derivatized beads determined in units/ml plasma.

2.11 Platelet Interactions

Heparin has been reported to inhibit, (133, 134) enhance, (135, 136) and have no effect at all upon platelet function. (137) Due to both the heterogeneous nature of heparin preparations and the numerous methods of testing platelet adhesion, aggregation and activation, the precise effect of heparin is difficult to discern. Nevertheless, it appears that heparin potentiates platelet adhesion. Because platelets behave differently when in the presence of other cellular material than in plasma, or after washing and resuspending, retention tests were done using whole blood and platelet rich plasma. Platelet activation was measured using the release of Platelet Factor 4 from the α granules.

2.11.1 Platelet Retention

Platelet retention by the various surfaces was measured by exposing whole blood or platelet rich plasma (PRP) to derivatized beads as a function of contact time and counting the platelets left in the fluid. The tubes were previously coated with PEO-bis chloroformate (MW 18,000) as described in Section 2.10.1. Eighty mg of beads were added to each tube and equilibrated with PBS for 2 hours. The PBS was withdrawn with a glass pipet immediately before adding either whole blood or PRP. Whole blood was collected from the author using the double syringe technique into 3.8 percent sodium citrate (nine parts blood to one part citrate) and used either as is, or PRP was prepared by centrifugation. The supernatant plasma was collected and pooled for subsequent platelet testing. In the first series of tests, 2 ml whole blood were added to the tubes containing the derivatized beads, stirred gently with a glass pipet, and incubated for times ranging from 0 to 30 minutes at 37°C. The tubes were stirred every 5 minutes. The whole blood was then withdrawn and spun for 15 minutes at 2500 g and the plasma separated from the cells. This plasma was then counted for platelets in a Coulter Counter. In the second series of experiments, 2 ml PRP was incubated with the derivatized beads for various time periods and counted. This was done to determine if the presence of other cellular material had any effect on the behavior of platelets exposed to the surfaces. Controls consisted of blood or PRP which was incubated in the PEO tubes with clean glass beads, without any beads, and with APS derivatized beads. A plot of exposure time versus number of platelets was determined for each of the surfaces exposed to whole blood and PRP. All surfaces were tested in triplicate from each of two batches of blood and averages determined.

2.11.2 Platelet Factor 4 Release

Platelet Factor 4 levels in collected plasma exposed to the derivatized beads were determined by bovine PF4 RIA reagents (Abbott Laboratories). The test is a competitive radioimmunoassay in which nonradioactive PF4 in plasma, and buffer, competes with a constant amount of ^{125}I-PF4 for binding sites in a constant, limited amount of bovine PF4 antiserum. The percentage of radioactive PF4 bound to the antiserum is therefore inversely proportional to the concentration of nonlabeled PF4 in the test samples. Again, tubes for these experiments were prepared with PEO-bis chloroformate (MW 18,000) as described above. Eighty mg of derivatized beads were pre-equilibrated with PBS, then exposed to 1 ml of plasma for 30 minutes at 37°C. Fifty ul of dilution buffer, nonlabled bovine PF4 standards (in concentrations ranging from 50 ng/ml to 1000 ng/ml), or 50 ul of the plasma which had been exposed to the derivatized beads were added to 250 ul of the ^{125}I-PF4 solution. Two hundred fifty ul of PF4 antiserum were added and the tubes incubated at room temperature for 2 hours after which 1 ml of 73 percent saturated ammonium sulfate was added. The tubes were then incubated between 10 and 60 minutes and centrifuged at 1500 g for 20 minutes. The supernatant was carefully decanted and the excess supernatant on the rim of each tube was blotted with tissue paper. The total ^{125}Iodine in the precipitate was then counted with a gamma counter. The percent bound, expressed as cpm in 250 ul of the ^{125}I-PF4 solution multiplied by 100, was determined for each tube. A standard curve was prepared by plotting percent bound versus standard PF4 concentrations. By locating percent bound of the unknown test sample on the standard curve, the concentration of PF4 in the test samples was determined. Each PF4 standard and test sample was evaluated in triplicate.

CHAPTER 3

RESULTS

3.1 APS Coupling to Quartz Plates and Beads

3.1.1 XPS Characterization of Surface

The vapor phase silanized quartz substrates were characterized using XPS by monitoring the nitrogen and silicon signals. Generally, an atomic percentage of nitrogen in the range of 5.5 to 8 percent before hydration in PBS was considered to be complete surface coverage. Surfaces falling outside of this range were not used. The percents of nitrogen, carbon, silicon, and oxygen were plotted as function of soaking time in PBS buffer to determine the stability of the APS surface (Fig. 14). After soaking in PBS, the nitrogen 1S signal appears as a split doublet at 394.8 and 393.1 ev which are presumably due to the presence of NH_2 and NH_3+ (Fig. 15). The area of both of these peaks was combined as the total nitrogen signal. As can be seen in Fig. 14, the nitrogen signal decreased slightly in the first hour, and then remained fairly constant after that time with a final value of 5 percent. This is also reflected by the constant value of the silicon signal during the period of hydration. Each point on the graph represents a minimum of four samples. The elemental percentages found on the clean quartz controls are, as would be expected, significantly lower (Fig. 16). An alternate method of analyzing these data is to plot the ratio of the nitrogen signal of the APS layer to the silicon signal arising from the quartz substrate. However, each molecule of APS has a single atom of silicon which contributes to the overall silicon signal. This must then be subtracted from the total silicon

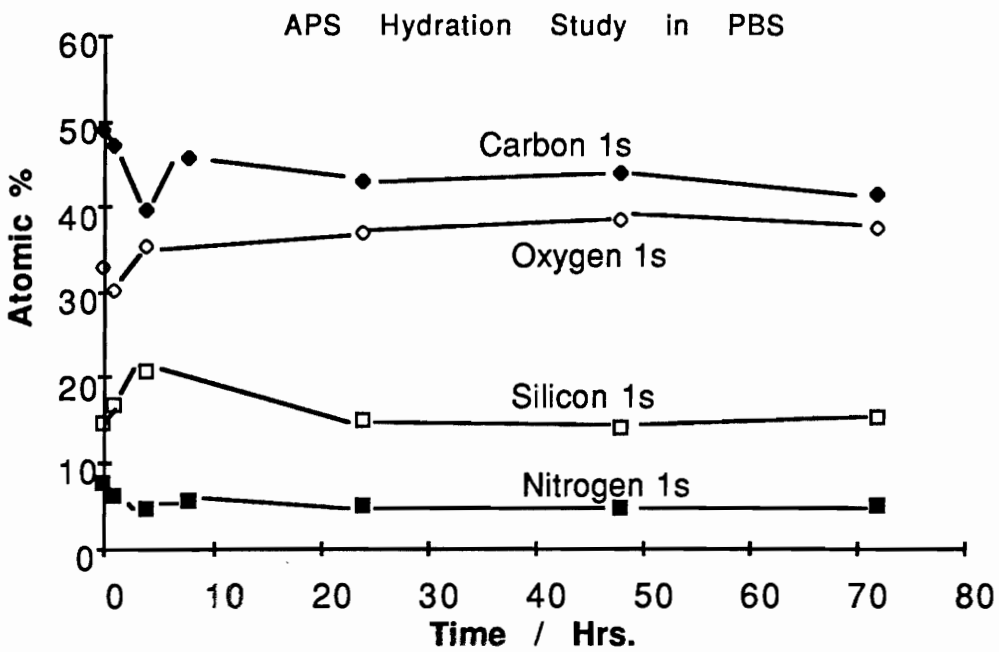

Figure 14. The XPS elemental analysis of quartz surfaces derivatized with γ - aminopropyltriethoxy silane following exposure to PBS for various times.

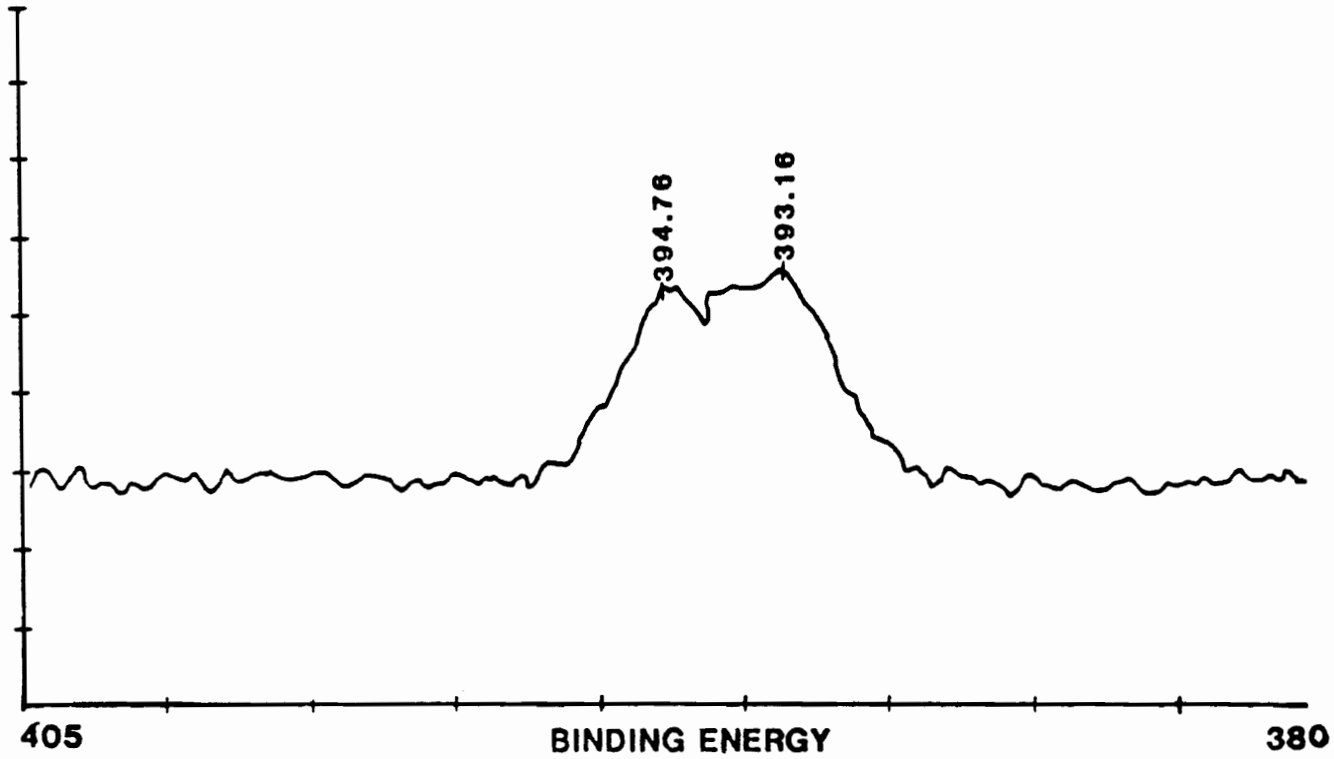

Figure 15. The XPS spectrum of the nitrogen 1S signal of APS-coupled quartz slides following exposure to PBS. The doublet presumably is due to the presence of NH_2 and NH_3.

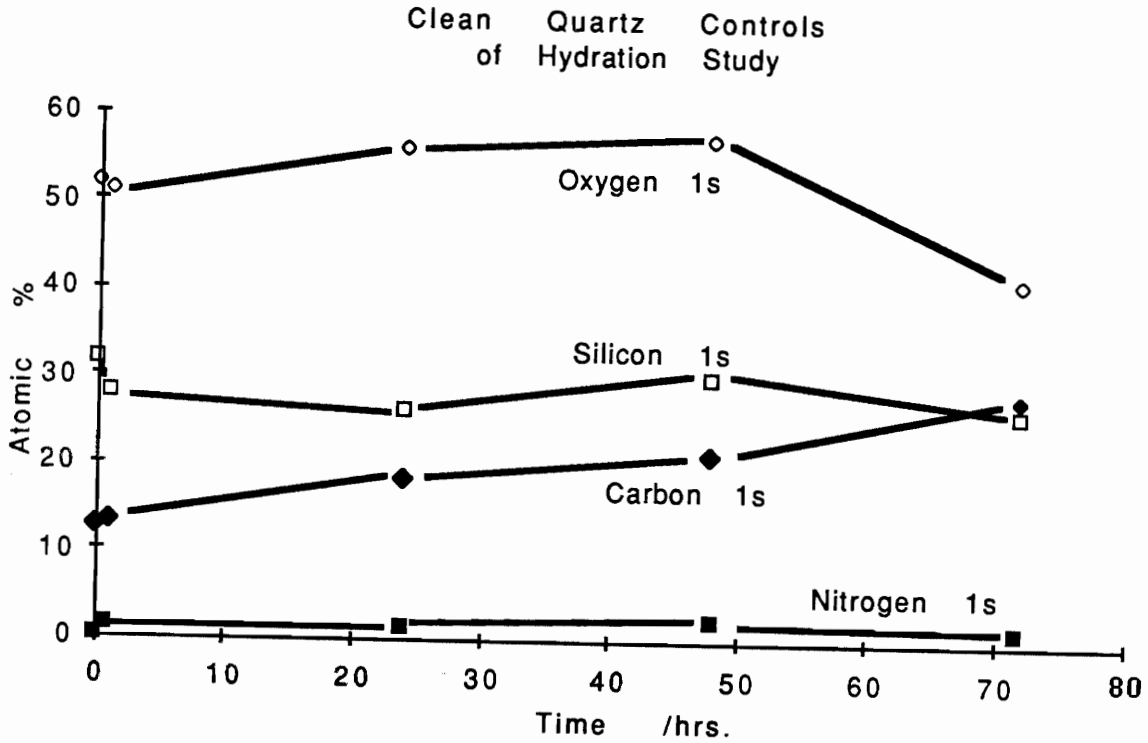

Figure 16. The XPS elemental analysis of clean quartz slides following exposure to PBS for various times.

percentage. Assuming three attachment sites for each APS molecule, an atomic ratio for a multilayer of APS and quartz is N:Si:C:O of 1:1:3:1.5 and 0:1:0:2, respectively. The N/Si ratios of the APS and clean quartz controls are plotted in Fig. 17.

3.1.2 Variable Angle Thickness

Variable angle XPS was used to estimate the thickness and homogeneity of the APS layer on the quartz substrates. This technique allows a calculation of the thickness or the percent coverage of an overlayer on a substrate. According to the equation for a uniform overlayer:

$$\frac{I_b}{I_a} = \frac{\lambda_b}{\lambda_a} \exp\left(t_b / \lambda_b \sin\theta - 1\right) \qquad (7)$$

where

I_a is the integrated area of the substrate (in this case the 2S peak of silicon)

I_b is the integrated area of the overlayer (in this case the 1S peak of nitrogen of the APS)

λ_a is the mean free path of the silicon 2S electron (calculated by the Ashley method (125) to be 35.1Å)

λ_b is the mean free path of the nitrogen 1S electron (calculated by the Ashley method (125) to be 43.7Å)

θ is the photoelectron take off angle.

Using equation (7) above, a uniform overlayer of various thicknesses yields the curves seen in Fig. 18. The astericks on the graph represent the actual data obtained in this experiment and do not fit well with any of the curves. For this

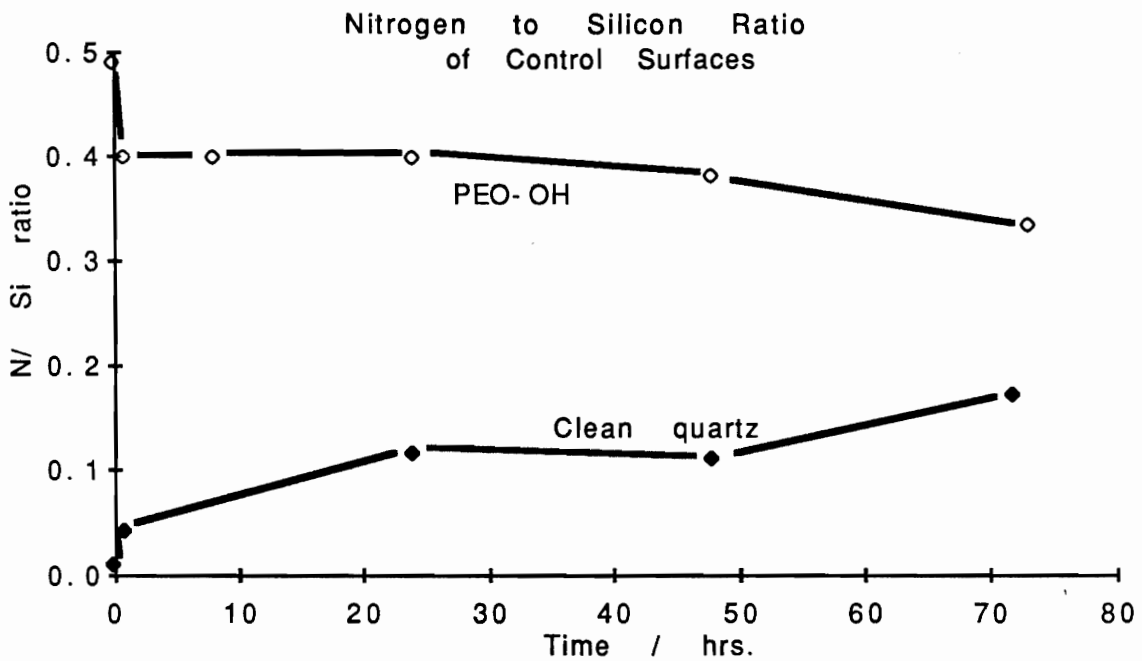

Figure 17. The ratio of the nitrogen to silicon XPS signals of APS and clean quartz control surfaces following exposure to PBS for various times.

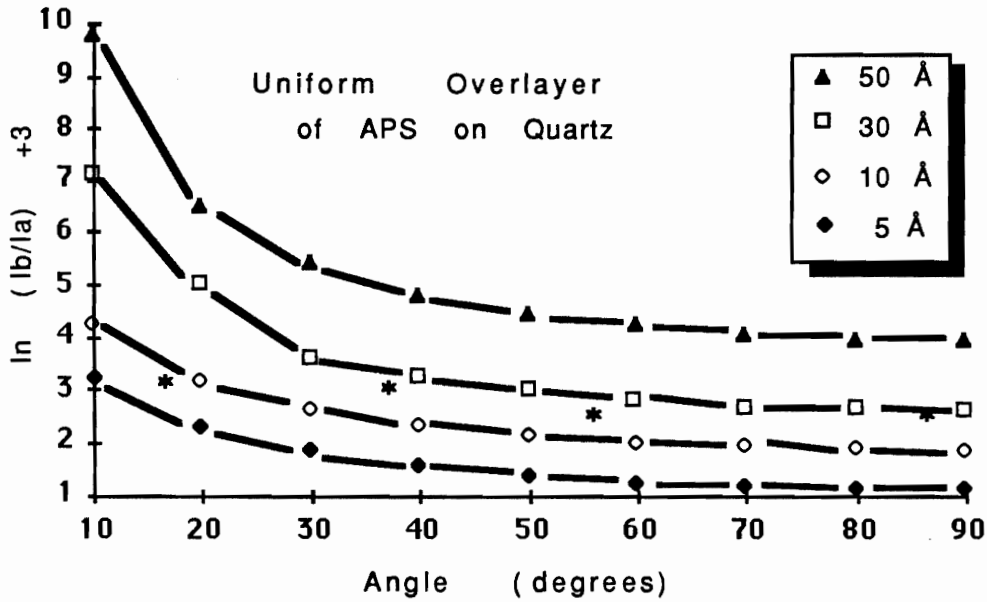

Figure 18. Plot of the equation for a theoretical uniform overlayer of APS on quartz of various thicknesses. The astericks (*) indicate actual data obtained in variable angle XPS experiments.

reason, modeling of the surface with a patchy overlayer was done using various thicknesses for "t" in the equation:

$$\frac{I_b}{I_a} = \frac{\gamma \lambda_b \; 1-\exp(-5_b/\lambda_b \sin\theta)}{(1-\gamma)\,\lambda a + \gamma \lambda_a \exp(-t_b/\lambda_b \sin 0)} \qquad (8)$$

where

γ is the fraction of the surface covered by the overlayer and other symbols are as defined in equation (7).

An overlayer thickness of 10, 20 and 50 Å yields the curves expressed in Figs. 19-21. The fractional surface coverage is given by the different curves. The astericks plotted on the graph are the actual data obtained at take off angles from 4^0 to 85^0. Using a least squares best fit, the data correspond most closely to an overlayer of 50 Å of APS on the quartz substrate and 50 percent coverage. This is contrary to popular belief that vapor phase silanization using this method creates a homogeneous monolayer; however, each asterick on the graph represents three samples, each silanized in separate reactions. The error in these experiments was no greater than plus or minus 10 percent of the area of the atomic signals.

3.1.3 Wilhelmy Plate Characterization

The measured contact angles on the APS silanized slides after soaking in PBS for various periods of time are shown in Fig. 22. As can be seen in the figure, clean glass with no previous soaking in PBS produced a 0° contact angle with no hysterisis. After exposure to PBS, the contact angle increased to $10.7 \pm 2.3^\circ$ for the advancing angle and $4.5 \pm 1.7^\circ$ for the receding angle over the test period of 72 hours. This is presumably due to contamination of the PBS during the course of the experiment which caused adsorption of contaminants onto the

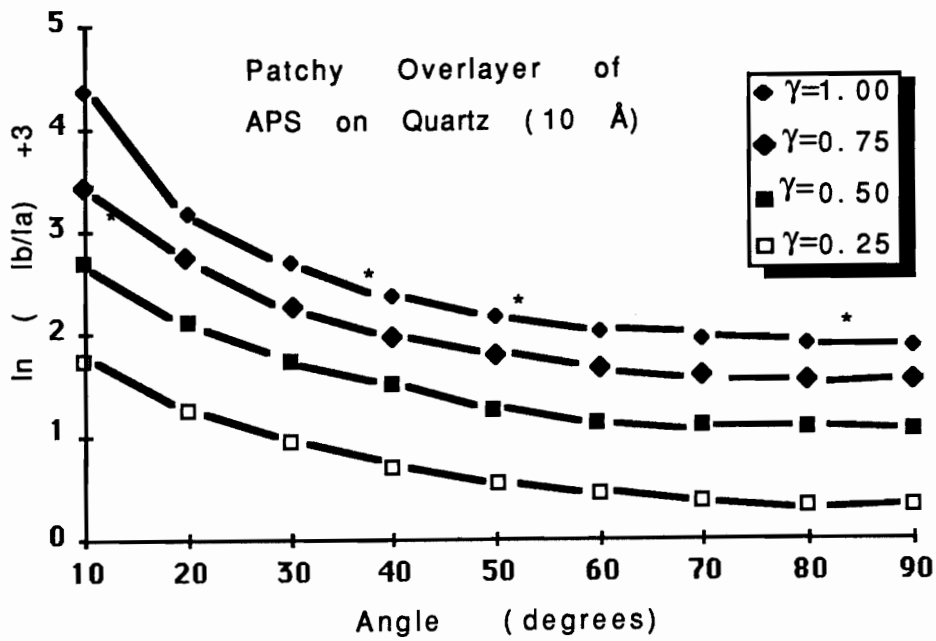

Figure 19. Plot of the equation for a theoretical 10 Å patchy overlayer of APS on quartz for varying surface coverages (γ). The astericks (*) indicate actual data obtained in variable angle XPS experiments.

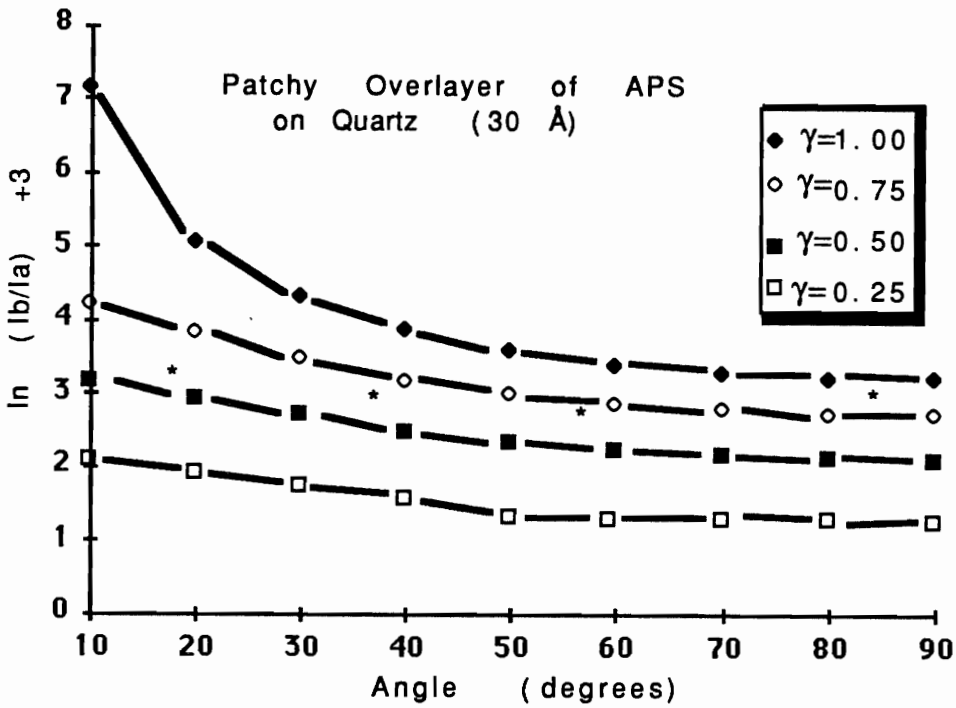

Figure 20. Plot of the equation for a theoretical 30 Å patchy overlayer of APS on quartz for varying surface coverages (γ). The astericks (*) indicate actual data obtained in variable angle XPS experiments.

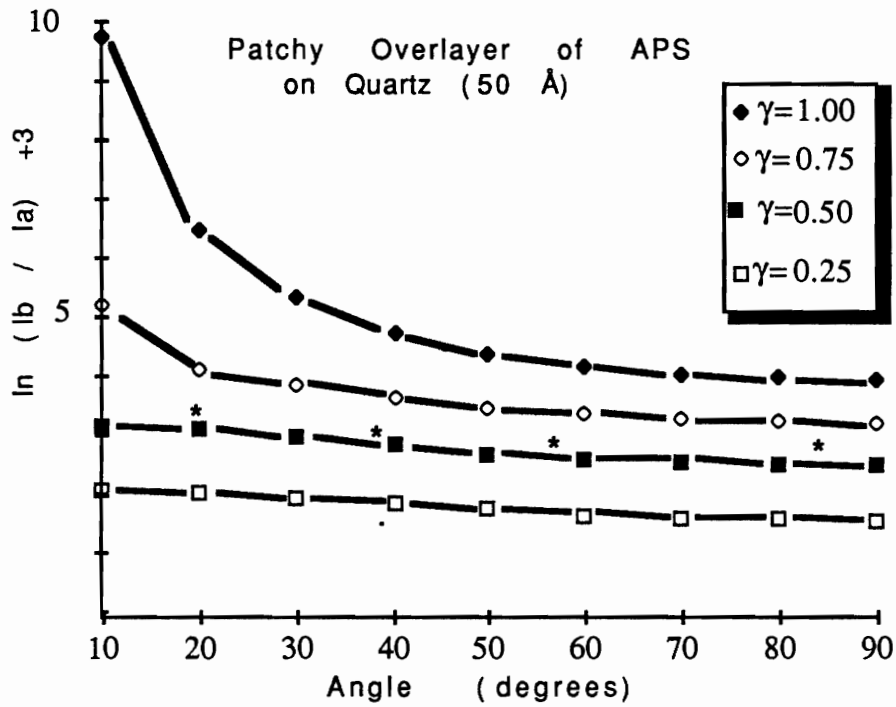

Figure 21. Plot of the equation for a theoretical 50 Å patchy overlayer of APS on quartz for varying surface coverages (γ). The astericks (*) indicate actual data obtained in variable angle XPS experiments.

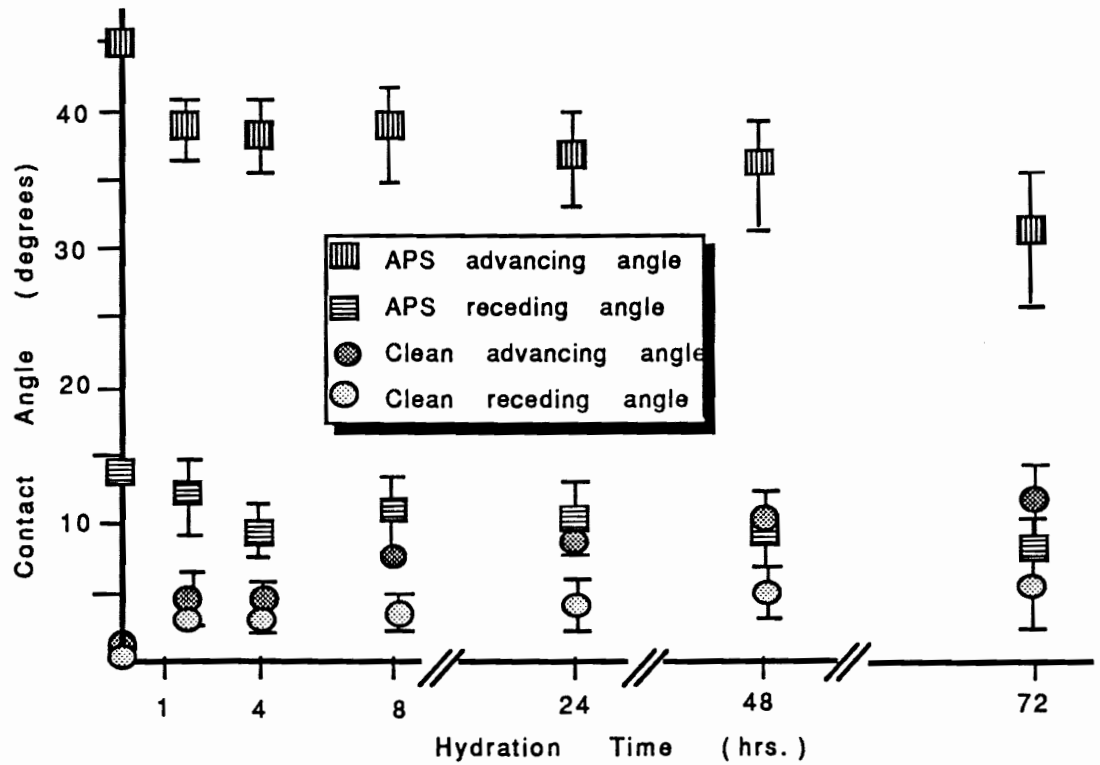

Figure 22. The contact angles of clean and APS derivatized quartz measured by the Wilhelmy Plate method as a function of hydration time in PBS.

quartz. The APS contact angles were also found to vary over the time of hydration. Before hydration, the angles were very reproducible yielding values of 43.5 $\pm$ 2.1° and 11.8 $\pm$ 1.7° for the advancing and receding angles, respectively. This represents five separate reactions of vapor phase silanization with triplicates of each reaction. However, over the course of hydration, the angles were found to vary significantly as can be seen in the figure and the large standard deviations of $\pm$ 10o. Following hydration, the advancing angle was found to be 30.9 $\pm$ 12.8° and the receding angle of 8.1 $\pm$ 5.6°. This was not reflected in the results of the XPS characterization as discussed above.

As a side study, the stability of the APS layer following exposure to different buffers and ionic strengths was analyzed. Soaking in borax pH 9.7 and ionic strength of 0.20 for only 4 hours produced 61.4° and 8.1° for the advancing and receding angles, respectively. Similarly, exposure to an acetate buffer of pH 3.7 and ionic strength of 0.19 produced advancing and receding angles of 53.0° and 16.3°, respectively. For both of these buffers, the angles were found to be unstable following the second pass into the contact angle water, indicating the APS had probably come off into the water. This presumably resulted in a change of the surface tension of the water, thus invalidating the measurements.

3.2 Poly(ethylene oxide) Coupling to Quartz Plates and Beads

3.2.1 XPS Characterization of Surface

All surfaces were XPS analyzed for PEO coverage following the coupling reactions by monitoring the carbon 1S, oxygen 1S, nitrogen 1S, silicon 2S, and sulfur 2P signals. Fig. 23a shows a carbon 1S XPS spectrum of pure PEO (MW 6,000). The peak at 285.6 ev (charge referenced to C 1S, 284.0) corresponds with a carbon bonded to an ether oxygen and hence is monomodal since all the carbons

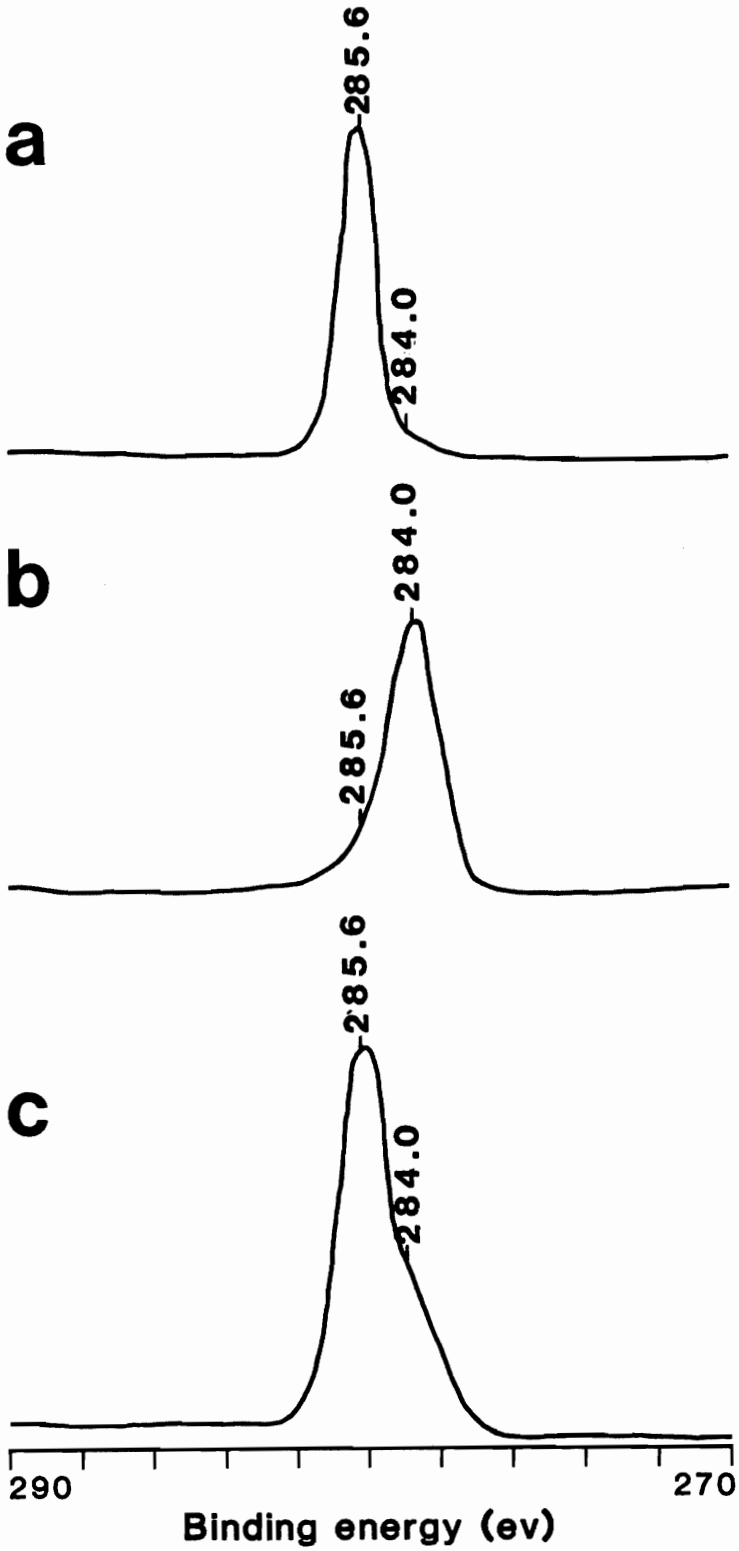

Figure 23. The carbon 1S XPS spectra of surfaces analyzed. a) pure PEO; b) aliphatic carbon of an APS silanized quartz slide; c) PEO immobilized onto quartz via APS.

in PEO are equivalent. The carbon 1S spectrum of Fig. 23b shows the aliphatic carbon peak of an APS silanized quartz slide with the peak at 284.0 ev. Fig. 23c is again the carbon 1S spectrum; this time it is a spectrum of a quartz slide to which PEO has been bound via the APS coupling agent. The aliphatic carbon of the APS layer is evident as a distinct shoulder on the lower binding energy side of the other carbon peak. It is the ether carbon component of the total carbon 1S spectrum which has been used to monitor the stability of the PEO on the surface. This can be seen in the curve resolved carbon 1S spectrum of Fig. 24.

Figs. 25-32 show the elemental percentages of the four derivatives for the two molecular weights used in this study after various times of hydration in PBS buffer. The carbon signal plotted in these graphs is the total carbon detected on the surface and therefore also reflects the carbon component of the attached APS. The same data of the control, a clean quartz slide, were seen in Fig. 17.

It is perhaps more beneficial to compare the percent of the total carbon signal due to the ether carbon component. It is the ether carbon signal which reflects the amount of PEO on the surface. Fig. 33 is the ether carbon signal of the control surfaces to which underivatized PEO was physically adsorbed. From Figs. 33 and 34, it is apparent that some of this adsorbed PEO remained on the APS surface after the rinse but prior to the hydration in PBS. The slightly higher initial C/Si ratio of 3.0 and the ether carbon content of 32 percent are higher than the same values of the clean quartz control surfaces. The adsorbed PEO partially desorbed during the three day PBS soak as reflected by the slight decrease of these curves with time. Final parameters for the APS controls were C/Si of 2.0 and 2.3 for the molecular weights 6,000 and 18,000, respectively. Final values for the ether carbon content are 22 percent for MW 6,000 and 18 percent MW 18,000.

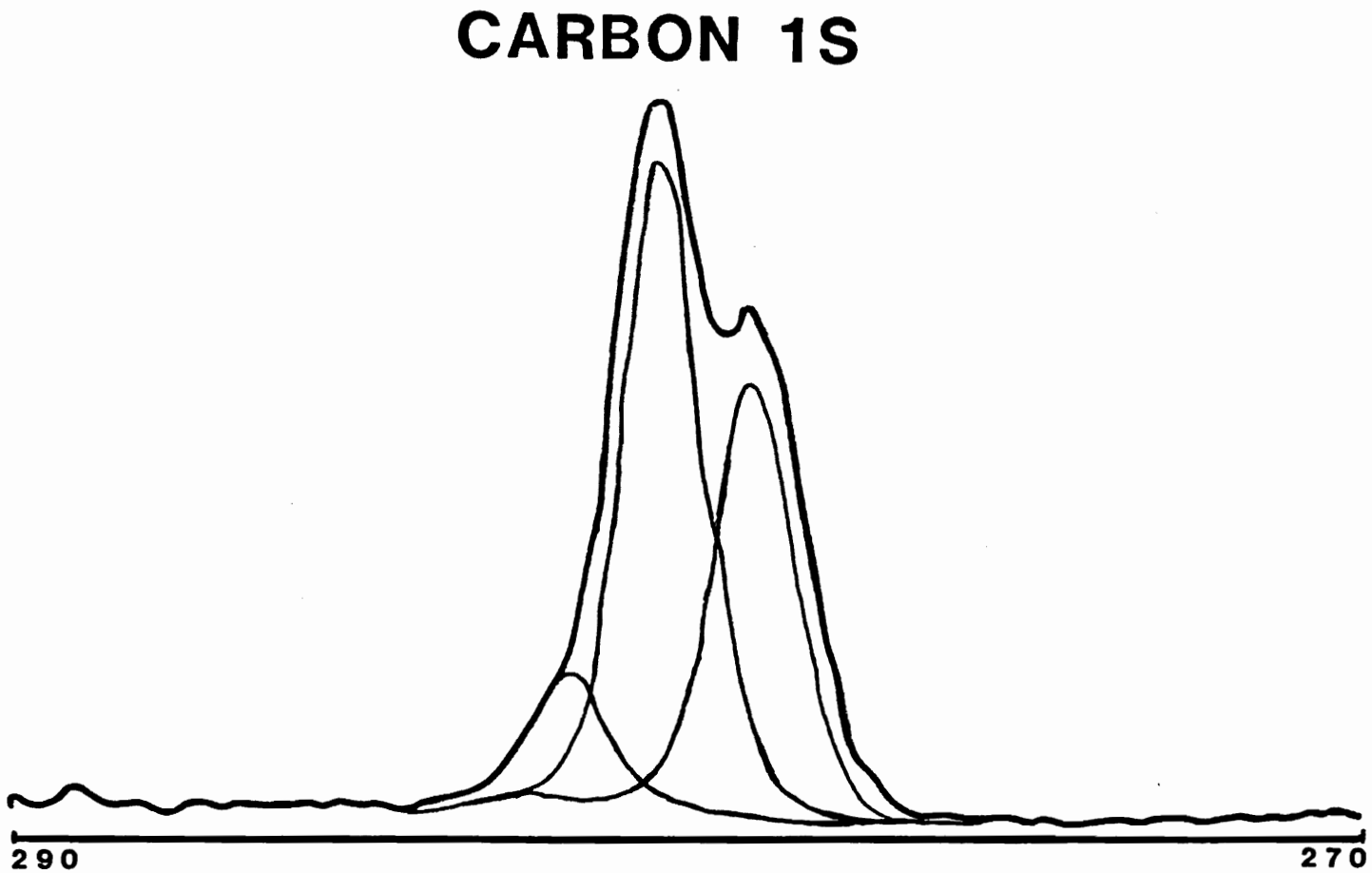

Figure 24. The curve-resolved carbon 1S spectrum of PEO immobilized on quartz via APS coupling agent. It is the ether carbon component of the carbon 1S signal that was used to monitor the stability of the PEO grafted surface.

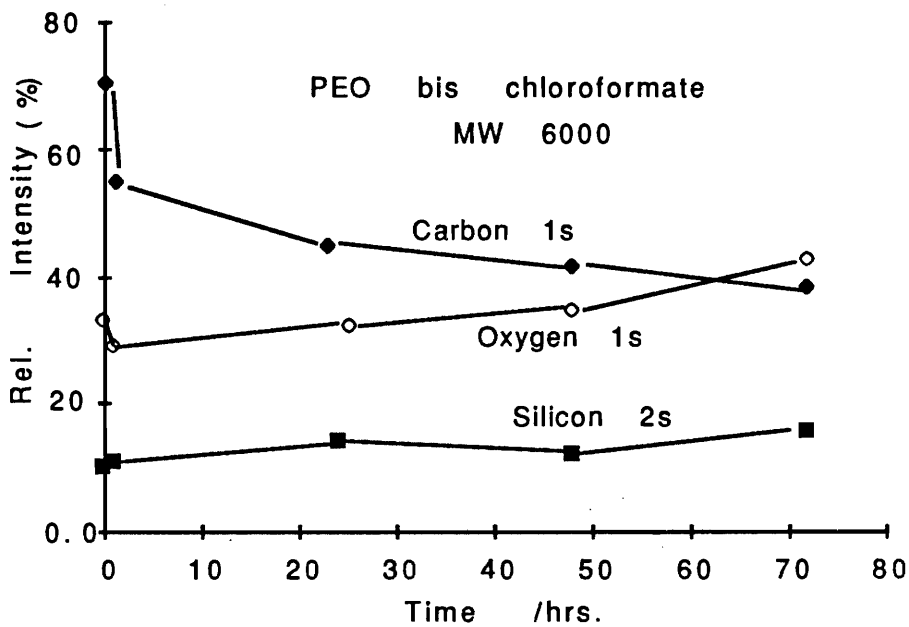

Figure 25. The total XPS elemental signals of PEO-bis chloroformate MW 6,000 immobilized onto a quartz slide as a function of hydration time in PBS.

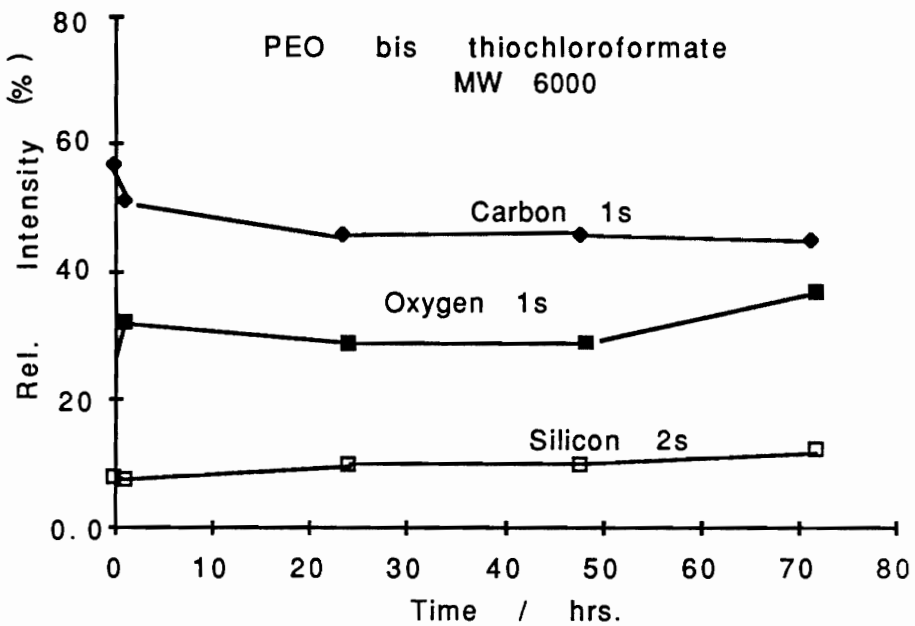

Figure 26. The total XPS elemental signals of PEO-bis thiochloroformate MW 6,000 immobilized onto a quartz slide as a function of hydration time in PBS.

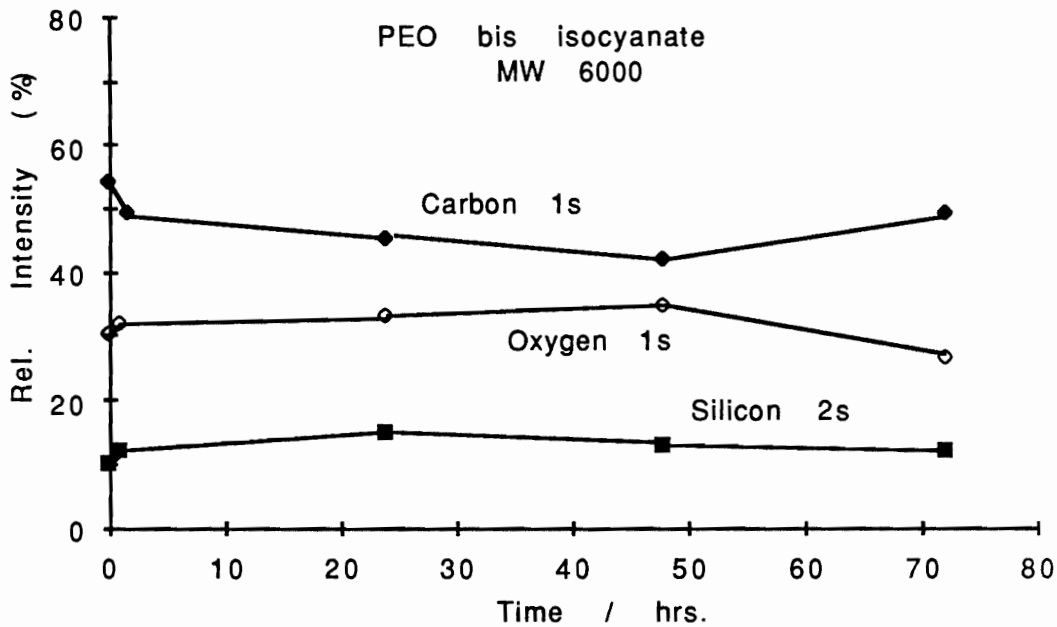

Figure 27. The total XPS elemental signals of PEO-bis isocyanate MW 6,000 immobilized onto a quartz slide as a function of hydration time in PBS.

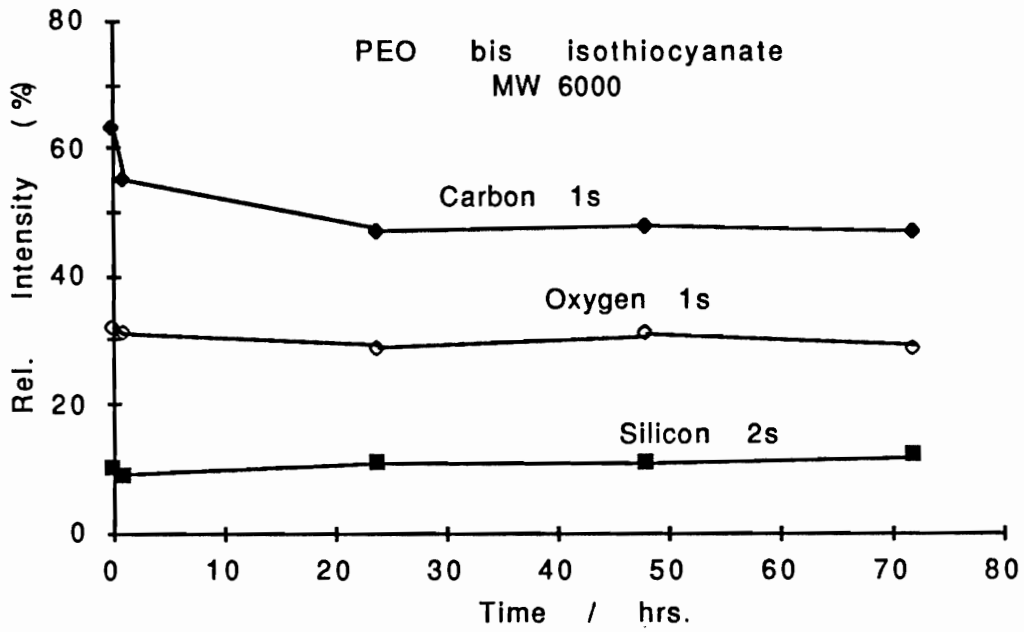

Figure 28. The total XPS elemental signals of PEO-bis isothiocyanate MW 6,000 immobilized onto a quartz slide as a function of hydration time in PBS.

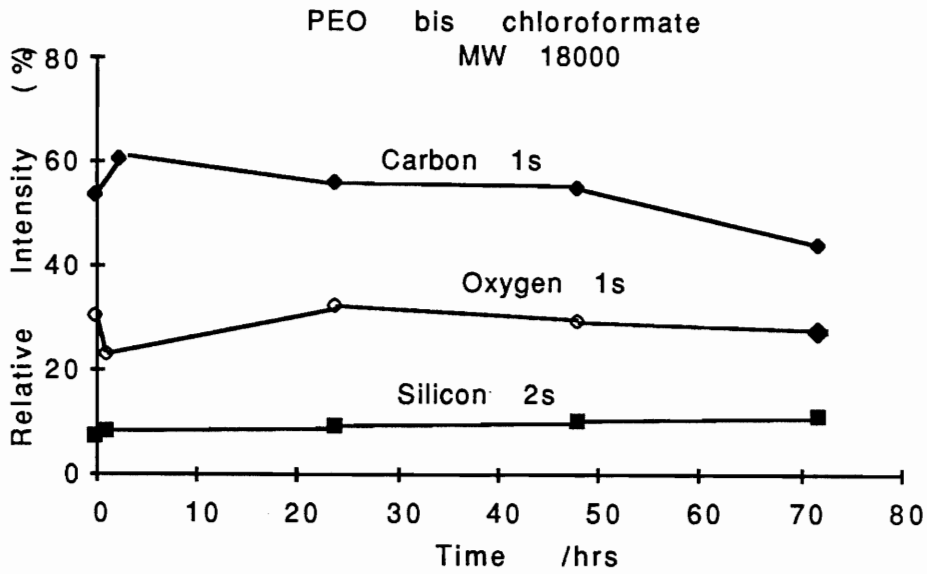

Figure 29. The total XPS elemental signals of PEO-bis chloroformate MW 18,000 immobilized onto a quartz slide as a function of hydration time in PBS.

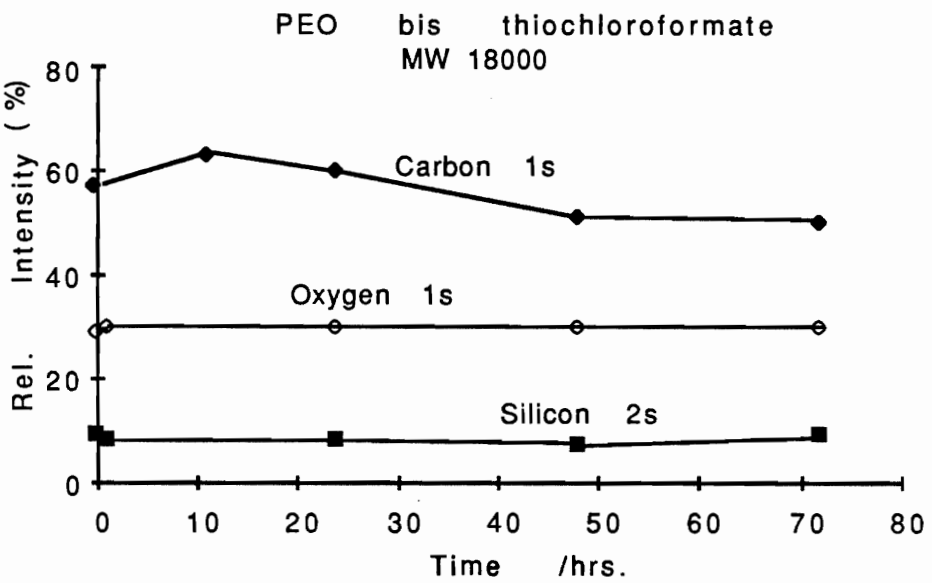

Figure 30. The total XPS elemental signals of PEO-bis thiochloroformate MW 18,000 immobilized onto a quartz slide as a function of hydration time in PBS.

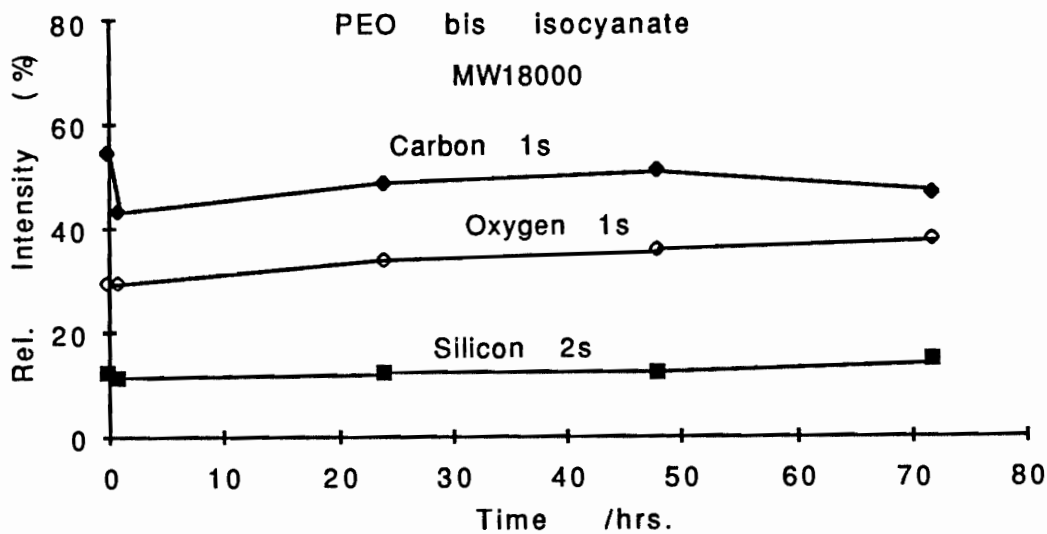

Figure 31. The total XPS elemental signals of PEO-bis isocyanate MW 18,000 immobilized onto a quartz slide as a function of hydration time in PBS.

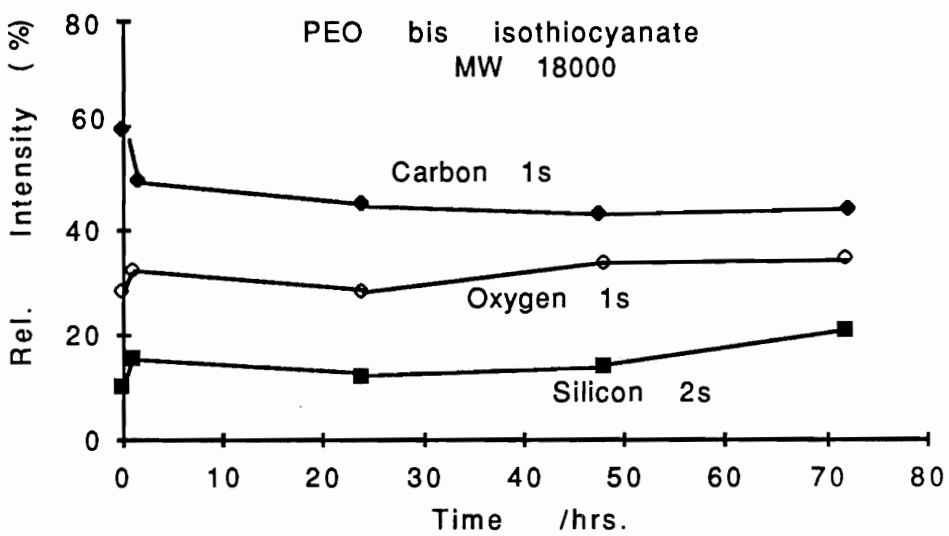

Figure 32. The total XPS elemental signals of PEO-bis isothiocyanate MW 18,000 immobilized onto a quartz slide as a function of hydration time in PBS.

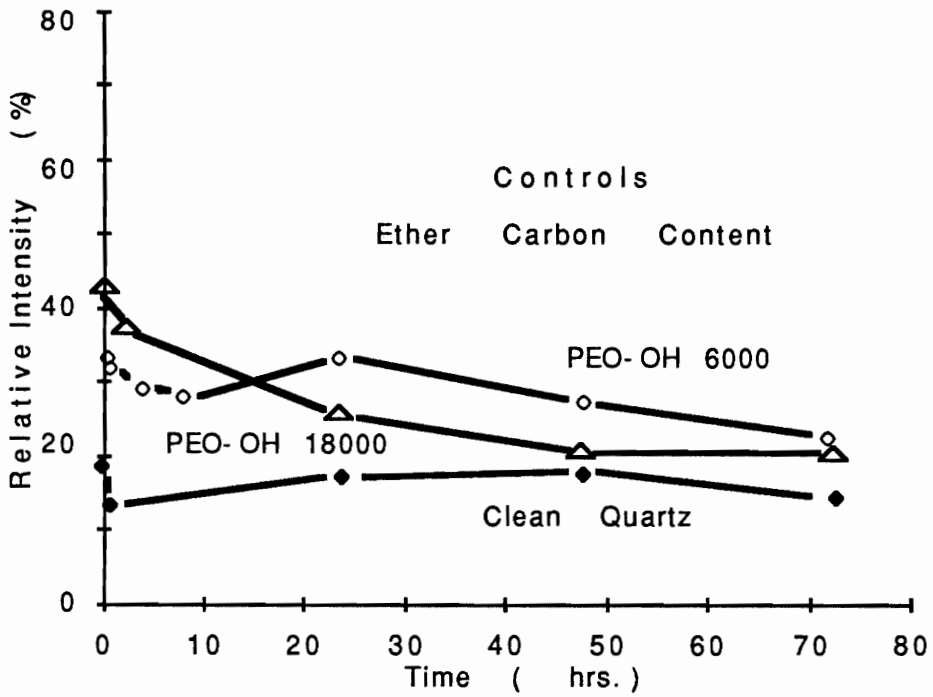

Figure 33. The percent of the total carbon XPS signal due to the ether carbon component of the control surfaces. The underivatized PEO was physically adsorbed to the APS/quarts surfaces and slowly leached from the surface.

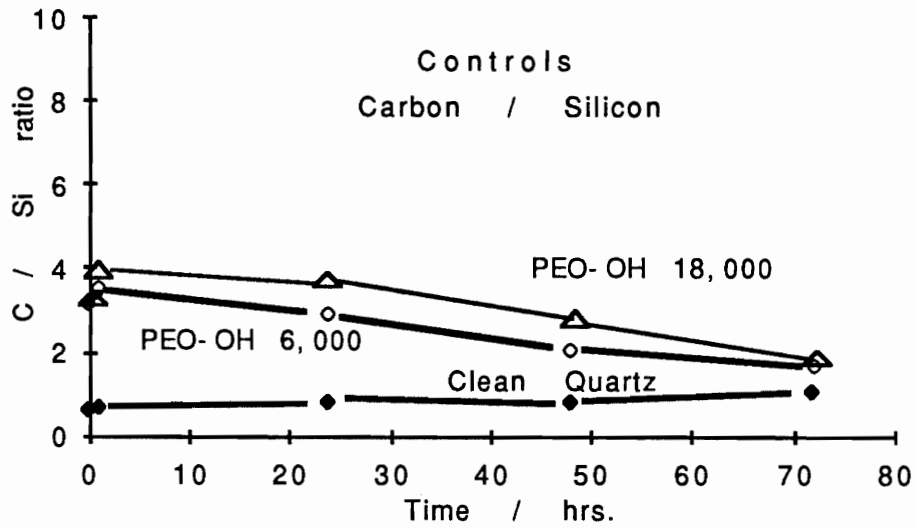

Figure 34. The carbon to silicon ratio of the XPS elemental analysis of control surfaces as a function of hydration time in PBS.

The ether carbon contents of four MW 6,000 PEO derivatives are expressed in Fig. 35. The C/Si ratios of these same four derivatized surfaces are plotted in Fig. 36. What is most striking about both these graphs is the very high degree of coupling of the PEO chloroformate and thiochloroformate derivatives, which initially have an average ether carbon content of 70 percent for the chloroformate and 78 percent for the thiochloroformate. This is indicative of a surface very rich in PEO. However, the PEO layer resulting from these two derivatives appears to be somewhat less stable than the isocyanate and isothiocyanate derivatives. This is reflected by the decrease to a final value of approximately 32 percent ether carbon, a C/Si ratio of 3.4, for the thiochloroformate, ether carbon of 30 percent, and C/Si of 3.0 for the chloroformate derivative.

Similar trends, although less dramatic, are observed in the 18,000 molecular weight derivatives seen in Fig. 37. The decrease in the initial values for ether carbon of 69 percent and 72 percent for the chloroformate and thiochloroformate of 44 percent and 50 percent again tend to indicate less stability of the urethane linkages involved in the chloroformate reactions.

The two cyanate derivatives of both molecular weights have a lower degree of PEO coupling than the chloroformates. This is based on an initial average ether carbon content of 65 percent and 58 percent for the 6,000 isocyanate and isothiocyanate, respectively, and 53 percent and 49 percent for the 18,000 molecular weight isocyanate and isothiocyanate derivatives, respectively. These appear more stable over the 3 day hydration period. Final values for the ether carbon content of the cyanate derivatives are: 40 percent for isocyanate 6,000; 45 percent for isothiocyanate MW 6,000; 53 percent for the isocyanate MW 18,000 and 49 percent for the isothiocyanate MW 18,000.

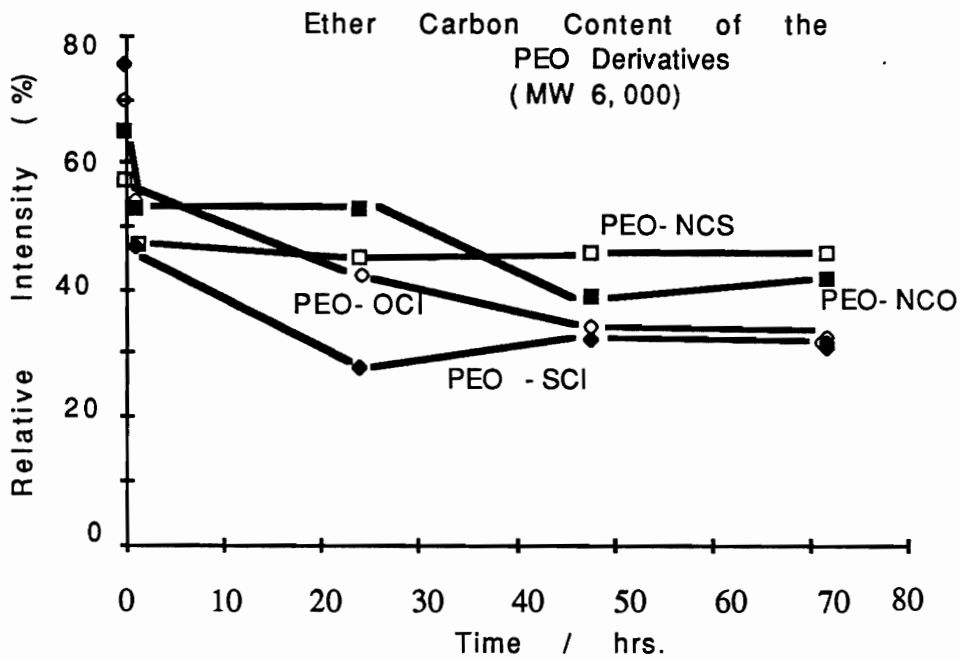

Figure 35. The percent of the total carbon XPS signal due to the ether carbon component of the four PEO derivatized surfaces MW 6,000 as a function of PBS exposure time.

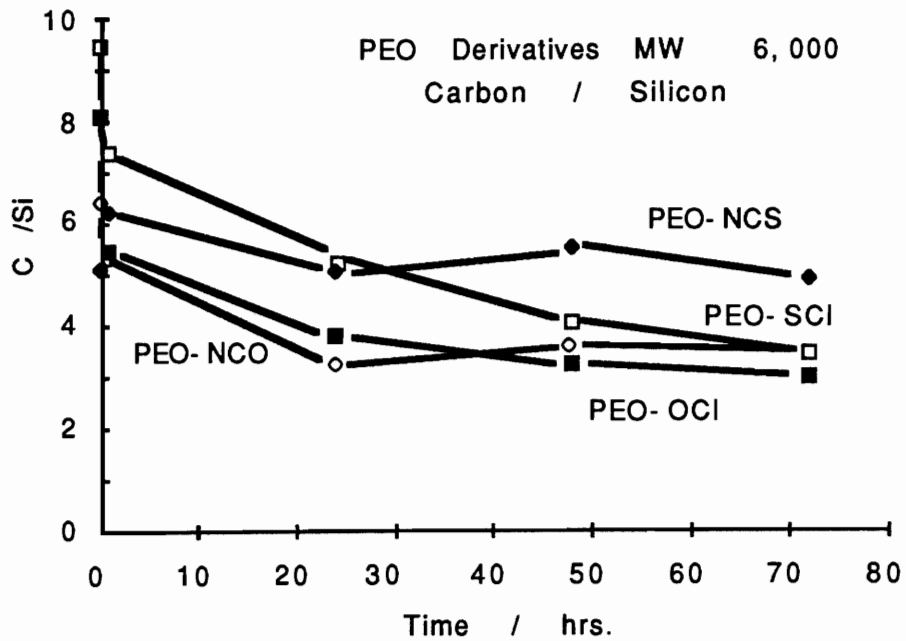

Figure 36. The carbon to silicon ratio of the XPS elemental analysis of the four PEO derivatized surfaces MW 6,000 as a function of PBS exposure time.

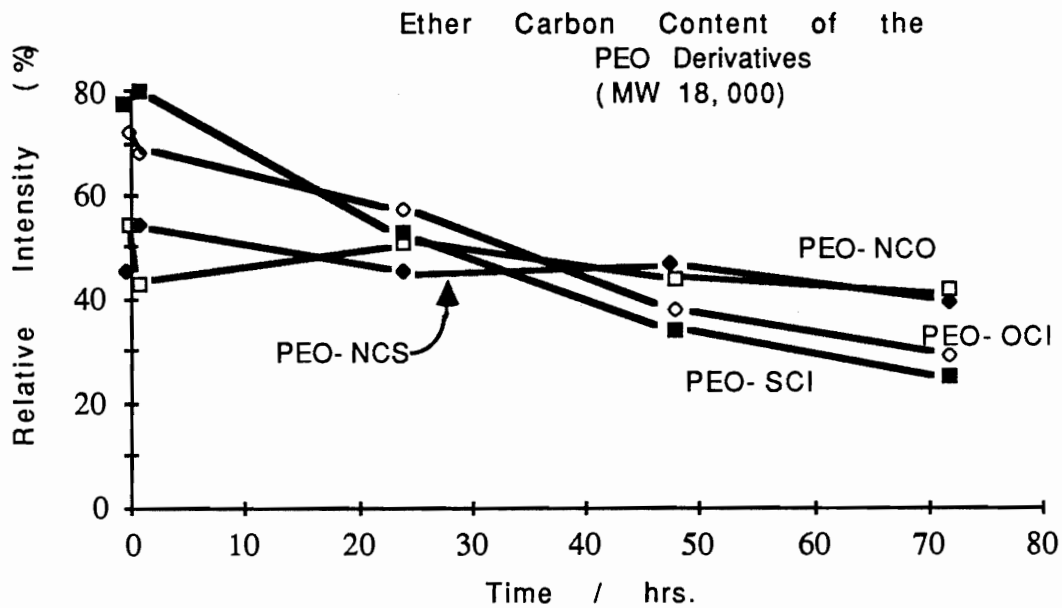

Figure 37. The percent of the total carbon XPS signal due to the ether carbon component of the four PEO derivatized surfaces MW 18,000 as a function of PBS exposure time.

Again, this is reflected in the C/Si ratios for the cyanate derivatives seen in Figs. 36 and 38. The values of 3.8 and 4.0 for the MW 6,000 derivatives compare similarly with the 4.5 and 4.0 for the 18,000 MW derivatives.

The quartz beads were similarly XPS characterized; however, less extensive testing was performed, to demonstrate the stability of the PEO coatings. Table II summarizes the results of a single study, involving triplicate samples for each case. As mentioned in Section 2.2.1, the beads were pressed into indium foil for analysis in the spectrometer. Although indium was detected in the scans, any hydrocarbon contamination on the foil did not enter into the elemental percentages for the PEO. This was conveniently avoided due to the lack of conductivity of the glass beads leading the peaks to be charge shifted to lower binding energies. Distinct peaks of elements coming from the indium were discernable as can be seen in the carbon 1S spectrum seen in Fig. 39. The small peak at 284.2 ev is presumably hydrocarbon contamination on the indium foil.

3.2.2 Variable Angle XPS Thickness

Variable angle XPS analysis, modeling the thickness and homogeneity of the PEO layer, was performed using isocyanate derivatives of 6,000 and 18,000 molecular weights. In this case, the APS and PEO were assumed to be a homogeneous overlayer. Data were calculated according to the equations given above using λ for the carbon 1S peak of PEO of 30.8 Å and 35.1 Å for the silicon 2S peak of the quartz substrate. The results of these calculations for uniform and patchy overlayers of various thicknesses were plotted and the best fit graph is shown in Fig. 40. The actual values obtained for the 6,000 MW are represented by the astericks on the graphs. Only the ether carbon component of the total carbon signal was used in these calculations. Again, a least squares analysis of the data indicates that the PEO overlayer fits most closely with the

Table II

Elemental Analysis of PEO Stability
on Glass Beads

Time	C	O	N	Si
1	51	36	2	11
8	47	37	2	14
24	43	37	2	15
48	42	36	2	14
72	42	38	2	15

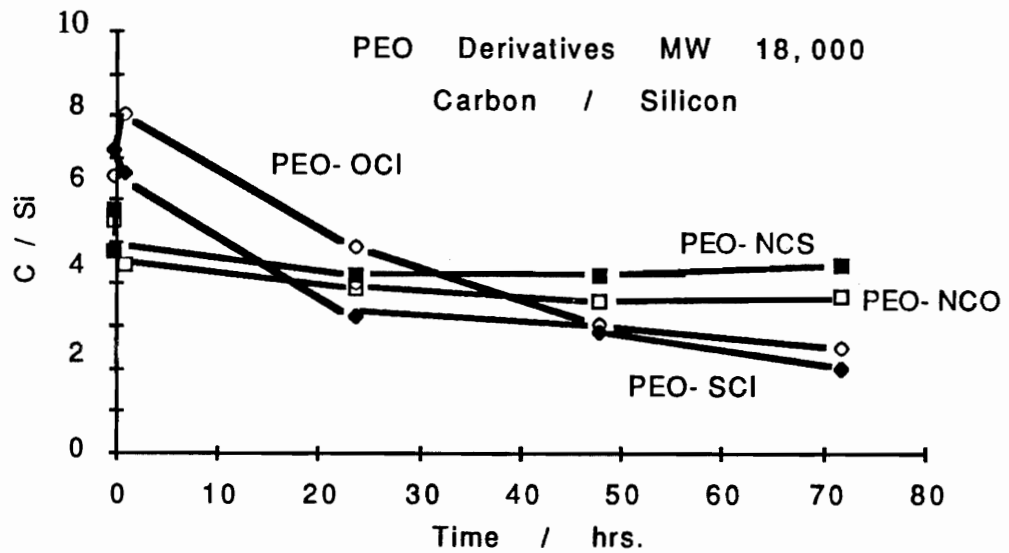

Figure 38. The carbon to silicon ratio of the XPS elemental analysis of the four PEO derivatized surfaces MW 18,000 as a function of PBS exposure time.

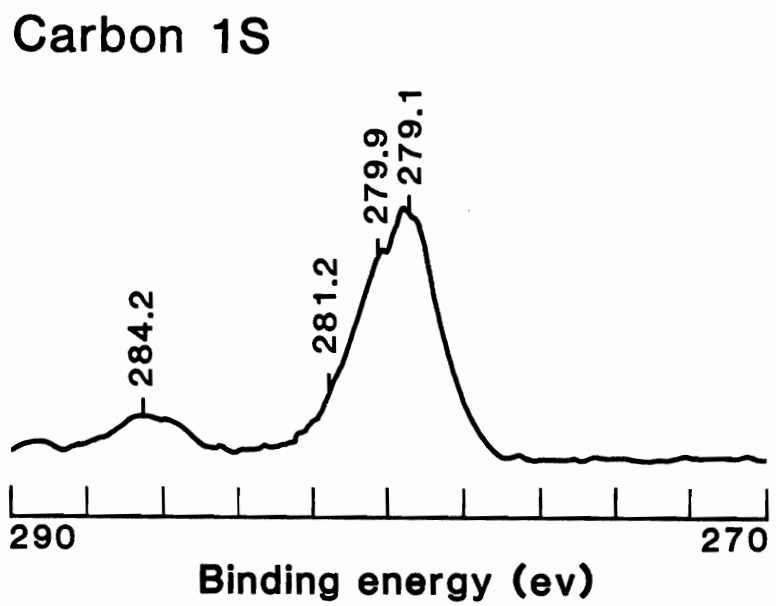

Figure 39. The carbon 1S spectrum of PEO derivatized glass beads. The small peak at 284 ev is the hydrocarbon contamination of the indium foil on which the sample beads were run.

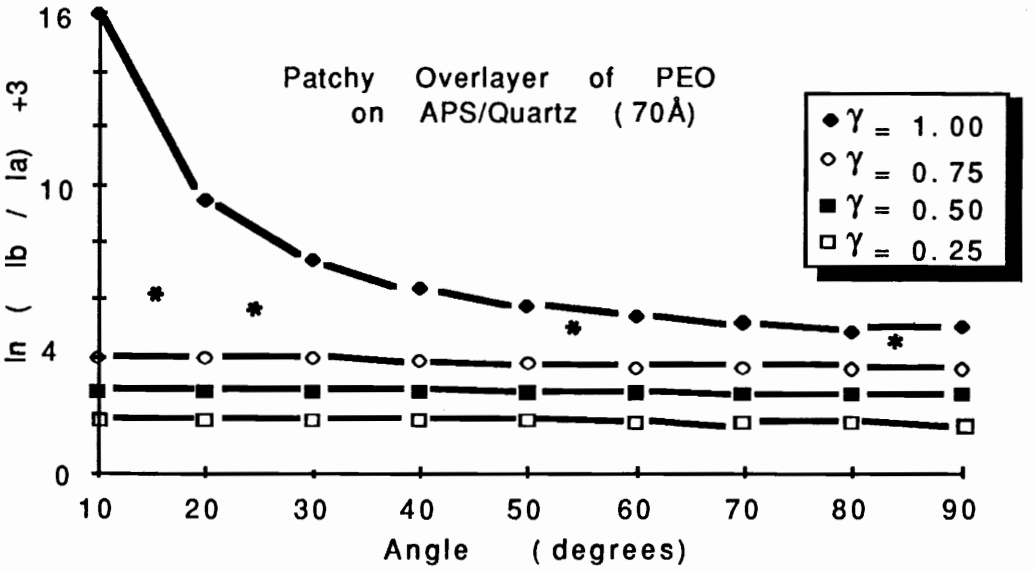

Figure 40. Plot of the equation for a theoretical 70 Å patchy overlayer of PEO on APS derivatized quartz for varying surface coverages (γ). The astericks (*) indicate actual data obtained in variable angle XPS experiments.

equation of a patchy 70 Å thick overlayer with 80 percent surface coverage. There was little detectable difference in the 6,000 and 18,000 molecular weights. This is presumably due to the collapsed nature of the polymer layer in the vacuum of the XPS spectrometer and will be discussed further in Section 4.1.

3.3 Heparin Coupling to Quartz Plates and Beads

3.3.1 XPS Stability Characterization of Surfaces

The heparin coupled surfaces were XPS analyzed for carbon 1S, oxygen 1S, nitrogen 1S, silicon 2S, and sulfur 2P. Pure as received heparin was compared with the heparin coupled surfaces. Table III shows the elemental analysis of the pure heparin powder and heparin immobilized via PEO-bis chloroformate and PEO-bis thiochloroformate (MW 3,400). The sulfur content of the pure heparin was found to be 6.9 percent. If the sulfur content is calculated by atomic ratios from the known heparin structure, this compares favorably with expected values. Of course, the sulfur content cannot be calculated exactly as a result of the heterogeneous nature of the heparin structure. If the PEO derivativized slides contained a thick homogeneous layer of heparin, the sulfur content should be about 7 percent. It will be remembered that XPS scans the top 50 Å of the surface, and since there is silicon detected from the substrate, it may be concluded that either the layer of PEO/heparin is less than this thickness or there is incomplete surface coverage by the overlayer. This will be discussed in the next section.

The sulfur 2P signal shown in Fig. 41 was used to monitor the stability of the heparin on the surface following exposure to PBS. The top spectrum is the sulfur 2P peak of pure heparin. The lower spectrum is immobilized heparin on a PEO-bis isothiocyanate spacer. The peak at 162.5 ev binding energy of the lower spectrum is the charge shifted 2P sulfur peak of heparin. The high resolution of

Table III

Elemental Content of Heparin and Heparin Derivatized PEO Surfaces (MW 3,000)

DESCRIPTION	C	O	N	Si	S	%CO
Na-heparin powder	45.5	45.3	2.5	0	6.9	
PEO-OCl + heparin	55.1	34.3	4.6	2.2	3.7	64.3
PEO-SCl + heparin	51.5	39.5	3.6	1.2	4.2	73.1

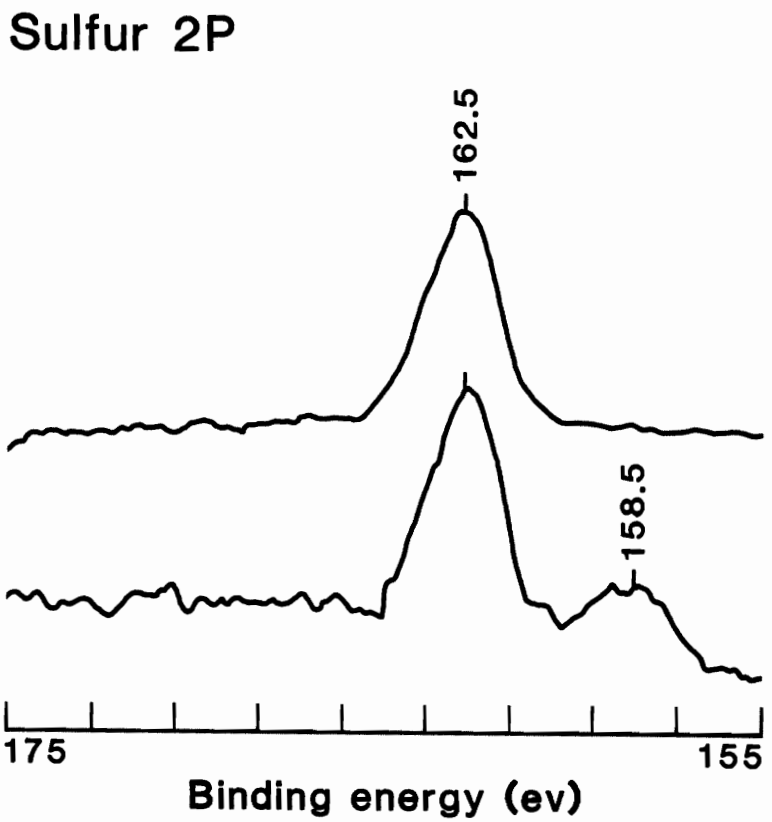

Figure 41. The sulfur 2P XPS signal from heparin. a) pure heparin powder; and b) heparin immobilized via PEO-bis isothiocyanate. The sulfur of the isothiocyanate is charge shifted enabling differentiation of the sulfur of heparin.

these spectra enables the sulfur 2P of the isothiocyanate PEO to be differentiated from the sulfur 2P of the heparin due to the less electronegative environment of the PEO alkyl sulfur. Only that portion of the sulfur 2P peak due to the heparin was used in the calculations.

Fig. 42 shows the sulfur content of the four MW 6,000 derivatized surfaces as a function of time. The clean quartz controls and a PEO-bis isothiocyanate derivatized slide without heparin are also plotted for comparison. The initial decrease in the sulfur signal indicates the heparin, like the PEO surfaces, was probably incompletely rinsed, resulting in unbound heparin on the surface. Over the 3 days tested, the heparin did not continue to leach from the surface after the initial loss.

The sulfur content of the cyanate derivatives was constantly higher after the 3 day soak than that of the chloroformate derivatives. This may not be statistically significant based on the margin of error of 10 percent for these data, but apparently the chloroformate/heparin derivatives are slightly less stable than the cyanate derivatives.

Fig. 43 shows the results of heparin coupling stability of the 18,000 MW derivatives. Again, after an initial loss from the surface, the sulfur content remains stable for a period of 3 days. This indicates a surface rich in heparin. The chloroformate derivatives appeared slightly less stable than the cyanate derivatives, as was true for the lower molecular weight surfaces. The clean quartz controls also appear on the graph. Data from the surface to which underivatized PEO was physically adsorbed, then reacted with heparin also appear on this graph. There is some binding of the heparin to this surface as can be seen by the 1.5 percent sulfur content. Presumably, this is bound via the free amine groups of the APS which would be expected to bind with the carboxylic groups of the heparin to a suface but does not benefit from the protein

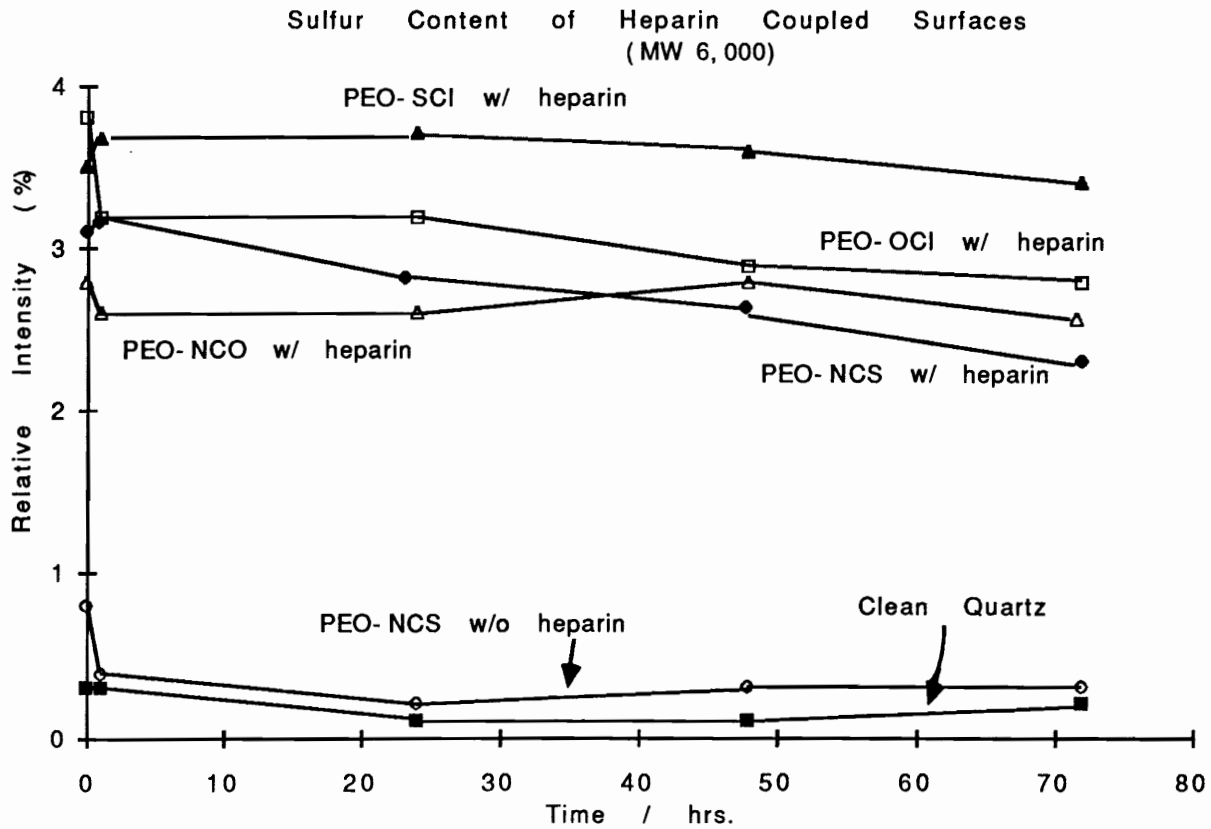

Figure 42. The sulfur 2P XPS signal of the four PEO/heparin surfaces MW 6,000 as a function of PBS exposure time.

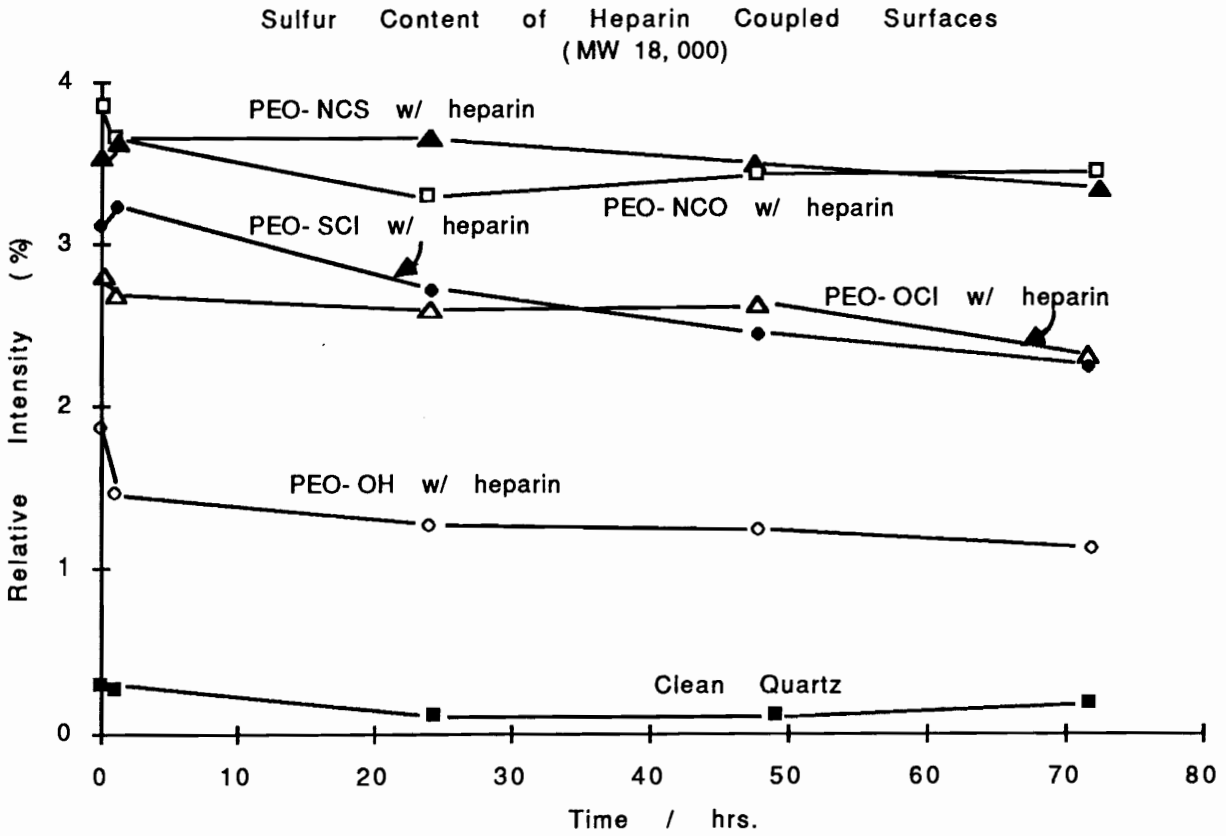

Figure 43. The sulfur 2P XPS signal of the four PEO/heparin surfaces MW 18,000 as a function of PBS exposure time.

resistance properties the PEO affords. This also involves blocking the heparin carboxylic groups which are necessary for activity.

3.3.2 Variable Angle XPS Thickness

Two different molecular weights of the PEOs with immobilized heparin were analyzed by variable angle XPS. The value used in the calculations for the mean free path (λ) of the sulfur 2P electron was 34.9 Å, while the photoelectron take off angle was varied from 4° to 80°. The calculations assumed the overlayer (APS, PEO and heparin) was homogeneous. The data were plotted on graphs of a patchy overlayer model of thicknesses from 70 Å to 100 Å. The assumption is not strictly valid but can be justified by the organic nature of the overlayer as opposed to the silicon substrate. This approach produced a large scatter in the data, presumably due to the small sulfur signal arising only from the heparin. Therefore, the intensity of the total carbon signal was used to account for the APS, PEO and heparin layers. The data were replotted using 30.8 Å for λ of the overlayer and fit to the curves modeling a patchy overlayer of 90 Å (Fig. 44) with 95 percent coverage. Considering the collapsed nature of the overlayer under the strong vacuum of the XPS spectrometer, this probably has little relevance to the thickness of the PEO/heparin layer in solution, where it is free to extend out from the surface with considerable mobility. It may be that if only 80 percent of the surface has grafted PEO, the heparin, while attached to one end of the PEO chain, actually lies collapsed in the "valleys" between the "mountains" of PEO. Perhaps more relevant is the concentration of the surface bound heparin.

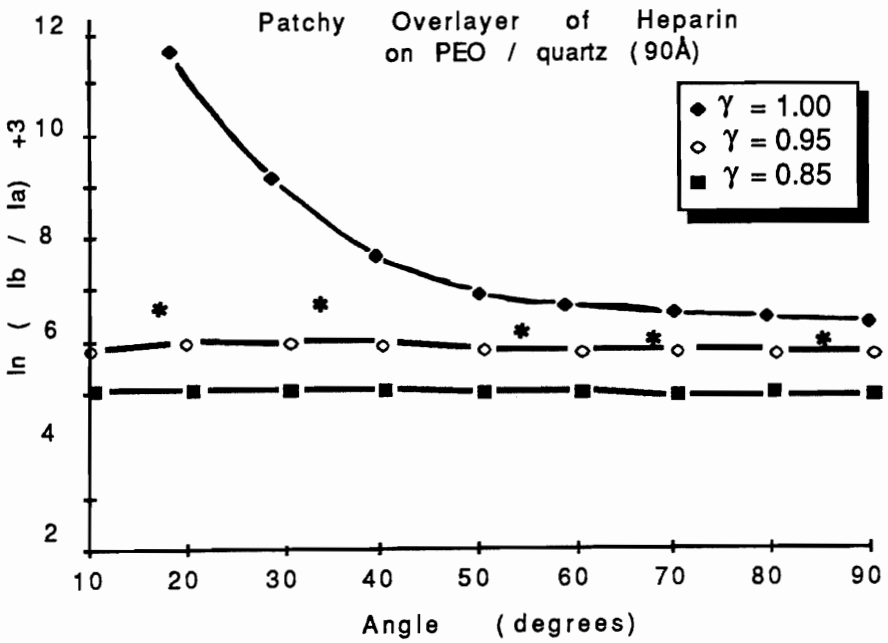

Figure 44. Plot of the equation for a theoretical 90 Å patchy overlayer of heparin on PEO coupled quartz surfaces for varying surface coverages (γ). The astericks (*) indicate actual data obtained in variable angle XPS experiments.

3.3.3 Quantitation

XPS is only relatively quantitative; therefore, for absolute quantitation the amount of heparin on the surface was measured using tritium labeled heparin. The dpm of the three replicates for each sample with known weights of beads were averaged and the amount of heparin calculated. Two different calculations were completed. In the first, the dpm/mg of beads were calculated, averaged for all five amounts of each molecular weight, and divided by the specific activity of the heparin to yield the amount of heparin per mg of beads. The second calculation used the surface area of the beads of each sample, calculated by the known weight and the density (2.0 g/cm^3) to obtain ug/cm^2.

The five weights of beads used for the 6,000 molecular weight derivatives averaged 53.9 $\pm$ 6.5 dpm/mg of beads. The 18,000 molecular weight derivatized surfaces were slightly less than this: 42.3 $\pm$ 5.1 dpm/mg of beads. One possible explanation for this result, is that the heparin immobilization method requires a totally organic solvent system. Formamide is not a particularly good solvent for PEO which may have caused the PEO chains to collapse and coil among themselves, prohibiting the reactive end groups from coupling with the heparin. In the case of the 18,000 MW derivatives, increased chain length may translate to more densely coiled chains on the surface.

Another possible explanation for the lower amount of heparin with longer chains, is that heparin may have multiple attachment sites; i.e., one molecule of heparin may be coupled with more than one PEO chain. This could result from the higher flexibility of the longer chains.

Expressing the amount of heparin per unit surface area, the derivatives ranged from 1.159 to 0.945 ug/cm^2 and 0.936 to 0.672 ug/cm^2 for the 6,000 and 18,000 molecular weight derivatives, respectively (Table IV). All values are on the low end or lower than obtained by other investigators immobilizing heparin

Table IV

Quantitation of Surface Immobilized
Tritiated Heparin

	Surface	average dpm/mg beads	surface bound mg/cm^2
without heparin	Clean	1×10^{-4}	2.15×10^{-6}
	PEO-NCO 18,000	1×10^{-4}	2.15×10^{-6}
with heparin	PEO-NCO 6,000	53.9	1.052
	PEO-NCO 18,000	42.3	0.901

via other methods. However, comparison is difficult due to major differences in method of surface attachment, derivatization of the heparin prior to immobilization, and the substrate used. What is more important is the activity of the heparin expressed as an activity per unit surface area. It is this figure which expresses the usefulness of the surface.

3.4 Protein Adsorption Studies

3.4.1 Total Internal Relfection Fluorescence (TIRF)

In order to test whether or not the intrinsic fluorescence of the protein was quenched by PEO, bulk transmission spectra were taken in the presence and absence of PEO ranging in concentration from 5×10^{-2} to 5×10^{-6} M. Fig. 45 shows the results. The two most concentrated solutions of PEO attempted, 5×10^{-2} and 2.5×10^{-2} M, caused precipitation of the protein. At 5×10^{-3} M PEO concentration, there was approximately a 15 percent reduction in the signal due to the presence of the PEO. This is very near the concentration required for precipitation of the protein. However, this is a bulk transmission experiment and extrapolation of these results to a surface on which the PEO is immobilized and protein near in solution assumes that the quantum yield of the protein does not change upon adsorption. This has been shown to be erroneous by Reinecke in the case of IgG adsorption to clean quartz. (138) For this reason, quantitation of the adsorbed protein was not attempted. Only relative comparisons of the TIRF signal can be made with any validity.

Table V reports the fluorescent signal of the adsorbed protein on the surfaces of clean quartz, APS derivatized quartz, PEO-bis chloroformate (MW 3,400) and a PEO derivatized surface to which heparin has been coupled. The top number of each group is the signal prior to the buffer flush and represents both the bulk and adsorbed protein. The bottom number of each box is the signal

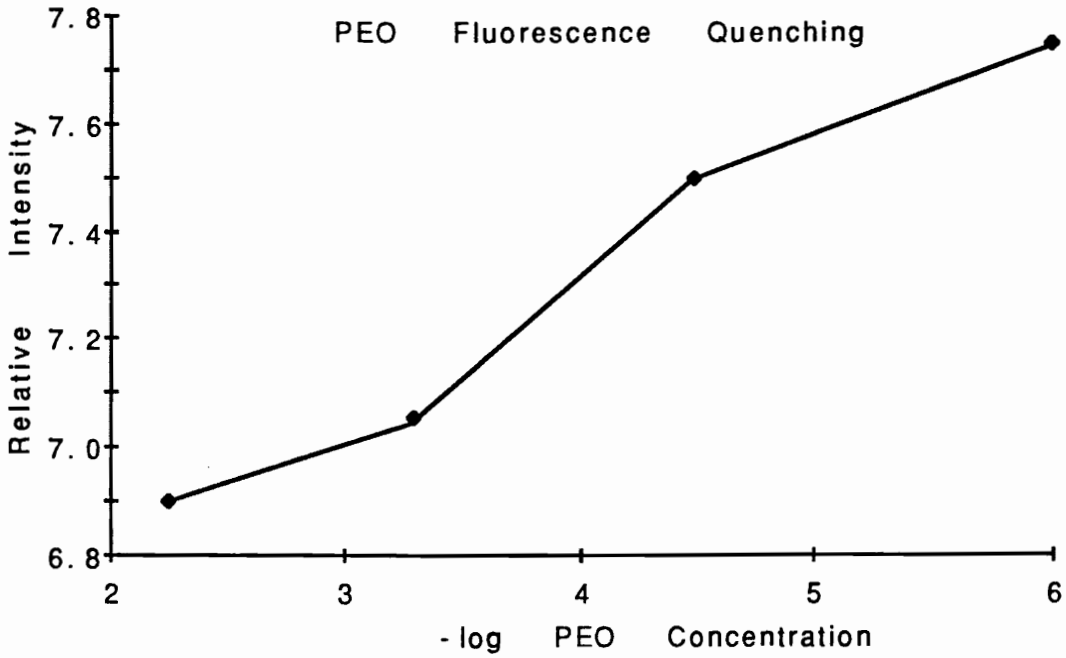

Figure 45. Quenching of the TIRF signal due to the presence of increasing concentrations of PEO.

Table V

Protein Adsorption From Solution
Measured by Total Internal
Reflection Fluorescence

	Clean Quartz	APS Quartz	PEO/APS Quartz	Heparin/PEO APS Quartz
0.25 mg/ml AT-III	445 175 (21)	1980 1300* (12)	505 90 (13)	335 140 (17)
0.50 mg/ml AT-III	1215 375 (7.5)	2075 1450* (56)	727 123 (19)	535 190 (18)
1:10 dilution Plasma	3875 2575 (73)	5414 3750* (63)	1608 134 (27)	1580 335 (37)

arising strictly from protein adsorbed on the surface. All values have been corrected for background. This was a step isotherm experiment with solutions of higher concentration being adsorbed subsequently. As expected, the clean quartz control adsorbs protein from even the dilute solution of AT-III and adsorbs more from increasingly concentrated solutions.

The APS derivatized surface shows anomalous behavior. During the adsorption of the tryptophan standards, the signal increased to the values given in the top of each box. Subsequent flushing with buffer did not bring the signal back to background levels. This is apparently due to binding of the free amine groups of the APS to the carboxylic groups of the tryptophan. Before standards were run, the background signal was 373. Following the standards, the background was 1127. Subtracting this from the signal following buffer flush, the corrected values for APS are 173, 323, and 2623 for the 0.25, 0.50 mg/ml AT-III and plasma, respectively.

The PEO derivatized surface showed the least protein adsorption from all three solutions. While some adsorption was noted by the 134 value following adsorption of the diluted plasma, this can be considered negligible in reference to the control surfaces. These data represent the results of four different experiments for each surface. The standard deviation is given in parentheses.

The heparin coated surfaces adsorbed slightly more protein than the PEO derivatized surfaces, but considerably less than either of the control surfaces. This follows the expected results that the heparin would bind the AT-III; however, nonspecific adsorption of the heparinized surface would be minimized by the presence of the PEO. Plasma levels of AT-III in the normal human male are approximately 0.2 $\pm$ .05 mg/ml. This is approximately equal to the concentration of AT-III of the first step of this isotherm experiment. However, at the higher concentration of AT-III used in the next step, slightly more protein

was adsorbed by the heparin surface. This would indicate that the surface bound heparin was not saturated by the less concentrated AT-III solution.

Heparin is known to bind numerous other plasma proteins. This may account for the increase in the fluorescent signal following the diluted plasma adsoprtion. Still, this adsorption is nearly an order of magnitude less than either of the control surfaces indicating that the nonspecific adsorption seen on the other surfaces has been minimized by the presence of the PEO.

3.4.2 ^{125}I-Labeled Proteins

The results of two bovine serum albumin adsorption experiments are given in Table VI. In the first experiment, the ratio of unlabeled to labeled protein was 100:1, and for the second the ratio was 84:1. Each chip was individually measured for exact surface area, three chips of each derivative and molecular weight were counted. Two derivatives, PEO-bis chloroformate and PEO-bis isothiocyanate, were used being representative of the least and most stable of the four derivatives tested for aqueous stability. The amounts of BSA adsorbed on clean quartz and APS derivatized quarts agree with each other well and are not significantly different from values of IgG found on the same surfaces by Reinecke. (138)

All four of the PEO derivatized surfaces showed reduced adsorption by nearly a factor of 10 than either of the controls. Interestingly, there is a factor of two difference between the chloroformate derivatives of different molecular weights but not an appreciable difference for the cyanate derivatives. Nagaoka, using varying lengths of PEO as the soft segment of a block copolymer system, found that no difference in the protein adsorption characteristics could be detected after $n \geq 100$. (9) For PEO molecular weight 6,000, n = 135 units and for the MW 18,000, n is approximately 400 units. Possible explanations for the

Table VI

Adsorbed ^{125}I-Proteins Onto PEO and PEO/Heparin Surfaces

SURFACE	BOVINE SERUM ALBUMIN	HUMAN ANTITHROMBIN-III
Clean Quartz	0.571 + 0.038	0.691 + 0.145
APS Quartz	0.379 + 0.051	0.429 + 0.125
PEO-OH (adsorbed)	0.296 + 0.067	0.312 + 0.045
PEO-OCl 6,000	0.073 + 0.011	0.127 + 0.015
PEO-OCl 18,000	0.034 + 0.025	0.091 + 0.025
PEO-NCS 6,000	0.081 + 0.027	0.025 + 0.015
PEO-NCS 18,000	0.062 + 0.033	0.098 + 0.048
PEO-OCl 6,000 + HEPARIN	0.084 + 0.012	0.857 + 0.015
PEO-OCl 18,000 + HEPARIN	0.058 + 0.029	0.593 + 0.048
PEO-NCS 6,000 + HEPARIN	0.080 + 0.014	0.863 + 0.045
PEO-NCS 18,000 + HEPARIN	0.072 + 0.029	0.800 + 0.016

observed results might be due to the difference in stability of the derivatives. This will be discussed in Section 4.2.

The surfaces with the immobilized heparin did not adsorb more albumin than the PEO surfaces without heparin. This is as expected; albumin is not known to specifically bind heparin.

The results of the single adsorption experiment using AT-III are also found in Table VI. Although triplicates of each surface were tested, only enough protein was available for adsorption from a single solution of AT-III. Assuming the results of this single experiment are valid, all surfaces adsorbed more AT-III than albumin. The clean quartz adsorbed 0.69 ug/cm^2 as opposed to 0.57 ug/cm^2 for albumin and the APS adsorbed 0.43 ug/cm^2 of AT-III and only 0.38 ug/cm^2 albumin. All proteins are known to have different adsorption characteristics on different surfaces which is one reason that blood materials interactions is such a complex field. The PEO coupled surfaces, while exhibiting the same trends seen with the albumin adsorption, show considerably more adsorption of AT-III than albumin. Still, the amount of protein on these surfaces is less by a factor of three than the controls. However, no difference was found between the two molecular weights of PEO.

An interesting finding of this experiment is the immobilized heparin surfaces adsorbed four times more AT-III than the PEO surfaces without heparin. This alone indicates that the heparin has retained at least some of the AT-III binding activity in the immobilized state. Apparently, the heparin immobilization procedure did not block the necessary AT-III lysine binding site.

Quantitation of adsorbed protein by radiolabeling procedures is controversial. Conflicting results have been reported for preferential adsorption of labeled or unlabeled protein. Bornzin and Miller found no change in the adsorption of albumin on silicone rubber and Cuprophan or fibrinogen on silicone

rubber. (139) Horbett found similar results for fibrinogen, hemoglobin, albumin, and lgG on polyethylene. (140) However, Van Der Sheer showed significant alteration in the adsorption properties of human serum albumin on polystyrene latex. (141) In any case, preferential binding appears to be dependent on the surface, radionuclide, and the protein used and caution must be exercised when interpreting results.

No tests were performed in this study to determine preferential binding of the labeled protein. The only conclusion that can be drawn is that these results support those seen in the TIRF experiments using unaltered protein. The PEO surfaces adsorb less total protein than the controls, and less than the heparinized surfaces in the case of the AT-III.

3.5 Whole Blood Clotting Times

The PEO derivatized surfaces, of both molecular weights, were tested for whole blood clotting times. This was done as a screen to determine which of the derivatives would be tested further for heparin activity. The results are shown in Table VII, where the number of triplicate tests run is indicated by n and the standard deviation is given in parentheses. As was mentioned previously, the heparinized surfaces initially failed to clot the blood and required more extensive washing procedures. The results in the table are those obtained following the extra rinsing procedures.

The PEO surfaces without heparin produced a slight increase in clotting time over the controls, with both molecular weights averaging approximately 17 minutes. There was no detectable difference in the two molecular weights or between any of the four derivatives. The surfaces with the immobilized heparin produced significant increases in the time required to clot the blood. The only difference between the four derivatives coupled with heparin was noted in the

Table VII

Whole Blood Clotting Times

Surface	MW 18,000	MW 6,000
Clean Glass n=5	6 (±0.9)	---
APS Glass n=5	17 (±1.5)	---
PEO(adsorbed) n=3	9 (±3.0)	8.5 (±2.0)
PEO-OCl n=5	18 (±4.0)	16 (±3.5)
PEO-SCl n=5	12 (±3.0)	17 (±3.0)
PEO-NCO n=7	21 (±1.5)	17 (±3.0)
PEO-NCS n=7	18 (±2.5)	21 (±2.5)
PEO OCl HEP n=8	89 (±5.5)	98 (±6.0)
PEO-SCl HEP n=8	109 (±4.0)	106 (±7.0)
PEO-NCO HEP n=8	82 (±3.0)	78 (±5.0)
PEO-NCS HEP n=8	79 (±2.0)	85 (±6.0)
Beads first soaked in PBS for 72 hours pH 7.4:		
CLEAN n=3	6.5 (±1.0)	---
PEO-OCl HEP n=5	69 (±4.5)	---
PEO-SCl HEP n=5	87 (±5.0)	---
PEO-NCO HEP n=5	53 (±6.0)	---
PEO-NCS HEP n=5	63 (±7.5)	---

thiochloroformate derivatized surface. No explanation for this is apparent except that the standard deviation of the eight tests run is larger for this sample. Again, there was no detectable difference between the two PEO molecular weights.

In addition to the new rinsing procedures, beads exposed to PBS for 72 hours were also tested for clotting times in order to determine if there was loss of activity after this time period. A 25 percent decrease in the time to clot was observed. This loss of activity could have resulted from two sources: either there was leaching from the surface leading to a decrease in the amount of heparin available, or the heparin which was present lost activity due to degradation. Leaching of the surface bound heparin is unlikely based on the results of the radiolabeled and XPS stability analyses; however, degradation would not be expected to occur under these conditions. Heparin is a very stable molecule.

The beads and tubes had a total surface area of approximately 66 cm^2. Using the average amount of heparin of 0.75 ug/cm^2 determined from the ^3H-labeled heparin, this translates to 3 mg total heparin in 1 ml of blood for each sample.

3.6 Activated Partial Thromboplastin Times

A standard curve was generated by using known amounts of heparin in plasma. Known weights of PEO derivatized beads were incubated with the same plasma used in the generation of the standard plot, and APTTs were determined. Since no detectable differences in the whole blood clotting time were observed between the two molecular weights, only the 18,000 MW derivatives were tested. From the standard curve, amounts of heparin per ml plasma were calculated.

The APTT of the various quantities of immobilized heparin beads is given in Fig. 46. The well washed heparin/PEO beads demonstrated anticoagulant activity as shown by the prolonged APTT. The increase in clotting time was directly proportional to the amount of heparinized beads added to the plasma. PEO derivatized and clean beads without heparin had no significant effect on the clotting times.

Activities of the immobilized heparin as determined by APTT tests and the average activity of heparin/mg (average of 1.05 ug/cm^2 and 0.90 ug/cm^2 for the 6,000 and 18,000 molecular weights, respectively) are presented in Table VIII. These data are averages of the various amounts of beads used to calculate activity. The standard deviations are given in parentheses. The control surfaces, the clean, APS and PEO derivatized beads without heparin were found to have less than 0.001 U/ml plasma. The heparin, as received, was reported to have an activity of 157 U/mg. Based on the APTT test, the bound heparin appeared to have approximately 25 percent of the activity of the comparable amount of heparin in solution. There appeared to be no significant differences in these values for the two derivatives or for the two molecular weights of PEO used. The 18,000 molecular weight derivatives, while having less immobilized heparin on the surface (dpm/mg beads), did not have less activity per mg of heparin as can be seen in the table. For this reason, it was important to report the activity of the heparin in U/mg heparin rather than in U/mg beads.

The activity of these surfaces is significantly higher than that reported by Sefton using Diosynth heparin immobilized to poly(vinyl alcohol) beads. (142) However, he notes that the size of beads used had a large influence on the resultant activity; the smaller the beads the higher the activity observed. The beads used in this study were 50 um. The smallest beads used by Sefton were 105

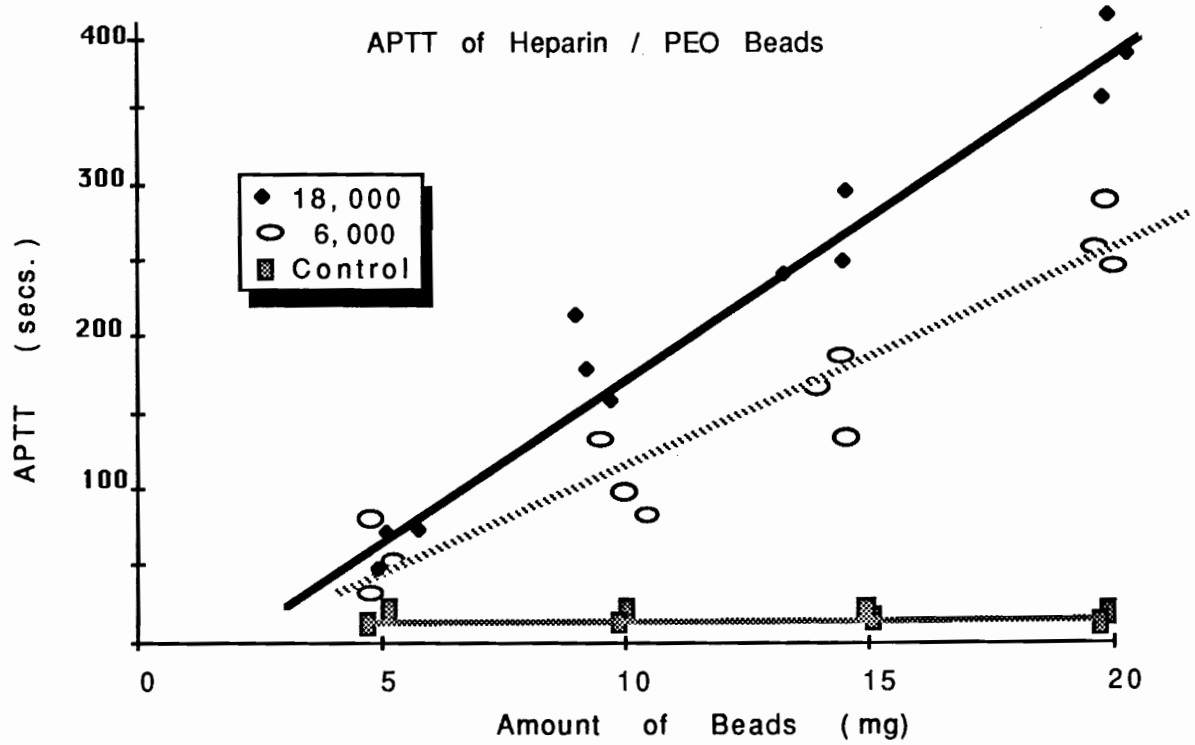

Figure 46. The Activated Partial Thromboplastin Times of various quantities of immobilized heparin/PEO glass beads.

Table VIII

Activity of Immobilized Heparin
Surfaces Determined by APTT

SURFACE	HEPARIN CONC. (U / ml plasma/ mg beads)	HEPARIN ACTIVITY (U / mg Heparin)
PEO- OCI 6,000	3.3×10^{-2}	39.4 (+ 3.6)
PEO- NCS 18,000	2.64×10^{-2}	37.9 (+ 4.9)

um and found to have only 0.26 percent activity. No reasons were suggested for this size/activity relationship.

Ebert *et al.* found a difference in activities of immobilized heparins on diaminoalkane-agarose dependent upon chain length of the spacer for attachment and chemistries of immobilization reactions. (143) Prior to immobilization, Ebert *et al.* used various derivatization procedures with little loss of activity. While it is difficult to directly compare amounts of heparin on the surface because they report amount/cc swollen gel, the time to clot of the immobilized heparins was very similar to the results found here.

3.7 Platelet Retention

The retention of platelets by the derivatized surfaces was determined using both whole blood and platelet rich plasma (PRP) in order to see if the presence of other cellular material influenced the adsorption behavior of platelets. The platelets present in the plasma, following incubation with derivatized beads, were counted, normalized to the amount of heparin present and plotted as a function of time of incubation. Fig. 47 shows the results of typical curves generated in these experiments.

A modification of Merrill and Salzman's mean platelet retention index (73) was developed in order to report a single value reflecting the adsorption behavior of platelets by these surfaces. The mean platelet retention index ($\bar{p}$) is defined by:

$$\bar{p} = 1 - \left(\frac{1}{n_t} \sum_{1}^{n_t} r_t\right)$$

where:

$$r = \frac{\text{number of platelets at time t}}{\text{number of platelets at time O}}$$

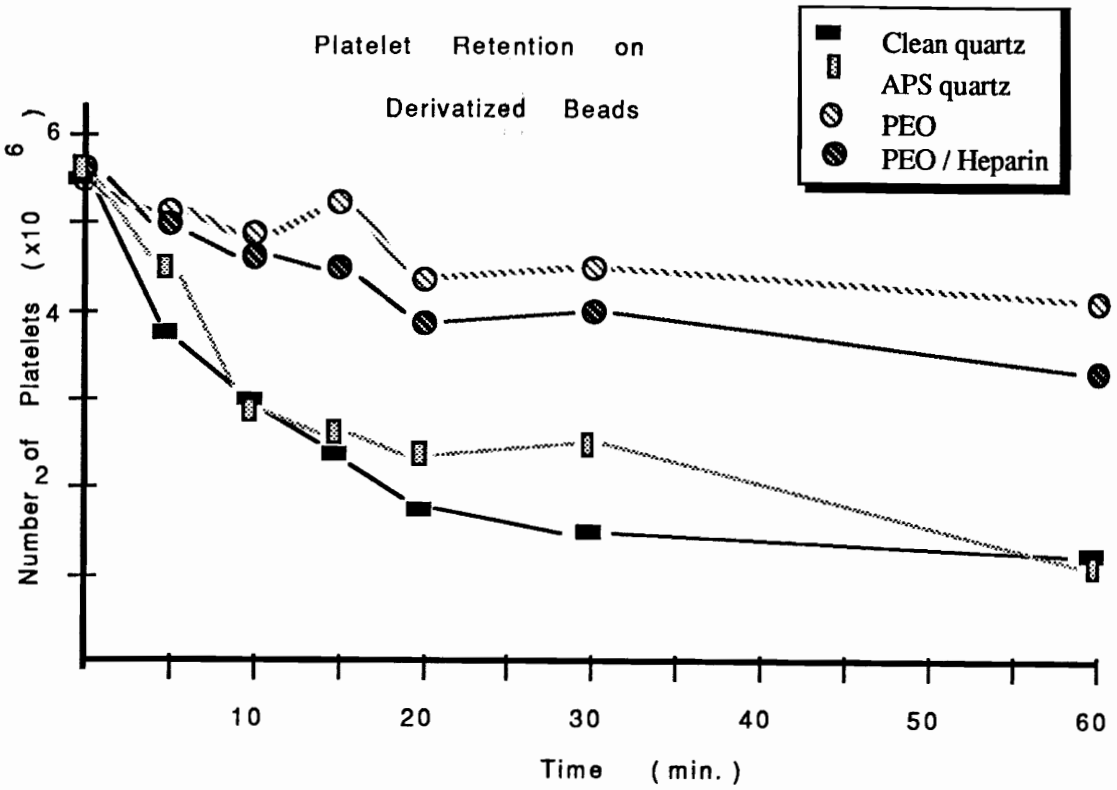

Figure 47. A typical curve generated in the platelet retention studies using immobilized heparin beads plotted as a function of whole blood incubation time.

This convenient index premits the comparison of different surfaces regardless of the amount of time of exposure. Table IX reports the indices of retention found by all surfaces tested using both whole blood and PRP. Values were normalized to clean glass. All PEO surfaces without heparin had values for the retention index significantly below those of the controls. All surfaces with immobilized PEO/heparin complexes had an intermediate value between the controls and the PEO without heparin. This indicates that there are virtually no platelets retained by the PEO coupled surfaces supporting the theory of Nagoaka and others that PEO adsorbs minimal numbers of platelets. It also indicates that the heparin surfaces have a slightly higher affinity for platelets than PEO by itself, although the heparin surfaces adsorb significantly fewer platelets than any of the surfaces without PEO or heparin.

The conclusion that PEO is an efficient surface for minimizing platelet retention is also valid with heparin immobilized to the PEO chains. This is presumably due to the high flexibility of the PEO chains on the surface which exclude platelets from interacting. Previous studies of the interactions of heparin and platelets are conflicting. The presence of heparin causes markedly greater platelet retention on glass bead columns. (144, 145) Heparin has been shown to independently induce and potentiate platelet aggregation and release reactions caused by exogenous agents; high molecular weight heparin fractions being more deleterious to platelet functions than low molecular weight fractions. Platelet interaction studies by Salzman *et al.* on a cellulose/ethylene imine/heparin surface demonstrated high degrees of platelet adhesion *in vitro.* (146) The authors concluded the adverse platelet interactions were due to increased fibrinogen adsoprtion. If this result is true, then the PEO/heparin system would eliminate such problems by the exclusion of all nonspecifically adsorbed proteins.

Table IX

Mean Platelet Retention Index for Whole Blood and Platelet Rich Plasma

	Surface	$\bar{\rho}$ Whole Blood	$\bar{\rho}$ PRP
no heparin	Clean Quartz	1.00	1.00
	APS Quartz	0.86	0.83
	PEO-OCl 6,000	0.25	0.27
	PEO-OCl 18,000	0.14	0.21
	PEO-NCS 6,000	0.21	0.30
	PEO-NCS 18,000	0.19	0.24
with heparin	PEO-OCl 6,000	0.77	0.71
	PEO-OCl 18,000	.068	0.59
	PEO-NCS 6,000	0.72	0.67
	PEO-NCS 18,000	0.65	0.61

There was little difference observed in the platelet retention index when the surfaces were exposed to either whole blood or platelet rich plasma. While the numbers of platelets retained by the surfaces in the presence of other blood components, i.e., whole blood, were considerably more (4.3×10^6 versus 3.2×10^6 after one hour exposure time), this is not reflected when the data are normalized for the number of platelets in the whole blood or PRP before exposure.

3.8 Platelet Factor 4 Release

The adsorption of platelets does not necessarily correlate with their activation. Activation and degranulation of platelets were monitored in platelet rich plasma exposed to the heparin surface. Initially, 120 mg of beads of the PEO-bis chloroformate were incubated for various lengths of time before measuring the PF4 release. The standard curve is shown in Fig. 48 and the sample results are shown in Fig. 49. In the period from 0 to 60 minutes exposure time, no difference in the PF4 plasma levels was observed. The PEO surfaces without heparin show slightly less PF4 released than the controls, but the heparin coupled surfaces were indistinguishable from the controls for each of the times tested. Very little difference (less than 10 percent) was seen between plasmas exposed for 5 minutes and those exposed for 60 minutes.

The next set of experiments measured PF4 levels in plasma after 1 hour of exposure to differently derivatized beads. A standard curve was generated for each test. The results were normalized for the amount of heparin on the beads. No difference was noted in the PF4 levels between any of the derivatives or between the heparin coupled beads and the controls. The PEO surfaces without heparin again had only slightly less PF4 bound than either the controls or the heparinized surfaces. The average level of PF4 was 20 ± 1.6 ng/ml plasma in all

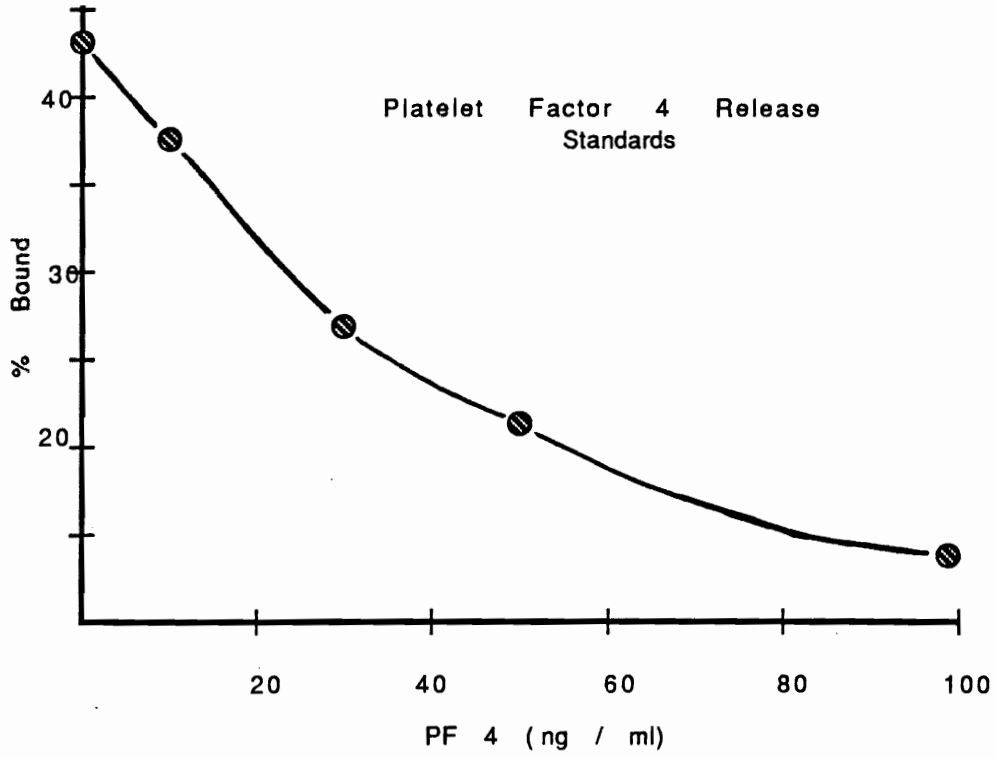

Figure 48. A typical standard curve generated during each series of the sample Platelet Factor 4 release studies.

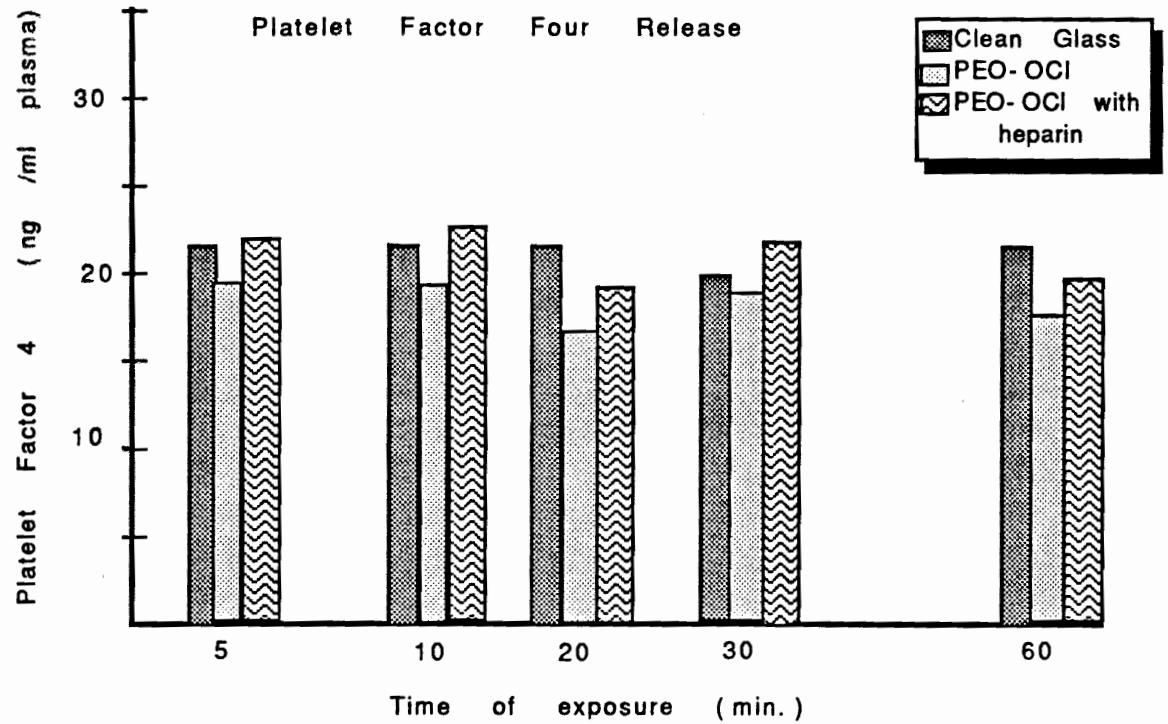

Figure 49. Platelet Factor 4 levels in plasma exposed to derivatized beads for various times with and without heparin.

the PEO derivatized surfaces regardless of the time of incubation. The controls and the heparinized surfaces averaged approximately 23 $\pm$ 0.9 ng/ml plasma.

Relating these data to those of platelet retention reported in the previous section, some interesting facts emerge. The PEO surfaces without heparin retained significantly less platelets than either the controls or the PEO surfaces onto which heparin was immobilized. The fact that no difference is seen in the PF4 levels of the control and sample surfaces indicates that the adherent platelets on the PEO apparently are more highly activated to release their granule contents. Why this should occur is unclear. It may be that the sensitivity of the PF4 assay is not adequate to distinguish between small variations in low levels of PF4. Or the conclusion may be reached that while PEO surfaces do not permit much adsorption of platelets due to the reasons discussed above, those that do avoid the steric and entropic repulsion and reach the surface are activated by the immobilized PEO. Why this might happen is subject for speculation.

CHAPTER 4

DISCUSSION

4.1 Poly(ethylene Oxide) Derivatization

Poly(ethylene oxide) and its derivatives are widely used in various branches of industry. Replacement of the hydroxyl groups by primary amine groups has been reported by a variety of methods, some of which have minimal chain scission or branching problems. (147, 148, 149) The method reported here uses very mild conditions without the use of pyridine which has been reported to cause chain scission in the preparation of diamino PEO. (150) An 85 percent conversion of PEO to PEO-diamine was found by titration with perchloric acid and acetic acid anhydride. This produced a highly soluble, amine terminated polymer for reaction with phosgene. More direct routes have been reported for the isocyanate derivatization of PEO; however, this method was found to produce little chain branching, scission and a highly water soluble polymer. However, infrared spectroscopy showed the end product to be quite labile unless stored under nitrogen. This is one advantage of the method reported here.

The coupling reaction to the primary amine of the APS coupling agent occurred readily for all the derivatives tested. The chloroformates appear to couple more readily but are slightly less stable once immobilized than the isocyanate derivatives. The difference in stability between the isocyanate and chloroformate terminated derivatives could possibly be due to the relative instability of the resulting urethane linkage when bonded to APS with respect to the urea linkages formed by the isocyanate and isothiocyanate derivatives. The

urea linkage is presumably stabilized in the aqueous solution by the resonance cation:

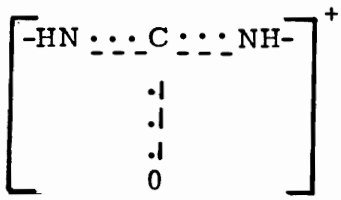

This same linkage is involved in the immobilization of the heparin to the PEO isocyanate derivatives. These also were found to be more stable.

The stability of these surfaces was monitored for three days. Longer term testing is necessary before this surface modification technique could become practical. However, a number of practical applications such as blood oxygenators and dialyzers could benefit from a protein resistant surface for even short times.

A large number of factors are involved in the stability of a polymer grafted to a surface and immersed into an aqueous salt medium. It is well known that aliphatic ethers react with oxidizing agents such as oxygen to form hydroperoxides which can degrade, generally by chain scission. (33) This reaction may be catalyzed by certain metals such as ferrous, copper and silver ions. Bailey, Callard and Lundberg, in an unpublished study, found that aqueous solutions of PEO undergo a rapid decrease in viscosity at pH 4 if the solutions are contacted with an iron rod. (121)

Solutions of PEO are also sensitive to light exposure. (151) Significant decreases in viscosity due to ultraviolet light can be attributed to a free radical degradation mechanism. (152) In the immobilization reactions of this thesis, although the initial coupling reaction was carried out under nitrogen, no rigorous precautions were taken to exclude air and room light. The slides of the PBS

hydration study were handled using steel forceps which could have been a source of ions leading to chain degradation. Although the pH of the solution was 7.4, it may have caused chain scission. Even so, the XPS data indicate a surface rich in PEO, particularly for the 6,000 isocyanate and isothiocyanate derivatives. The greater stability of these derivatives would be expected over the higher molecular weight derivatives since the higher polymers are more susceptible to degradation. (152, 153)

4.2 Protein Resistance of PEO Surfaces

The four derivatives of PEO did not show significantly different abilities to resist protein adsorption (Table VI). This is not unexpected as there would be little difference in the surface seen by the proteins. The isocyanate derivatives are amine terminated and the chloroformate functionalities revert to hydroxyl groups after exposure to water. The small difference these end groups make in comparison to the long polymer chain is probably negligible. With no difference observed between the derivatives in terms of protein adsorption, it would then be beneficial to use the one providing the most stability; i.e., one of the isocyanate or isothiocyanate derivatives for further testing.

An interesting point is the difference between the amount of protein adsorped by the chloroformate derivatives of different molecular weight but not by the different molecular weight cyanate derivatives. A possible explanation for this might be the fact that the chloroformate surface has less PEO on the surface as exhibited by the 35 percent ether carbon content as compared to the 45 percent for the cyanate derivatives. Although there was no difference in the surface coverage determined by the variable angle XPS data, the layer under the conditions of the XPS spectrometer is collapsed and condensed. The surface density of the grafted PEO under fully hydrated conditions may allow for much

greater flexibility of the less densely packed polymer surface. Why this is true for the chloroformate derivatives and not for the isocyanate or isothiocyanate derivatives remains unclear. Tanford found that the excluded volume of a surface decreases as the molecular crowding increases. (154) This is to say, there should be an optimal packing density of polymer chains on the surface to promote protein resistance. Nagaoka reports the surface mobility of grafted PEO chains is maximal when n, the number of repeat units is near 100. This translates to a molecular weight of approximately 4,500 (155). The protein resistance of a surface was found to be more effective if long chains with free ends were grafted to a surface rather than formed in a network or block system.

The conditions in this study were optimized for maximum PEO coupling to the surface by varying the concentration of the PEO in solution. No attempt was made to determine the protein resistance of surfaces without the maximum amount of PEO coupled to them. Other than the TIRF studies in which a PEO of 3,400 MW was used, no lower molecular weight PEO was tested for the protein resistance behavior. There would, of course, be advantages to using the lowest molecular weight PEO possible which still minimizes the protein adsorption. Lower molecular weight derivatives of the PEO are easier to synthesize and more efficiently coupled to the surface. Higher molecular weight polymers are more subject to chain scission and branching. From the results of the protein binding studies, it may be concluded that the 6,000 molecular weight derivatives do not adsorb sufficiently more protein as to necessitate using any longer chains.

The amount of protein adsorbed by these PEO grafted surfaces is very similar to those reported by Nagaoka using methoxy poly(ethylene glycol) monomethacrylate with PEO side chains of various chain lengths. With n=100, the hydrogels synthesized by this group, with a water content of 45 percent, were found to have a 0.1 ug/cm^2 which was considered to be negligible. (155)

Pekala and Merrill found that the surface of polyurethanes, with increasing molecular weight of the PEO block, consisted of at least 95 percent of the ethylene oxide of the PEO block. This surface, which is highly swollen with bound water, did not favor the adsorption of platelets. (156) The picture which emerges from this and other investigations is the extension of the PEO chains from the surface, whether those chains are incorporated into the network or grafted on the surface. The repulsive forces which prohibit protein adsorption are generated by the loss of possible chain conformations as the volume available to the grafted chains is reduced due to the approaching species, i.e., the protein and polymer chains.

The dynamic nature of protein adsorption to polymer surfaces has been investigated extensively. Reports using protein solutions show isotherms with monomolecular layer formation on the surface which fail to adsorb more protein with higher bulk protein concentration. However, in the long-term implants, multilayers are formed due to the rearrangement and exchange of protein by the surfaces. Adsorption must be considered a time dependent process. Matsuda has proposed a multilayer proteinaceous passivation mechanism for long term antithrombogenicity which requires up to 2 weeks before hematological parameters return to normal levels. (157) However, in order for irreversible adsorption and adhesion to occur, blood components have to be in contact with the surface more than a certain measure of time. The rapid mobility of the hydrated PEO chains may prevent stagnation of the blood components on the surface because the contact time is too short.

The protein concentration in plasma is quite high (approximately 8g/dl) compared to those used in the radiolabeled protein adsorption experiments. This gives a different physiochemical process for adsorption. In a highly concentrated system such as plasma, the PEO chains may find it thermodynamically favorable

to collapse. They may even be forced to "give up" some of their associated water due to osmotic increases. From indications in the whole blood clotting tests of this thesis, in which the PEO surfaces slightly increased the time to clot by a stagnant system, this seems unlikely. The surface is apparently still very hydrophilic and the PEO chains probably in the extended form.

4.3 Heparin Immobilization

Using a completely organic solvent system for the immobilization reactions, heparin was coupled to various chain lengths of two derivatized PEOs. The amount of heparin coupled to the surface was found to be a function of the molecular weight of the PEO, but not the type of derivative, i.e., the formation of a urethane linkage versus a urea linkage. The coupling presumably occurred through the free amines and hydroxyl groups present on the heparin molecule. Thus, by virtue of the method of attachment, the problems encountered when using the carboxylic groups for the site of attachment were avoided. Blockage of the carboxylic groups has been shown to cause loss of anticoagulant activity; however, free amines of heparin can be blocked with no loss in activity. (118) Any reaction with the carboxylic groups of the heparin and the functional groups of the PEO would form unstable intermediates and would necessarily rearrange to couple with the free amines or the hydroxyls of the heparin.

Another of the major benefits of this method of immobilization is that a totally organic solvent system prevents the possibility of inter- and intra-molecular crosslinking of the heparin. This has been a problem encountered by other investigators requiring prior blockage of the carboxylic groups before immobilization, then reactivating them to produce maximum activity. The use of the pyridine catalyst in the reaction functions to increase the basicity of the hydroxyl groups rendering them more reactive. Merrill has proposed affixing the

heparin molecule by an end unit derived from the polypeptide serine and not by any of the side groups on the polysaccharide units (personal communication). Here again, the problem may be encountered requiring blockage of the carboxylic groups on the saccharide units.

The amounts of heparin on the surface were found to be a function of the molecular weight of the PEO chains. The lower molecular weight derivatives coupled slightly more heparin than the higher molecular weight polymers. Higher yields of immobilized heparin may be attainable in different solvent systems; however, for the reasons stated above, aqueous systems would not be advisable. Heparin is virtually insoluble in most common organic solvents. In terms of amount of heparin per mg of beads, the 6,000 MW derivatives had 0.87 ug heparin/mg and the 18,000 MW had 0.62 ug heparin/mg of beads. This compares to the immobilized heparin/agarose surfaces of Schmer containing five ug/mg of dry agarose when no spacer arm was used. Schmer also used a putrecine or -aminocaproyl- derivatized agarose to immobilize via the amine groups of heparin, and found much higher coupling efficiency, 60 ug/mg. Subsequently, the abilities of these surfaces to bind thrombin were also greater. It is difficult to compare amounts of heparin coupled to the results found by Ebert using derivatized Sepharose as they are expressed per mg of swollen beads. (118) However, Heyman, using similar methods of attachment, found amounts ranging from 1-4 ug/cm^2. (119)

The immobilized heparin was found to be stable after repeated washings with PBS, ethanol and methylene chloride as demonstrated by two techniques. First, using the sulfur 2P peak of the XPS spectrum, little loss was observed over the 3 day hydration period which was done prior to performing the activity assays (Table VIII). As can be seen in Fig. 41, the sulfur 2P peak of pure heparin powder occurs at approximately 162.5 ev binding energy and has an atomic

percent of 6.9 percent. The sulfur peak of heparin immobilized onto PEO-bis isothiocyanate (MW 6,000) is also seen in Fig. 41. It is quite easy to distinguish the sulfur from the thiocyanate as this is less electronegative and is not charge shifted, occurring at 158.5 ev. Since all the peaks and percentages are normalized for their Scofield cross sections and the number of scans, these data are directly comparable to those of Ebert, who monitored the 2S peak of immobilized heparin. (118) His pure heparin powder was found to have 5.3 percent sulfur content. The sulfur of the immobilized heparins accounted for only 0.25 percent of the total surface signal. The surface of the PEO/heparin demonstrated 2.5 percent sulfur content, which is 10 times more than that found by Ebert. So although the amounts of heparin on the surface are not comparable directly by radiolabeling experiments, the XPS analysis suggests that the PEO coupled heparin surface contains a much higher percentage of heparin available for interactions.

The second method to determine the stability of the immobilized heparin was to count successive washes of the labeled heparin beads which would indicate if heparin were leaching from the surface over time. Beads, which had been washed according to the final protocol developed prior to activity testing, had only 8.6×10^{-5} ug/cm^2. This amount slowly decreased to a final value of 9.2×10^{-6} ug/cm^2 in the tenth and final wash. Even if the quantities of all the washes are added together, they total far less than the minimum amount of heparin required for thrombo-resistance. (115) This is also far less than would be required to produce the elevation in clotting times which were observed in the activity assays.

4.4 Blood and Protein Interactions

Accomplishing the immobilization of heparin onto a surface is useless unless the activity of the heparin is established. With the stability of the heparin confirmed, the activities reported can be assumed to be a result of the immobilized heparin and not solution heparin which has leached from the surface. The results of the two clotting assays indicate significant increases in both the whole blood clotting time and the activated partial thromboplastin time. When comparing similar weights of beads, heparin coupled via the 18,000 MW PEOs was slightly less active than those of the 6,000 MW derivatives. When this is normalized for the differences in amount of heparin coupled to the surfaces, no difference was found in the activity of the immobilized heparins. Still the activity of the heparin accounts for only approximately 24 percent of the native heparin if the equivalent amount were in solution. Although this is higher than some investigators have reported, (145) others have been able to retain a greater percentage of the native heparin activity. (119)

The results of the platelet retention tests support the findings from other investigators. PEO is very efficient at minimizing platelet adhesion onto the surface and is still able to exert this influence even in the presence of the immobilized heparin. However, retention does not necessarily imply activation and release. Although controversial, soluble heparin has been shown to adversely interact with platelets, initiating aggregation and release of the contents of the α-granules. One of the substances released is Platelet Factor 4. PF4 has been shown to bind to heparin and inactivate it.

The activation of the platelets which did adhere to the heparin derivatized surfaces were not statistically different from the controls as measured by the percentage of bound PF4. Although the PEO/heparin surfaces were found to retain fewer platelets, there was no difference in the PF4 levels between these

surfaces and the controls. This indicates that a fewer number of platelets produced the same amount of PF4. This same observation was made for the PEO surfaces in the absence of immobilized heparin. On the other hand, the heparin coupled surfaces, which in the absence of PEO would be expected to activate α-granule release, showed no elevated levels of PF4 after exposure. This indicates that the immobilized heparin is not activating platelets as solution heparin has been reported to do. Presumably, this is due to the presence of the PEO chains. However, from the increase in clotting times obtained, the heparin is still capable of interacting with other coagulation factors.

4.5 Summary and Conclusions

The purpose of this dissertation, as stated in the introduction, was to investigate the properties of long poly(ethylene oxide) chains grafted to a surface in such a manner as to be capable of extension out from the surface. Due to the extension and the flexibility of the hydrophilic chains, an excluded volume is established, prohibiting other macromolecules from adsorbing to the surface. If this could be established, then the protein resistance of this surface could be utilized in conjunction with immobilized heparin. This would permit the extension of heparin out from the surface, mimicking solution activity towards particular coagulation factors. Optimally, the heparin activity could be maintained while still minimizing the nonspecific adsorption of proteins which otherwise could mask the heparin from further interactions.

From these studies the following conclusions are made:

1. By derivatizing various molecular weight poly(ethylene oxide) chains, highly reactive functional end groups may be formed which allow for straight forward coupling to free amines of an APS vapor-phase silanized surface. The reactions result in efficient transformation of the terminal hydroxyl groups to

chloroformate, thiochloroformate, isocyante or isothiocyanate groups depending upon the reagents used. The PEO-bis chloroformate and PEO-bis thiochloroformate, not unexpectedly, were more highly reactive, resulting in more efficient coupling to the surface. It would be expected that any surface containing free amines would be capable of reacting with the functional end groups of the derivatized PEOs. This chemistry is suitable for PEO immobilization onto the surface of urethanes which could be used for numerous applications requiring mechanical strength not inherent to the PEO.

2. The immobilized PEOs were characterized with respect to their stability in an aqueous salt medium and found to be stable over the period tested. The PEO-bis chloroformate and PEO-bis thiochloroformate have a higher degree of coupling to the surface than either the PEO-bis isocyanate or the PEO-bis isothiocyanate, but exhibit less stability in PBS solution. Presumably, this is due to the relative instability of the urethane linkage over the urea linkage, which possesses additional stability due to resonance of the adjacent double bonds. The thickness of the layer of polymer on the surface was investigated and no difference in thickness or degree of surface coverage was observed using variable angle XPS. It must be remembered that in the XPS spectrometer the chains would necessarily be collapsed and highly condensed due to the high vacuum. If the lengths of the fully extended chains are calculated from bond distances, the 6,000 MW and 18,000 MW PEO chains are 375 Å and over 1000 Å long, respectively. Using terminally bonded PEO chains on polystyrene latex particles dispersed in water, Cosgrove found that the segment density of PEO tails (MW 4,800) extended 30nm from the surface. (27) This is good evidence that the chains do extend fully into the solution.

3. The method of attachment of the PEO chains, permitting extension out from the surface, is successful in excluding proteins from the surface. This was

demonstrated by the TIRF technique which monitors the protein bound to the surface *in situ*. The PEO coupled surfaces were found to adsorb virtually no protein from two different concentrations of AT-III and from serum when adsorbed from flowing solutions. In the radiolabeled experiments, which necessitates that the protein be eluted from the surface, very little protein was detected in the wash. The 18,000 MW chloroformate surface was slightly more efficient at resisting adsorption than the 6,000 MW derivatives, but the same trend was not evident in the isocyanate derivatives. The reason for this discrepancy remains unclear. The chloroformate derivatives were more resistant to protein adsorption than the isocyanate derivates when comparing equal molecular weights. This may be a function of the amount of PEO coupled to the surface. The density of the isocyanate derivatives may have required tighter packing of the chains limiting the flexibility of the individual chains.

4. The functional groups on the immobilized PEO were capable of binding to the hydroxyl and amine groups of heparin provided that they were not first exposed to atmospheric water vapor. This caused the hydrolysis of the functional end groups. The primary amines resulting from PEO end group hydrolysis should have been capable of binding heparin via the carboxylic groups of the heparin molecule. Much less heparin was found on the surface when conditions permitted end group hydrolysis as demonstrated by the small sulfur 2P XPS peak. However, with reactive chlororformate and isocyanate groups, the immobilization of the heparin is quite straightforward.

5. The immobilized heparin surfaces were characterized in terms of amount, stability and thickness of the layer. XPS data showed very little decrease in the total sulfur signal after the first hour of hydration in PBS buffer. This was confirmed by the radiolabeled heparin experiments designed to monitor leaching of the surface heparin. When the heparin surfaces were washed

adequately with distilled water, ethanol, and methylene chloride, no solution heparin was found in the subsequent water washes. The layer of immobilized heparin was found to cover approximately 95 percent of the surface although this represents the collapsed layer under vacuum conditions. The amount of heparin on the surface was found to be approximately 1.0 ug/cm^2 with slightly less on the 18,000 MW PEO surfaces. The reason for the decreased amount of heparin on the higher molecular weight polymer chains is unclear, but may be a result of using an organic solvent system for the immobilization reaction. The higher polymer may have been more highly coiled and therefore less accessible to the solution heparin. However, the organic solvent system used in this method of immobilization does not permit inter- and intramolecular crosslinking of the heparin molecules.

6. The immobilized heparin is capable of binding AT-III as demonstrated in the TIRF and radiolabeled protein experiments. In the flowing solutions of the TIRF experiments, PEO surfaces without heparin did not adsorb appreciable amounts of AT-III or other proteins from serum, but when heparin was coupled to the PEO chains, some protein adsorption was observed. The TIRF experiments indicated that the heparin was not saturated in its ability to bind proteins. More AT-III was adsorbed when the solution concentration was doubled (twice that of physiological concentration) and from serum. The increase of the fluorescent signal resulting from serum adsorption, probably indicates other proteins were binding to the immobilized heparin. The amount of protein adsorbed by the immobilized heparin was still less than the control surfaces by nearly a factor of five. The ability of heparin to perform its anticoagulant function was demonstrated by the major increases in whole blood clotting and activated partial thromboplastin times. When normalizing to the weight of heparin on the surface, no difference between the different molecular weight spacers was noted

in the activity of the heparin as determined by APTT. Although the PEO and PEO/heparin surfaces demonstrated a significantly lower mean platelet retention index, there was no statistical difference observed between any of the surfaces, either between the surfaces with or without heparin and the controls in the amount of PF4 bound. This indicates that the platelets were activated to a greater degree by the PEO and the PEO/heparin surfaces, if the platelet retention experimental conditions can be assumed to produce similar results as those used in the PF4 assay. The PEO surfaces without heparin did not show any less PF4 than the controls or the heparinized surfaces. This is not corroborated by other investigators who report that PEO is inert towards platelets. Why this has been found in this study warrants further investigation.

7. The activity of the immobilized heparin was shown not to be due to heparin released from the surface and in solution. This was demonstrated by monitoring the amount of radiolabeled heparin from the surface in successive washes of the surface. XPS monitoring of the heparin sulfur 2P peak demonstrated no loss from the surface during hydration over a 3-day time period. Also, heparin, which failed to clot whole blood after nearly an hour, was withdrawn and placed in a tube containing clean glass beads. All of the samples clotted within 9 minutes, indicating that no depletion of the coagulation factors had occurred.

8. Even though the molecular weight of heparin ranges from 5,000 to 30,000, the presence of this large molecule was shown not to mask the benefits of grafted PEO on the surface. Although, the APTT and PF4 levels were not quite as "good" as with PEO chains without heparin, they were consistently better than the controls.

I have demonstrated the feasibility of a PEO-heparin surface and some of the potential benefits in terms of protein and platelet compatibility. It is hoped

that, with further testing, long chain PEO can be grafted to a mechanically suitable polymer in such a manner as to permit attachment of heparin. If the grafting procedure allows for the extension of the PEO chains into solution, this surface should also minimize nonspecific protein adsorption. The *in vivo* results of such a device would have far ranging potential, if its efficiency could be established.

4.6 Future Studies

4.6.1 Derivatization of Graft Materials

The ultimate test of the effect of PEO-heparin complexes must be on a mechanically suitable polymer. PEO, with terminal hydroxyl groups, offers a wide variety of methods to terminally graft the chains onto another polymer. The hydroxyl groups are easily replaced by other functionalities or may be used directly to couple to reactive groups on the polymer surface. The amines of urethanes offer an excellent opportunity for grafting PEO chains in a manner similar to those used in this dissertation. Diamino PEO could be esterified with alcohols in an acid catalyzed reaction to permit direct attachment to poly-amino acids. Aqueous irradiation may be used to graft PEO to crosslinked hydrogels.

The extent of grafting to any substrate material must be studied on a case by case basis. If the PEO is crosslinked, the network chain density should be determined, and its effects on the extension of the chains into solution. The free PEO tails must then be available for the covalent attachment of heparin. Since heparin also possesses a number of functional groups, there are many varieties of possible mechanisms for its immobilization.

The blood compatibility, protein adsorption and coagulation activation characteristics of these surfces would be an interesting extension of this study.

4.6.2 *In-Vivo* Characterization

As mentioned previously, favorable *in-vitro* results do not necessarily correlate with *in-vivo* biocompatibility. Both acute and chronic thromboresistance of the PEO/heparin grafted surfaces must be tested *in-vivo*. The *in-vivo* stability of the surface is critical and should be studied. Cannulae with grafted PEO/heparin could be implanted and studied for the thromboresistance in both arterial and venous flow.

4.6.3 Feasibility for Long Term Applications

Any immobilized material, particularly a drug, is susceptible to enzymatic degradation. The long term potential of an immobilized heparin via PEO chains needs to be investigated. However, due to the degradation of the heparin, and the instability of the grafted PEO, long term applications may not be feasible. However, it may be that the presence of the PEO/heparin complex offers short term passivation which later may be replaced by inert proteineceous film deposits. This phenomenon has been observed on long term artificial heart implants. (164) If the PEO/heparin can remain active until the hypercoaguability of the blood resulting from surgery returns to normal, the benefits are obvious.

Also, there are a number of short term applications which could significantly benefit from a protein resistant surface. The left ventricular assist device (LVAD), currently being tested for short term (i.e., 2 weeks) use, offers an excellent surface which could benefit from an immobilized heparin surface which minimizes protein resistance. Blood oxygenators, used during open heart surgery, could be rendered much less detrimental to the blood, if the blood contacting surfaces had a grafted PEO/heparin complex on them. Certainly passivation of dialysis membranes might be achieved through this approach. The possibilities are numerous.

REFERENCES

1. Didisheim, P., "Comparative Hematology in the Human, Calf, Sheep, and Goat: Relevance to Implantable Blood Pump Evaluation," **Am. Soc. for Artif. Intern. Org. J. 8** (3) 123-127 (1985).

2. Anderson, J.M. and Kottke-Marchant, K., "Platelet Interactions with Biomaterials and Artificial Devices," CRC **Critical Reviews in Biocompatibility, 1** (2) 111-204 (1984).

3. Didisheim, P., **Guidelines for Blood-Material Interactions,** Report of the National Heart Lung and Blood Institute Working Group. U.S. Dept. of Health and Human Services, NIH publication no. 85-2185 (1985).

4. Soderquist, M.E. and Walton, A.G., "Structural Changes in Proteins Adsorbed on Polymer Surfaces," **J. Coll. and Inter. Sci., 75** 386-397 (1980).

5. Leninger, R.I., "Polymeric Materials That Don't Clot Blood," **Chem. Technol., 5** (3) 172-176 (1975).

6. Kim, S.W., and Feijen, J., "Surface Modification of Polymers for Improved Blood Compatibility," **Biocompatibility, 1** (3) 229-234 (1985).

7. Gott, V.L., Wiffen, J.D., and Dutoon, R.C., "Heparin Binding on Colloidal Graphite Surfaces," **Science, 142** 1297 (1963).

8. Mori, T., Nagaoka, S., Takiuchi, H., Kikuchi, T., Noguchi, N., Tansawa, H., and Noishiki, Y., "A New Antithrombogenic Material with Long Poly(ethylene Oxide) Chains.," **Trans. Am. Soc. Artif. Intern. Organs, 28** 459-463, 1982).

9. Nagaoka, S., Mori, Y., Takiuchi, H., Yokota, K., Tanzawa, H., and Nishiuimi, S., "Interaction Between Blood Components and Hydrogels With Poly(oxyethylene) Chains.," **Polymer Preprints, 24** (1) 67-68, (1983).

10. Matsuda, T. and Akutsu, T., "*In Vitro* and *In Vivo* Assessment of Blood/Material Interactions of Hydrophobic and Hydrophilic Segmented Polyurethanes.," Seattle American Chemical Society Meeting Abstracts, March (1983).

11. Hiatt, C.W., Shelvkov, A., Rosenthal, E.J., and Galimore, J.N., "Treatment of Controlled Pore Glass with Poly(ethylene Oxide) to Prevent Adsorption of Rabies Virus," **J. Chromatog., 58** 362, (1971).

12. Wasiewski, W., Fasco, M.J., Martin, B.B., Detwiler, J.C., and Fenton, J.W., "Thrombin Adsorption to Surfaces and Prevention with Polyethylene Glycol 6,000," **Thromb. Res. Brief Commun., 8** 881, (1976).

13. Merrill, E.W. and Salzman, E.W., "Polyethylene Oxide as a Biomaterial," **Amer. Soc. for Artif. Intern. Organs J., 6** 60-64, (1983).

14. Laurenco, A., **Compt. Rend. 49** 619 (1859).

15. Borguardt, U., Schnable, W., and Henglein, A., *"Pulsradiolytische Messung der Geschwindigkeitskonstentens der Kom ination on Polyathyloxid-Radi -linin wabri er Losung"*, **Macromol Chem., 127** 176 (1969).

16. Bailey, F.E., Jr. and Koleske, J.F., **Poly(ethylene Oxide),** Academic Press, New York, (1976).

17. Bluestone, S., March, J.E., and Flory, P.J., "The Interpretation of Viscosity-Temperature Coefficients for Poly(oxyethylene) Chains in a Thermodynamically Good Solvent," **Macromolecules, 7** 325, (1974).

18. Doolittle, A.K., **The Technology of Solvents and Plasticizers,** Wiley, New York, 836 (1956).

19. Rasch, M., *"Zur Hudratbildung Van Polyglydcolaterio- sungenn Amonaler Zahigkeif"* **Makromol, Chem., 73** 109 (1964).

20. Nemethy, G. and Scheraga, H.A., "Structure of Water and Hydrophobic Bonding in Proteins II. Model for the Thermodynamic Properties of Aqueous Solutions of Hydrocarbons," **J. Chem. Phys., 36** 3401 (1962).

21. Godovsky, Y.K., Slonimsky, G.L. and Garbar, N.M., "Effect of Molecular Weight on the Crystallization and Morphology of Poly(ethylene oxide) Fractions," **J. Poly Sci.,** Part C **38** (1), (1972).

22. Koenig, J.L. and Angood, A.C., "Raman Spectra of Poly(ethylene glycols) in Solution," **J. Poly Sci. (A2), 8** 1787 (1970).

23. Miyazawa, T., "Molecular Vibrations and Structures of High Polymers. I. General Method of Normal Coordinate Treatment of Internal Coordinate and Infrared Frequencies and Conformations of $(-CH_2-)_n$, $(-CH_2-O)_n$, and $(-CH_2-O-CH_2-)_n$" **J. Chem. Phys., 35** 693 (1961).

24. Liu, K-J, "Nuclear Magnetic Resonance Studies of Polymer Solutions. IV. Polyethylene Glycols," **Macromolecules, 1** 213-217 (1968).

25. Maxfield, J. and Shepard, I.W., "Conformation of Poly(ethylene oxide) in the Solid State, Melt and Solution Measured by Raman Scattering," **Polymer, 16** (7) 505-509 (1975).

26. Glass, J.E., "Adsorption Characterization of Water-Soluble Polymers: 1. Poly(vinyl alcohol) and Poly(vinyl pyrrolidone) at the Aqueous-Air Interface," **J. Phys. Chem., 72** 4450 (1968).

27. Cosgrove, T., Crowley, T.L. and Vincent, B. "An Experimental Study of Polymer Conformations at the Solid/Solution Interface," in **Adsorption from Solution,** 287-297 Academic Press, (1983).

28. Assarsson, P.G., Eirich, F.R., "Properties of Amides in Aqueous Solution. I. Viscosity and Density Changes of Amide-Water Systems. An Analysis of Volume Deficiencies of Mixtures Based on Molecular Size Differences (Mixing of Hard Spheres)," **J. Phys. Chem. 72** (8) 2710-2719 (1968).

29. Koenig, J.L. and Angood, A.C., "Raman Spectra of Poly(ethylene Glycols) in Solution," **J. Polymer Sci., (A2) 8** 1787 (1970).

30. Glass, J.E., "Adsorption Characterization of Water-Soluble Polymers: I. Poly(vinyl alcohol) and Poly(vinyl pyrrolidone) at the Aqueous-Air Interface," **J. Phys. Chem., 72** 4450 (1968).

31. Ryden, J. and Albertsson, P.A., "Interfacial Tension of Dextran - Polyethylene Glycol - Water Two Phase Systems," **J. Coll. and Inter. Sci., 37** (1) 219-222 (1971).

32. Hedman, P.O. and Gustafsson, J-G., "Protein Adsorbents Intended for Use in Aqueous Two - Phase Systems," **Analyt. Biochem., 183** 411-415 (1984).

33. Bailey, F.E., Jr. and Koleski, J.V., **Non-Ionic Surfactants,** (M.J. Schick, ed.) Dekker, (1966).

34. Smith, K.L., Winslow, A.E., and Peterson, D.E., "Association Reactions for Poly(alkylene oxides) and Poly(carboxylic acids)," **Ind. Eng. Chem., 51** 1361, (1959).

35. Lundberg, R.D., Bailey, F.E., and Callard, R.W., "Interactions of Inorganic Salts with Poly(ethylene Oxide)" **J. Poly Sci., (A-1) 4** 1563-1577 (1966).

36. Awano, H., Ono, K., and Murakami, K., "The Interaction of a Neutral Polymer with Small Ions in Solution. II. The Binding of Alkali Metal Ions to Poly(oxyethylene) in Several Organic Solvents," **Bull. Chem. Soc. Japan, 55** (8) 2530-2536 (1982).

37. Bailey, F.E., Jr. and France, H.G., "Molecular Association Complexes of Polymers. Urea and Thiourea Complexes of High Molecular Weight Poly(ethylene Oxide)," **J. Polymer Sci., 49** 397 (1961).

38. Hemalatha, S., Chandani, B., and Balasu-bramanian, D., "Complexation of Molecular Iodine by Linear Poly(ethylene Glycol)," **Spect. Letters, 12** (7&8) 535-541 (1970).

39. McPherson, A., Jr., "Crystallization of Proteins from Polyethylene Glycol," **J. Biol. Chem., 251** 6300-6303 (1976).

40. Hawk, G.L., Cameron, J.A., and Dufault, L.B., "Chromatography of Biological Materials on Polyethylene Glycol Treated Controlled-Pore Glass," **Preparative Biochem., 2** (2) 193-203 (1972).

41. Ingham, K.C., "Precipitation of Proteins with Polyethylene Glycol; Characterization of Albumin," **Archives of Biochem. and Biophys., 186** (1) 106-113 (1978).

42. Vincent, B., "The Van Der Waals Attraction Between Colloid Particles Having Adsorbed Layers. II. Calculation of Interaction Curves," **J. Coll. Inter. Sci., 42** (2) 270-285 (1973).

43. Topchieva, I.N., "Biochemical Applications of Poly-(ethylene Glycol):, ***Uspekhi Khimii*, 49** 494-517 (1980).

44. Knoll, D. and Hermans, J., "Polymer-Protein Interactions. Comparison of Experiment and Excluded Volume Theory," **J. Biol. Chem., 258** (9) 5710-5715 (1983).

45. Maroudas, N.G., "Polymer Exclusion, Cell Adhesion and Membrane Fusion," **Nature, 254** (24) 695-696 (1975).

46. Klein, J. and Luckham, P.F., "Forces Between Two Adsorbed Poly(ethylene oxide) Layers in a Good Aqueous Solvent in the Range of 0-150 nm" **Macromolecules, 17** 1041-1048 (1984).

47. Merrill, E.W. and Salzman, E.W., "Polyethylene Oxide as a Biomaterial," **Am. Soc. for Artif. Intern. Org. J., 6** (2) 60-64 (1983).

48. Bell, G.E., Dembo, M. and Bongrand, P., "Cell Adhesion: Competition Between Nonspecific Repulsion and Specific Bonding," **Biophys. J., 45** 1051-1064 (1984).

49. Lang, S.L. and Webster, D.F., "Wound Dressings for Burns," UK Patent Applications 2,093,702 and 2,093,703 (1982).

50. Castello, G. and D'Amato, G., "Evaluation of the Properties of Polyethylene Glycols as Stationary Phases in Gas-Liquid Chromatography," **J. Chrom., 90** 291-301 (1974).

51. Blomberg, L. and Wannman, T., "Some Factors Affecting the Properties of Thin Films of Carbowax 20M Intended for Deactivation of Glass Capillary Columns," **J. Chrom., 148** 379-387 (1978).

52. Matsumato, U., Shibusawa and Tanaka, Y., "Surface Affinity Chromatographic Separation of Blood Cells III. Effect of Molecular Weight on Polyethylene Glycol Bonded Stationary Phases on Elution Behavior of Human Blood Cells," **J. Chrom., 268** 375-386 (1983).

53. Hiatt, C.W., Shelokov, A., Rosenthal, E.J. and Galimore, J.M., "Treatment of Controlled Pore Glass with Poly(ethylene oxide) to Prevent Adsorption of Rabies Virus," **J. Chrom., 56** 362-364 (1971).

54. Ling, T.G.I. and Mattiasson, B., "Poly(ethylene Glycol)- and Poly(Vinyl Alcohol)-Substituted Carbohydrate Gels for "Mild" Hydrophobic Chromatography," **Chrom., 15** 293-297 (1983).

55. Haire, R.N., Tisel, W.A., White, J.G., and Rosenberg, A., On the Precipitation of Proteins by Polymers: The Hemoglobin-Polyethylene Glycol System," **Biopoly., 23** 2761-2779 (1984).

56. Roth, E.F., Jr., Bookchin, R.M. and Nagel, R.L., "*In Vitro* Assessment of the Interaction of Blood with Model Surfaces," **J. Lab. Clin. Med., 93** 867-871 (1979).

57. Laurent, T.C., "The Interaction Between Polysaccharides and Other Macromolecules. 5. The Solubility of Proteins in the Presence of Dextran," **Biochem. J., 89** 253 (1963).

58. Hasko, F., and Vaszileva, R., "Solubility of Plasma Proteins in the Presence of Polyethylene Glycol," **Biotech. and Bioeng., 24** 1931-1939 (1982).

59. Skoog, B., "Removal of Polyethylene Glycols from Immunoglobulin Samples By Adsorption Chromatography on Polystyrene Beads," **Experientia, 36** 1157-1158 (1980).

60. Thurow, H., and Geisen, K., "Stabilization of Dissolved Proteins Against Denaturation at Hydrophobic Interfaces," **Diabetalogia, 27** 212-218 (1984).

61. Suzuki, T., Kanbara, N., Tomano, T., Hayashi, N., and Shinohara, I., "Physiochemical and Biological Properties of Poly(ethylene Glycol) Coupled Immunoglobulin G," **Biochem. et Biophys. Acta, 778** 248-255 (1984).

62. Zalipsky, S., Gilon, C., and Zilkha, A., "Attachment of Drugs to Polyethylene Glycols," **Polymer J., 19** (12) 1177-1183 (1983).

63. Kim, S.W., Peterson, R.V., and Feijen, J., "Polymeric Drug Delivery Systems," in **Drug Design 10** Academic Press, New York, (1980) and references sited therein.

64. Abuchowski, A. and Davis, F.F., "Soluble Polymer-Enzyme Adducts," in **Enzymes as Drugs,** (J.C. Rolcenberg ed.) Wiley, 367-382 (1981).

65. Abuchowski, A., Van ES, T., Palczuk, N.C., and Davis, F.F., "Alteration of Immunological Properties of Bovine Serum Albumin By Covalent Attachment of Polyethylene Glycol," **J. Biol. Chem., 252** (11) 3578-3581 (1977).

66. Abuchowski, A. and Davis, F.F., "Preparation and Properties of Polyethylene Glycol-Trypsin Adducts," **Biochim. et Biophys. Acta, 578** 41-46 (1979).

67. Bade, K. and Mutter, M., "^{1}H-NMR Studies on Poly(oxyethylene)-Bound Oligopeptides," **Biopolymers, 22** 163-169 (1983).

68. Nagaoka, S., Mori, Y., Takiuchi, H., Yokota, K., Tanzawa, H. and Nishiumi, S., "Interaction Between Blood Components and Hydrogels with Poly(oxyethylene) Chains," **J. Biomed. Matrl. Res., 28** 459 (1982).

69. Mori, Y., Nagaoka, S., Takiuchi, H., Kikuchi, T., Naguchi, N., Tanzawa, H., and Noishiki, Y., "A New Antithrombogenic Material With Long Polyethyleneoxide Chains," **Trans. Amer. Soc. Artif. Intern. Org., 28** 459-463 (1984).

70. Nagaoka, S., Mori, Y., Takiuchi, H., Yokota, K., Tanzawa, H., and Nishiumi, S., "Interaction Between Blood Components and Hydrogels with Poly(oxyethylene) Chain," **Polymer Preprints, 24** (1) 67-68 (1983).

71. Lin, S.C., Beahan, P., and Hull, D., "The Protein Adsorption of Polymers Containing Ether Groups," **Society for Biomaterials** abstracts, **86** (1982).

72. Matsuda, T. and Akutsu, T., "*In Vitro* and *In Vivo* Assessment of Blood/Material Interactions of Hydrophobic and Hydrophilic Segmented Polyurethanes," **Amer. Chem. Soc.**, abstracts, **3** (1983).

73. Merrill, E.W., Salzman, E.W., Wan, S., Mahmud, N., Kushner, L., Lindon, J.N., and Curme, J., "Platelet-Compatible Hydrophilic Segmented Polyurethanes From Polyethylene Glycols and Cyclohexane Diisocyanate," **Trans. Am. Soc. Artif. Intern. Org., 28** 482-487 (1982).

74. Merrill, E.W. and Salzman, E.W., "Polyethylene Oxide as a Biomaterial," **Am. Soc. Artif. Intern. Org. J., 6** (2) 60-64 (1983).

75. McLean, J., "The Thromboplastic Action of Heparin," **Am. J. Physiol., 41** 250-257 (1976).

76. Riesenfeld, J., Hook, M., Lindahl, U., "Biosynthesis of Heparin, Concerted Action of Early Polymer-Modification Reactions," **J. Biol. Chem., 207** 421-425 (1982).

77. Jaques, L.B., "Heparin: a Unique Misunderstood Drug," **TIPS, 7** 289-291 (1982).

78. Rosenberg, R.D., Armand, G., and Lam, L., "Structure-Function Relationships of Heparin Species," **PANS (USA), 75** 3065-3069 (1978).

79. Rosenberg, R.O. and Lam, L., "Correlation Between Structure and Function of Heparin," **PANS (USA), 76** 1218-1222 (1979).

80. Lindahl, U., Backstrom, G., Hook, M., Thunberg, L., Franssan, L.A., and Linker, A., "Structure of the Antithrombin III Binding Site in Heparin," **PANS (USA), 76** 3198-3202 (1979).

81. Radoff, S. and Danishefsky, I., "Location on Heparin of the Oligosaccharide Section Essential for Anticoagulant Activity," **J. Biol. Chem., 259** (1) 166-172 (1984).

82. Lasker, S.E. and Stivala, S.S., "Physiochemical Studies of Fractionated Bovine Heparin: 1. Some Dilute Solution Properties," **Arch. Biochem. Biophys., 115** 360-372 (9165).

83. Hurst, R.E. and Poon, M-C, "Structure-Activity Relationships of Heparin: Independence of Heparin Charge Density and Antithrombin-Binding Domains in Thrombin Inhibition By Antithrombin and Heparin Cofactor III," **J. Clin. Invest., 72** 1042-1045 (1983).

84. Oosta, G.M., Gardner, W.T., Beelerand, D.L., and Rosenberg, R.O., "Multiple Functional Domains of the Heparin Molecule," **Proc. Natl. Acad. Sci. USA,** 78 (2) 829-833 (1981).

85. Rosenberg, R.D., "Biologic Actions of Heparin," **Seminars in Hematology, 14** (4) 427-439 (1977).

86. Rosenberg, R.D., "Chemistry of the Hemostatic Mechanism and its Relationship to the Action of Heparin," **Federation Proc., 36** (1) 10-18.

87. Salzman, E.W., Rosenberg, R.D., Smith, M.H., Lindon, J.N., and Faureau, L., "Effects of Heparin and Heparin Fractions on Platelet Aggregation," **J. Clin. Invest., 65** 64 (1980).

88. Jaques, L.P., "Heparin: An Old Drug with a New Paradigm, **Science, 206** 528 (1979).

89. Glueck, C.J., "Postheparin Lipoprotein Lipase," **New Eng. J. Med., 292** 1346 (1975).

90. Baylin, S.B., Bearen, M.A., Kraus, R.M., and Keiser, H.R., "Response of Plasma Histamine Activity to Small Doses of Heparin in Normal Patients and Patients with Hyperlipoproteinemia," **J. Clin. Invest., 52** 1985 (1973).

91. Kloppenborg, P.W.C., Casparie, A.F., Beuraad, T.J., and Mafoor, C.C.H., "Inhibition of Adrenal Function in Man by Heparin or Heparinoids," **Acta Med. Scand., 197** 99 (1975).

92. Rosenberg, R.D. and Damus, P.S., "The Purification and Mechanism of Action of Human Antithrombin-Heparin Cofactor," **J. Biol. Chem., 248** 6490 (9178).

93. Villanueva, G.B. and Danishefsky, I., "Evidence for a Heparin-Induced Conformational Change of Antithrombin III," **Biochem. Biophys. Res. Comm., 74** 803 (1977).

94. Anderson, L.O., Barrowcliffe, T.W., Homer, E., Johnson, E.A., and Sims, G.E.C., "Anticoagulant Properties of Heparin Fractionated by Affinity Chromatography on Matrix Bound Antithrombin III by Gel Chromatography," **Thromb. Res., 9** 515-583 (1976).

95. Stead, N., Kaplan, A.P., and Rosenberg, R.D., "Inhibition of Activated Factor XII by Antithrombin-Heparin Cofactor," **J. Biol. Chem., 251** 6481 (1971).

96. Rosenberg, J.S., McKenna, P., and Rosenberg, R.D., "Inhibition of Human Factor IXa by Human Antithrombin," **J. Biol. Chem., 25** 8883 (1975).

97. Damus, P.S. and Rosenberg, R.D., "Anticoagulant Action of Heparin," **Nature, 246** 355 (1977).

98. Griffith, M.J., "Heparin-Catalyzed Inhibitor/Protease Reactions: Kinetics Evidence for a Common Mechanism of Action of Heparin" **Proc. Natl. Acad. Sci., (USA), 80** 5460-5464 (1983).

99. Homer, E., Soderstrom, G., and Anderson, L.O., "Studies on the Mechanism of the Rate-Enhancing Effect of Heparin on the Thrombin-Antithrombin III Reaction," **Eur. J. Biochem., 93** 1 (1979).

100. Anderson, L.O., Engman, L., and Henningsson, E., "Cross-Immunoelectrophoresis as Applied to Studies on Complex Formation: The Binding of Heparin to Antithrombin III and the Antithrobin III-Thrombin Complex," **J. Immun. Meth., 14** 271 (1977).

101. Griffith, M.J., "The Heparin-Enhanced Antithrombin III-Thrombin Reaction is Saturable with Respect to Both Thrombin and Antithrombin III," **J. Biol. Chem., 257** 13899-13902 (1982).

102. Pomerantz, M.W. and Owen, W.G., "Heparin-Accelerated Inhibition of Activated Factor X by its Natural Plasma Inhibitor" **Biochim, et Biophys. Acta, 201** 387-390 (1978).

103. Gitel, S.N., in **Heparin: Structure, Function and Clinical Implications,** (R.A. Bradshaw and S. Wessler, eds.) Plenum Press, New York, 243-247 (1975).

104. Danishefsky, I., Ahrens, M., and Klein, S., "Effect of Heparin Modification on its Activity in Enhancing the Inhibition of Thrombin by Antithrombin III," **Biochim. et Biophys. Acta, 498** 215-222 (1979).

105. Gitel, S.N., "Heparin: Structure, Function, and Clinical Implications," **Adv. Exp. Med. Biol., 52** 243 (1975).

106. Ebert, C.D. and Kim, S.W., "Heparin - Polymers for the Prevention of Surface Thrombosis," in **Medical Applications of Controlled Release Technology Vol. 2,** CRC Press (R. Langer and D.L. Wise, eds.) 178-203 (1984).

107. Grode, G., Falb, R., and Anderson, S., "Development of Materials for Use in Circulatory Assist Devices," in **Artificial Heart Program Conference Proceedings,** U.S. Dept. of Health, Education and Welfare, National Institutes of Health 19-27, June 9-13 (1969).

108. Grode, G.A., Falb, R.D., and Crowley, C., "Biocompatible Materials for Use in the Vascular System," **J. Biomed. Mater. Res. Symp.,** 3 77-84 (1972).

109. Peppas, N., "New Hydropholic Copolymers for Biomedical Applications," Trans. Am. SOL. Artif. Intern. Org., **24** 404-410 (1978).

110. Lagergren, H.R. and Erikson, J.C., "Plastics with a Stable Surface Monolayer of Crosslinked Heparin: Preparation and Evaluation:, **Am. Soc. Artif. Intern. Org. Trans., 17** 10-12 (1971).

111. Schmer, G., "The Biological Activity of Covalently Immobilized Heparin," **Am. Soc. Artif. Intern. Org. Trans., 18** 321-324 (1972).

112. Labarre, D. and Jozefowicz, M., "Preparation and Properties of Heparin-Poly(methyl methacrylate) Copolymers," **J. Poly. Sci. 47** 131-137 (1974).

113. Labarre, D., Boffa, M.S., and Jozefowicz, M., "Properties of Heparin-Poly(methyl methacrylate) Copolymers II," **J. Biomed. Matrl. Res., 11** 283-295 (1977).

114. Danishefsky, I. and Tzeng, F., "Preparation of Heparin-Linked Agarose and its Interaction with Plasma," **Thromb. Res., 4** 237-364 (1974).

115. Gossen, M.F.A. and Sefton, M. V., "Heparinized Styrene-Butadiene-Sytrene Elastomers," **J. Biomed. Matrl. Res., 13** 347-364 (1979).

116. Muria, Y., Aoyugi, S., Kusada, Y., and Miyamoto, K., "The Characteristic of Anticoagulation by Covalently Immobilized Heparin," **J. Biomed. Matrl. Res., 14** 619-630 (1980).

117. Larsson, R., Eriksson, J.C., Lagergren, H.R., and Olsson, D., "Platelet and Plasma Coagulation Compatibility of Heparinized and Sulphated Surfaces," **Thromb. Res., 15** 157-167 (1976).

118. Ebert, C.D., "Evaluations of Diaminoalkane Mediated Immobilized Heparin," PhD. dissertation, Dept. of Pharmaceutics, Univ. of Utah, (1981).

119. Heyman, P.W., "Heparinized Polyurethanes: *In Vitro* and *In Vivo* Studies," master's thesis, Dept. of Bioengineering, Univ. of Utah, (1984).

120. Lindberg, B., Maripuu, R., Siegbahn, K., Larsson, R., Golander, C.-G., and Eriksson, J.C., "ESCA Studies of Heparinized and Related Surfaces, 1. Model Surfaces on Steel Substrates," **J. Coll. Interf. Sci., 95** (2) 308-321 (1983).

121. McGary, C.W., Jr., "Degradation of Poly(ethyleneOxide)," **J. Poly. Sci., 46** 51-57 (1960).

122. Dottavio-Martin, D. and Ravel, J.M., "Radiolabeling of Proteins by Reductive Alkylation with (14C) Formaldehyde and Sodium Cyanoborahydride," **Anal. Biochem., 87** 562-565 (1978).

123. Greenwood, F.C., Hunter, W.M., and Glover, J.S., "The Preparation of ^{131}I-Labelled Human Growth Hormone of High Specific Radioactivity," **Biochem. J., 89** 114 (1963).

124. Chuang, H.Y.K., King, W.F., and Mason, R.G., "Interaction of Plasma Proteins with Artificial Surfaces: Protein Adsorption Isotherms," **J. Lab. Clin. Med., 92** 483-496 (1978).

125. Andrade, J.D., "X-Ray Photoelectron Spectroscopy," 105-195, in **Surface and Interfacial Aspects of Biomedical Polymers,** Vol. 1 (J.D. Andrade ed.) Plenum Press, New York (1985).

126. Johnson, R.E., Jr., and Dettre, R.H., "Wettability and Contact Angles," in **Surface and Colloid Science,** (E. Matijeric ed.) Wiley Interscience, New York, 85-154 (1974).

127. Harrick, N.J., **Internal Reflection Spectroscopy,** Wiley, New York (1967).

128. Hlady, V., Van Wagenen, R.A., and Andrade, J.D., "Total Internal Reflection Intrinsic Spectroscopy Applied to Protein Adsorption," **Interfacial Aspects of Biomedical Polymers Vol 2: Protein Adsoprtion,** (J.D. Andrade, ed.) Plenum Press (1985).

129. Hirschfeld, T., "Total Reflection Fluorescence," **Can. Spectroscopy,** 10 128 (1965).

130. Van Wagenen, R.A., Rockhold, S., and Andrade, J.D., "Probing Protein Adsorption: Total Internal Reflection Intrinsic Fluorescence," in **Biomaterials: Interfacial Phenomena and Applications,** (S.L. Cooper and N.A. Peppas, eds.) Washington, D.C. American Chemical Society, 351-370 (1982).

131. Fareed, J., "New Methods in Hemostatic Testing," in **Perspectives in Hemostasis,** (J. Fareed, H.L. Mesmore, J.W. Fenton and K.M. Brinkhouse, eds.) Pergamon Press, New York, 310-347 (1981).

132. Spector, I. and Corn, M., "Control of Heparin Therapy with Activated Partial Thromboplastin Times," **JAMA, 201** 157-159 (1976).

133. Besterman, E.M.M. and Gillet, M.P.T., "Heparin Effects on Irreversible Platelet Aggregation," **Lancet, 2** 282 (1972).

134. Davies, J.A. and Manys, V.C., "Effect of Heparin on Platelet Monoloyer Adhesion, Aggregation, and Production of Malondialdehyde," **Thromb. Res., 26** 31 (1982).

135. Macintyre, D.E., Handin, R.I., Rosenberg, R., and Salzman, E.W., Heparin Opposes Prostanoid and Non-Prostanoid Platelet Inhibitors by Enhancement of Aggregation," **Thromb. Res., 22** 167 (1981).

136. Salzman, E.W., Rosenberg, R.D., Smith, M.H., Lindon, J.N., and Favreau, L., "Effect of Heparin and Heparin Fractions on Platelet Aggregation," **J. Clin. Invest., 65** 64 (1980).

137. O'Brien, J.R., Shoonbridge, S.M. and Finch, W.J., "Comparison of the Effect of Heparin and Citrate on Platelet Aggregation," **J. Clin. Pathol., 22** 28 (1969).

138. Reinecke, D.R., "Monitoring Protein Adsorption by Gamma Photon Detection: An *In Situ* Device to Calibrate a Total Internal Reflection Fluorescence System," master's thesis, University of Utah, (1985).

139. Bornsin, G.A. and Miller, I.F., "The Kineticks of Protein Adsorption on Synthetics and Modified Natural Surfaces," **J. Coll. Interf. Sci., 86** 539-559 (1982).

140. Horbett, T.A., "Adsorption of Proteins from Plasma to a Series of Hydrophilic-Hydrophobic Copolymers. II. Compositional Analysis with the Prelabeled Protein Technique, **J. Biomed. Matrls. Res., 15** 673-695 (1981).

141. Van Der Sheer, A., Feijen, J., Elhast, J.K., Krugers Dagneaux, P.G.L.C., and Smolders, C.A., "The Feasibility of Radiolabeling for Human Serum Albumin (HSA) Adsorption Studies," **J. Coll. Interf. Sci., 66** 136-145 (1978).

142. Sefton, M.V. and Goosen, M.F.A., "Irreversible Immobilization of Heparin for Biomaterials," in **Chemistry and Biology of Heparin,** (R.L. Lundblad, W.V. Brown, K.G. Mann and H.R. Roberts, eds.) 463-474 (1981).

143. Ebert, C.D. and Kim, S.W., "Immobilized Heparin: Spacer Arm Effects on Biological Interactions," **Thromb. Res., 26** 43-57 (1982).

144. Wallace, H.W., Brooks, H.A., Stein, T.P., and Zimmerman, N.J., "The Contribution of Anticoagulants to Platelet Dysfunction with Extracorporeal Circulation," **J. Thorac. Cardiovasc. Surg., 72** 735 (1976).

145. Lindon, J.N., Rodvien, R., Brier, D., Greenberg, R., Merrill, and Salzman, E.W., "*In Vitro* Assessment of Interaction of Blood with Model Surfaces," **J. Lab. Clin. Med., 92** 904 (1978).

146. Salzman, E.W., Rosenberg, R.D., Smith, M.H., Lindon, J.N., and Favreau, L., "Effect of Heparin and Heparin Fractions on Platelet Aggregation, **J. Clin. Invest., 65** 64 (1980).

147. Geckeler, K., "Functionalization of Soluble Polymers. 1. Replacement of the Hydroxyl Groups of Poly(oxyethylene) by Amino Groups," **Polymer Bulletin, 1** 427-431 (1979).

148. Mutter, M., "Soluble Polymers in Organic Synthesis: 1. Preparation of Polymer Reagents Using Polyethylene Glycol with Terminal Amino Groups as Polymeric Components," **Tetrahedron Lett.,** 2839-2842 (1978).

149. Broze, G., Lefebure, P.M., Jerome, R., and Teyssie, P., "Some New Easy Routes for the Specific Functionalization of Polymers by Pendant or End Amino Groups," **Makromol. Chem., 178** 3171-3174 (1977).

150. Harris, J.M., "Laboratory Synthesis of Polyethylene Glycol Derivatives," **JMS Rev. Macromol. Chem. Phys.,** c25(3) 325-373 (1985).

151. Walling, C., **Free Radicals in Solution,** Wiley, New York, (1957).

152. Minoura, Y., Kasuya, T., Kawamura, S., and Nakans, A., "Degradation of Poly(ethylene Oxide) by High Speed Stirring," **J. Polymer Sci., A-2, 5** 125, (1967).

153. Nakano, A. and Minoura, Y., Degradation of Polymers by High Speed Stirring," **J. Appl. Polymer Sci., 15,** 927, (1971).

154. Tanford, C., **Physical Chemistry of Macromolecules,** Wiley, New York, (1963).

155. Nagaoka, S., Mori, Y., Takiuchi, H., Yokota, D., Tanzawa, H., and Nishimi, S., "Interaction Between Blood Components and Hydrogels with Poly(oxyethylene) Chains" **Amer. Soc. Artif. Intern. Org. J.,** 28 459 (1982).

156. Pekala, W. and Merrill, E.W., "XPS Determination of Molecular Rearrangement at the Surface of a Crosslinked Polymer System," **J. Coll. Interf. Sci., 101** (1) (1984).

157. Matsuda, T., Takano, H., Hayashi, K., Tanaka, Y., Takaichi, S., Umezu, M., Nakamura, T., Iwata, H., Nakatani, T., Tanaka, T., Takatani, S., and Akutsu, T., "The Blood Interface with Segmented Polyurethanes: Multilayered Protein Passivation Mechanism," **Am. Soc. Artif. Inter. Org. Trans., 30** 352-357 (1984).

158. Coleman, D.L., Meuzelaar, H.L.C., Kessler, T.R., McClennen, W.H. and Gregonis, D.E., "Retrieval and Analysis of a Clinical Total Artificial Heart," **J. Biomed. Matls. Res.,** submitted for publication.